Aus der Klinik für Urologie
der Heinrich-Heine-Universität Düsseldorf
Univ.-Prof. Dr. med. Peter Albers

An analysis of CD24 interaction partners in a pan-urological context, along with an assessment of its suitability as a therapeutic target

Dissertation

Zur Erlangung des Grades eines Doktors der Medizin
der medizinischen Fakultät der Heinrich-Heine-Universität Düsseldorf

vorgelegt von
David Julian Thomas
2024

Examiner Details

Als Inauguraldissertation gedruckt mit Genehmigung der medizinischen Fakultät der Heinrich-Heine-Universität Düsseldorf

gez.:

Dekan: Prof. Dr. med. Nikolaj Klöcker

Erstgutachter: Prof. Dr. rer. nat. Daniel Nettersheim

Zweitgutachterin: PD Dr. rer. nat. Doreen M. Floß

List of own Publications

Teile dieser Arbeit wurden veröffentlicht in:

Christian Söhngen, David J. Thomas, Margaretha A. Skowron, Felix Bremmer, Markus Eckstein, Anja Stefanski, Marc D. Driessen, Gamal A. Wakileh, Kai Stühler, Peter Altevogt, Dan Theodorescu, Rüdiger Klapdor, Axel Schambach, Daniel Nettersheim, (2023), CD24 targeting with NK-CAR immunotherapy in testis, prostate, renal and (luminal-type) bladder cancer and identification of direct CD24 interaction partners, The FEBS journal, (Volume 290, Issue 20), Pages 4864-4876

Zusammenfassung

Testikuläre Keimzelltumoren (TGCTs) sind urologische Malignitäten, die vor allem junge weiße Männer in westlichen Ländern betreffen, typischerweise im Alter von 15 bis 44 Jahren. Obwohl TGCTs insgesamt relativ selten sind und als die 29. häufigste Krebsart gelten, unterstreicht ihre zunehmende Inzidenz und ihre Auswirkungen auf junge Männer ihre Bedeutung, insbesondere im Hinblick auf die potenziellen langfristigen Folgen der Chemotherapie.

CD24, ist ein Membranprotein, das an verschiedenen zellulären Prozessen wie Migration, Invasion, Proliferation und Metastasierung beteiligt ist. In dieser Studie untersuchten wir die Rolle von CD24 bei der Beeinflussung der Empfindlichkeit gegenüber verschiedenen Medikamenten sowie dessen Interaktion mit anderen Proteinen in embryonalen Karzinomen (EC) und anderen urologischen Krebserkrankungen wie dem Urothelkarzinom (UC), dem Nierenzellkarzinom (RCC) und dem Prostatakarzinom (PC). Darüber hinaus erforschten wir das Potenzial von CD24 als Ziel für Immuntherapie in diesen Krebserkrankungen.

Um den Einfluss von CD24 auf die Therapieantwort zu bewerten, verwendeten wir CD24-Knockout-Zellen (Δ*CD24*), die mit verschiedenen Medikamenten behandelt wurden, und maßen die Zellüberlebensfähigkeit mithilfe von XTT-Zellviabilitätstests. Anschließend identifizierten wir Interaktionspartner von CD24 durch Co-Immunopräzipitationen gefolgt von Flüssigchromatographie-Massenspektrometrie (LC-MS). Darüber hinaus untersuchten wir die Wirksamkeit der Behandlung von EC-Zelllinien mit natürlichen Killerzellen, die mit einem chimären Antigenrezeptor gegen CD24 ausgestattet waren (NK-CAR-CD24), und bewerteten das Zellüberleben erneut durch XTT-Zellviabilitätstests.

Unsere Ergebnisse zeigten keinen signifikanten Unterschied im Überleben zwischen Δ*CD24*-Zellen und Wildtyp-Zellen bei der Medikamententestung. Obwohl die identifizierten Interaktionspartner von CD24 zwischen EC-Zellen und pan-urologischen Zellen variierten, waren diese jedoch an ähnlichen biologischen Prozessen wie Proteinbindung, Transport und posttranslationalen Modifikationen beteiligt. Zusätzlich zeigte die Behandlung mit NK-CAR-CD24 vielversprechende Wirksamkeit und Spezifität bei der gezielten Bekämpfung von $CD24^+$ Zellen in EC.

Zusammenfassend trägt unsere Studie dazu bei, die Rolle von CD24 bei urologischen Krebserkrankungen zu verstehen und sein Potenzial als therapeutisches Ziel, insbesondere im Kontext der Immuntherapie, hervorzuheben. Weitere Forschungen in diesem Bereich versprechen, die Behandlungsmöglichkeiten für Patienten mit TGCTs, insbesondere rezidivierenden TGCTs, sowie anderen urologischen Malignitäten zu verbessern.

Summary

Testicular germ cell tumors (TGCTs) are urological malignancies primarily affecting young white men in Western countries, typically between the ages of 15 and 44. While TGCTs are relatively rare overall, ranking as the 29th most common cancer, their increasing incidence and impact on young men underscore their significance, particularly considering the potential long-term consequences of chemotherapy.

One intriguing target in TGCTs is CD24, a membrane protein implicated in various cellular processes such as migration, invasion, proliferation, and metastasis. In this study, we investigated the role of CD24 in influencing sensitivity to different drugs, its suitability as a immunotherapeutic target, and its interaction with other proteins in embryonal carcinomas (EC) and other urological cancers including urothelial carcinoma (UC), renal cell carcinoma (RCC), and prostate carcinoma (PC). Our main aim is to overcome cisplatin resistance and introduce novel therapeutic avenues.

To assess the impact of CD24 on therapy response, we utilized CD24-knockout cells (ΔCD24) treated with various drugs and measured cell survival using XTT cell viability assays. Subsequently, we identified interaction partners of CD24 through Co-Immunoprecipitation followed by liquid mass chromatography-mass spectrometry (LC-MS). Furthermore, we investigated the efficacy of treating EC cell lines with natural killer cells equipped with a chimeric antigen receptor against CD24 (NK-CAR-CD24), evaluating cell survival through XTT cell viability assays.

Our results revealed no significant difference in survival between ΔCD24 cells and wild-type cells in drug testing. While the identified interaction partners of CD24 varied between EC cells and pan-urological cells, both sets were enriched for proteins involved in similar biological processes such as protein binding, transport, and post-translational modifications. Additionally, treatment with NK-CAR-CD24 showed promising efficacy and specificity in targeting CD24+ cells in EC.

Despite CD24 not affecting drug response in ECs, it remains an intriguing target for further investigation. Our findings shed light on the molecular functions of CD24 and its role in cellular differentiation. Additionally, treatment with NK-CAR-CD24 showed promising efficacy and specificity in targeting CD24+ cells in EC, warranting further exploration in other cell lines and potentially in vivo studies.

In conclusion, our study contributes to understanding the role of CD24 in urological cancers and highlights its potential as a therapeutic target, particularly in the context of immune therapy. Further research in this area holds promise for advancing treatment options and improving outcomes for patients with TGCTs, especially relapsing TGCTs and other urological malignancies.

List of Abbreviations

Abbreviation	Name
°C	degree celsius
µl	microliter
µm	micrometer
µM	micromolar
4-1BB / CD137	tumor necrosis factor ligand superfamily member 9
ADC	antibody-drug conjugate
ADCC	antibody-dependent cellular toxicity
Akt	protein kinase B
ALL	acute lymphatic leukemia
APS	ammonium peroxydisulfate
ARF	ADP-ribosylation factor
ATM	Ataxia-telangiectasia, mutated
BAP1	BRCA1 associated portein-1
BCA	bicinchoninic acid
Bcl-2	B-cell lymphoma 2
BCG	Bacillus Calmette-Guérin
BRAF	proto-oncogene B-RAF
BRCA	breast cancer susceptibility gene 1
BSA	bovine serum albumin
CAR	chimeric antigen receptor
CC	choriocarcinoma
CCNB	human cyclin B
ccRCC	clear cell renal carcinoma
CD133	cluster of differentiation 133
CD171	cluster of differentiation 171
CD19	cluster of differentiation 19

Abbreviation	Name
CD24	cluster of differentiation 24
$CD24^-$	CD24 negative
$CD24^+$	CD24 positive
CD28	cluster of differentiation 28
CD3ζ	cluster of differentiation 3ζ
CD44	cluster of differentiation 44
CD8α	cluster of differentiation 8α
CDKN2A	cyclin-dependent kinase inhibitor 2A
CKAP4	cytoskeleton-associated protein 4
Co-IP	co-immunoprecipitation
Cond	condition
cRCC	chromophobe renal cell carcinoma
CRISPR/CAS9	cluster of differentiation 9
CSC	cancer stem cell
CTLA-4 / CD152	cytotoxic T-lymphocyte - associated protein 4
CXCR4	c-x-c chemokine receptor type 4
DAMP	danger-associated molecular pattern
DMEM	Dulbecco's Modified Eagle Medium
DMF	dimethylformamide
DMSO	dimethyl sulfoxide
DNA	deoxyribonucleic acid
DNAM-1 / CD226	DNAX accessory molecule-1
DNAX	
DRM	detergent-resistant membrane

Abbreviation	Name
E/T	effector/target
EC	embryonal carcinoma
EDTA	ethylenediaminetetraacetic acid
EGFR	epidermal growth factor
EMA	European Medicines Agency
ERK	extracellular signal-regulated kinases
ETC	electron transport chain
FC	fold change
FCS	fetal calf serum
FDA	Food and Drug Administration
FITC	fluorescein isothiocyanate
FOXA1	forkhead box protein 1
GCNIS	germ cell neoplasia in situ
GCTs	germ cell tumors
GDF3	growth differentiation factor-3
GEM	glycolipid enriched membrane
GPI	glycosylphosphatidylinositol
GSK3β	glycogen synthase kinase-3 beta
GSTM1	glutathione S-transferase mu 1
GTP	guanosine-5'-triphosphate
h	hour
HCC	hepatocellular carcinoma
HMGB1	high mobility group box 1
HNSCC	head and neck squamous cell carcinoma
HOXB13	homeobox protein hox-B13
HSA	heat stable antigen

Abbreviation	Name
HSP	heat shock protein
IFN	interferon
IgG	immunoglobulin G
IL2	interleukin 2
ISUP	International Society of Urological Pathology
ITAM	immunoreceptor tyrosine-based activation motif
kDa	kilo Dalton
KDM5C	lysine (K)-specific demethylase 5C
KIR	killer Ig-like receptor
L1CAM	L1 cell adhesion molecule
LC-MS	liquid chromatography-mass spectrometry
LD50	median lethal dose
Lu-PSMA	lutetium 177 prostate-specific membrane antigen
M	molar
mAB	monoclonal antibody
MAPK	mitogen-activated protein kinase
MEM	minimum essential media
MET	mesenchymal-epithelial transition
MIBC	muscle-invasive bladder carcinoma
MICA	human major histocompatibility complex class 1 chain-related gene A
MICB	human major histocompatibility complex class 1 chain-related gene B
min	minute
ml	milliliter
mM	millimolar
mm^2	square millimeter

Abbreviation	Name
MMP2	matrix metalloproteinase 2
mRNA	messenger ribonucleic acid
MS	mass spectrometry
mTOR	mammalian target of rapamycin
MVAC	Methotrexate, Vinblastine, Adriamycin, Cisplatin
MYO1C	myosin 1 C
N/A	not available
NAT2	N-acetyltransferase 2
NCR	natural cytotoxicity receptor
NEAA	non-essential amino acid
NK-cell	natural killer cell
NK-92-CD24-CAR	natural killer cell with a chimeric antigen receptor against CD24
NKG2D / CD 159	receptor for natural killer cells
nM	nanomolar
NMIBC	non-muscle-invasive bladder cancer
NPM	nucleophosmin
OV	oncological virus
PAMP	pathogen-associated molecular pattern
PARP	poly (ADP-ribose) polymerase
PBRM1	polybromo 1
PBS	phosphate-buffered saline
PBS-T	phosphate-buffered saline and tween
PC	prostate cancer
PD-L1 / PD-1	programmed death ligand 1
Pen	penicillin
pg	picogram
PGC	primordial germ cell

Abbreviation	Name
PI	propidium iodide
PI3K	phosphoinositide 3-kinase
PIP2	phosphatidylinositol 4,5-biphosphate
PMSF	phenylmethylsulphonyl fluoride
pRCC	papillary renal cell carcinoma
PROM1 / CD133	prominin 1
PSA	prostate-specific antigen
PTEN	phosphate and tensin homolog deleted on chromosome ten
PTK	protein-tyrosine kinases
PVDF	polyvinylidene
qRT-PCR	quantitative reverse transcription polymerase chain reaction
-R	resistant
RalA	ras related protein A
RalB	ras related protein B
RCC	renal cell carcinoma
RNA	ribonucleic acid
Rpm	rounds per minute
RPMI	Roswell Park Memorial Institute
scFv	small chain variable fragment
SCID	severe combined immunodeficiency
SDS	sodium dodecyl sulfate
SETD2	SET domain containing 2
Siglec	sialic acid-binding immunoglobulin-type lectins
SOX2	sex-determining region Y-box 2
STAT3	signal transducer and activator of transcription 3
Strep	streptomycin

Abbreviation	Name
Syk	tyrosine-protein kinase SYK
TAA	tumor-associated antigen
TCGA	The Cancer Genome Atlas
TEMED	tetramethylethylenediamine
TFE3	transcription factor E3
TGCT	testicular germ cell tumor
TMD	transmembrane domain
TMPRSS2	transmembrane protease, serin 2
TMPRSS2-ERG	transmembrane protease serin 2- ETS-related gene fusion protein
TNFα	tumor necrosis factor-alpha
TP53	tumor suppressor gene 53
UC	urothelial carcinoma
US	United States of America
VHL	Von Hippel Lindau
WT	wild type
XTT	2,3-bis-(2-methoxy-4-nitro-5-sulfophenyl)-2H-tetrazolium-5-carboxanilide
YST	yolk sac tumor
ZAP70	zeta-chain-associated protein kinase 70
Δ*CD24*	CD24-deficient

Table of contents

Table of Figures

Table of tables

1 Introduction

Cancer continues to be one of the most relevant worldwide health risks and to this day still is the second most prevalent cause of death in Germany (Todesursachen in Deutschland 2023 - Statistisches Bundesamt). Urological malignancies such as testicular germ cell tumors (TGCT), and urothelial-, prostate- and renal cell cancers (UC, PC, RCC) remain a large part of this problem, especially in men. In the US alone over 7 million patient years were lost due to urological malignancies with TGCTs followed by PC being the main contributor (Kamel et al., 2012). This shows the relevance of urological malignancies and the need for further investigation into novel treatment options and tumor biology.

1.1 Impact of urological malignancies

TGCTs are urological malignancies that occur mainly in young white men in Western countries between the ages of 15 and 44. Overall TGCTs are relatively rare, being the 29th most common cancer, but an ongoing increase in incidence and their occurrence in young men mark them as highly relevant targets for study (Sung et al., 2021).

TGCTs can be separated into three different types, the most relevant being the type II-TGCT with a proportion of 95 % of total cases. Type I TGCTs are tumors occurring in children and arise from primordial germ cells (PGCs). They can be divided into prepubertal- teratoma and yolk-sac tumors (YST). Type III TGCTs are called spermatocytic seminoma and are generated through clonal expansion of the spermatogonium and are found outside the usual age spectrum in elderly men over 50 years of age. In contrast to type I and type III TGCTs, type II TGCTs evolve from a precursor lesion called germ cell neoplasia in situ (GCNIS). GCNIS eventually develops into seminoma (SE) or non-seminoma, where the non-seminoma can be further divided into a stem cell-like population the embryonal carcinoma (EC) which then further differentiate into teratoma (TE), YST, and choriocarcinoma (CC). TGCTs are tumors that respond to treatment well. First-line therapy for non-metastasized TGCTs is orchiectomy followed by, depending on the staging, chemo- or radiotherapy resulting in curation rates of 99 % (Cheng et al., 2018; Rajpert-De Meyts et al., 2016). The prognosis for metastatic tumors is far worse with 5-year survival rates of 90 %, 80 %, and 50 % depending on good, intermediate, or poor prognosis, respectively (Rajpert-De Meyts et al., 2016). Furthermore, relapse after first-line treatment occurs in 15-30 % of patients and can be associated with cisplatin resistance leading to poor survival rates caused by a lack of cisplatin alternatives (Albers et al., 2015). Cisplatin-based treatment also leads to a variety of adverse health outcomes like hearing impairment and tinnitus, peripheral neuropathy, Raynaud syndrome, cardiovascular disease, erectile dysfunction,

hypogonadism, depression, and more, while also raising the occurrence rate of secondary malignancies (Fung et al., 2017).

PC remains the most common tumor diagnosis in men and is still the fifth most common cause of death by cancer in Germany with 15072 deaths in 2021 which translates to 6.6 % of all cancer-related deaths (Todesursachen in Deutschland - Statistisches Bundesamt). PC can be classified into prognostic categories of low-risk, intermediate-risk, and high-risk tumors according to a combination of clinical tumor node metastasis (TNM) classification, Gleason- or International Society of Urological Pathology (ISUP) score, which is based on histological tumor architecture, and prostate-specific antigen (PSA) value (Mottet et al., 2021). Risk factors for PC include a family history of PC, germline mutations in genes like *BRCA1*, *BRCA2*, *ATM*, mismatch repair genes and single nucleotide polymorphisms (Rebello et al., 2021). Of these mutations, *BRCA2* and *HOXB13* lead to the highest risk of developing PC and they are predominantly involved in regulating cell growth, proliferation, apoptosis, and DNA damage repair (Bancroft et al., 2014; Karlsson et al., 2014). An important driver of tumorigenesis in non-metastatic PC is the fusion of transmembrane protease serine 2 (TMPRSS2) with electron transport chain (ETC) related gene and gain of function of FOXA1. In metastatic cancer, amplifications or gain of function of androgen receptor regulation genes or inactivation of androgen receptor repressing genes is seen most frequently (Rebello et al., 2021). Therapy depends highly on tumor stage and reaches from active surveillance to radical prostatectomy and ablative radiotherapy as curative options, which lead to good 10-year survival rates of 99 % in low to intermediate-risk cases (Rebello et al., 2021). High-risk and metastasized, as well as relapsing disease, show worse survival rates but can be treated with androgen deprivation therapy and depending on previous procedures and staging salvage-radiotherapy, chemotherapy, or radical prostatectomy. Even castration-resistant prostate carcinoma can be further treated via intensified androgen deprivation therapy, chemotherapy, and immunotherapy (Sipuleucel-T, PARP inhibitors) or more novel radionuclide (Radium-223)- and radiopharmaceutical (^{177}Lu-PSMA) therapy (Rebello et al., 2021). Nevertheless, all treatments for PC have side effects like erectile dysfunction, urinary incontinence, depression, cognitive impairment, loss of muscle mass, osteoporosis, impotence, and loss of libido, and classic chemotherapy-associated side-effects (Rebello et al., 2021). In summary, its high frequency and tendency to become hormone-resistant after some time justify intensive further research into novel treatment options for PC.

RCC is the most common malignant kidney disease and kidney cancer overall account for 3-5 % (including UC of the kidney) of all adult malignancies (Escudier et al., 2019). Risk factors for RCC include smoking, obesity, hypertension chronic kidney diseases, and a small part (3 %) are hereditary and associated with syndromes like von Hippel-Lindau. RCC can be divided into the most common clear cell RCC (ccRCC) and non-clear cell RCC which mostly consist of papillary RCC (pRCC) and chromophobe RCC (cRCC). Genetic mutations in ccRCC mainly appear in *VHL,* the earliest and

driving mutation, *PBRM1*, *SETD2*, *BAP1*, *KDM5C,* and *MTOR* genes while chromophobic RCC shows mutations in tumor suppressor gene 53 (*TP53*) and targets along the mTOR and PTEN pathways (Escudier et al., 2019; Hsieh et al., 2017). Papillary RCC can be divided into group 1 with *MET* or *EGFR* mutations and group 2 with *SETD2*, *CDKN2A,* and *TFE3* mutations or fusion (Escudier et al., 2019). Treatment for localized T1 tumors consists of partial or radical nephrectomy with 5-year disease-specific survival of 91.1 % in low-risk tumors and 80.4 % in intermediate-risk tumors (Escudier et al., 2019). More advanced local or metastatic ccRCC are treated with radical nephrectomy and cytoreductive surgery, immune checkpoint-, tyrosine kinase- and mTOR-inhibitors (Gkolfinopoulos et al., 2021; Hah & Koo, 2021). In contrast, non-ccRCC shows no evidence of response to immune checkpoint inhibitors, and clear treatment regimens remain to be found. This leads to an overall worse prognosis (Hsieh et al., 2017). Overall, the lack of early symptoms of RCC and their chemotherapy and radiation resistance led to many novel therapies being used in the treatment of RCC. Still, prognosis in advanced or metastasized cases remains poor and shows the need for novel therapies or improvements of existing ones.

Bladder cancer is the 12th most common cancer diagnosis worldwide and develops from the urothelial cells (Sung et al., 2021). Risk factors for bladder cancer can be genetic like single nucleotide polymorphisms in the genes slow acetylator N-acetyltransferase 2 (*NAT2*) or glutathione S-transferase mu 1 (*GSTM1*)-null leading to more carcinogen exposure, or they can be acquired like the two most important risk factors of tobacco smoking and occupational exposure to carcinogens like aromatic amines (Burger et al., 2013). UC can be separated into two prognostic groups: non-muscle-invasive bladder cancer (NMBIC) with good prognosis which makes up 80 % of the cases and muscle-invasive bladder cancer (MIBC) which makes up 20 % of cases and has comparatively poorer prognosis. NMBIC can be separated into three different subgroups, class 1 with luminal-like signatures, class 2 with luminal-like, epithelial-mesenchymal transition and cancer stem cell signatures, and class 3 with basal-like signatures, with class 2 having the worst prognosis. (Tran et al., 2020). MIBC can be further divided into six molecular subgroups which present different prognoses and clinical characteristics. These subgroups are luminal papillary, luminal non-specified, luminal unstable, stroma-rich, basal/squamous, and neuroendocrine-like bladder cancer (Kamoun et al., 2020; Tran et al., 2020). Luminal class overexpressed urothelial differentiation signatures, basal/squamous overexpressed basal differentiation signatures, and neuroendocrine-like neuroendocrine differentiation signatures (Kamoun et al., 2020). Therapy for NMBIC tumors consists of local resection and bladder instillation treatment with Mitomycin C or Bacillus Calmette-Guérin (BCG) solutions. Advanced MIBC can only be treated with radical cystectomy followed by or preceded by cisplatin-based chemotherapy in the form of Gemcitabine and Cisplatin or MVAC (Methotrexate, Vinblastine Silfate, Adriamycin, Cisplatin) although sensitivity to cisplatin varies between tumors and subgroups (Tran et al., 2020). Treatment of metastatic bladder cancer has seen vast advancements in the last decade with treatments based on antibody-drug conjugates like

Enfortumab-Vedotin and checkpoint inhibitors showing better results in overall survival than the previous standard treatments with cisplatin-based therapy ("EAU Guidelines. Edn. Presented at the EAU Annual Congress Paris 2024," 2024; Hoimes et al., 2023; O'Donnell et al., 2023). This even led to those treatments being introduced as first-line therapy. These novel developments show that there is still far more room for improvement in the treatment of MIBC using novel and more targeted therapeutics. (Patel et al., 2020; Tran et al., 2020)).

1.2 CD24: a membrane-bound tumor-associated signaling protein

Cluster of differentiation (CD)24 is a membrane-bound signaling protein first described in 1991 in human cells as an ortholog to mouse heat stable antigen (HSA), which plays a role in the maturation of hematopoietic cells in mice (Altevogt et al., 2021; Kay et al., 1991). In humans, CD24 is of special interest due to its role as a regulator of autoimmunity and its involvement in the regulation of cell migration, invasion, and proliferation in tumor cells (Fang et al., 2010; Kristiansen et al., 2004)).

CD24 is physiologically present in B-cells (Israel et al., 2005), T-cells (Hubbe & Altevogt, 1994; O. Li et al., 2004), neutrophilic granulocytes (Elghetany & Patel, 2002), developing neurons (Shewan et al., 1996), muscle fibers (Higuchi et al., 1999), keratinocytes (Magnaldo & Barrandon, 1996), pancreas (Cram et al., 1999) and prostate tissues (Lawson et al., 2007) and is generally expressed in cells with progenitor and metabolically active traits (Fang et al., 2010). The protein itself is very small with a protein core of 31-34 amino acids and a glycosylphosphatidylinositol(GPI)-anchor connects CD24 to the cell membrane. Nevertheless, CD24 shows extensive *N*- and *O*-glycosylation with 14-16 described O- and 2 N-glycosylation sites which resemble cell surface mucin (Altevogt et al., 2021; X. Li et al., 2022). This glycosylation leads to CD24 being a highly variable protein with molecular weights ranging between 20 kDa and 70 kDa depending on cell type and tissue (Fang et al., 2010).

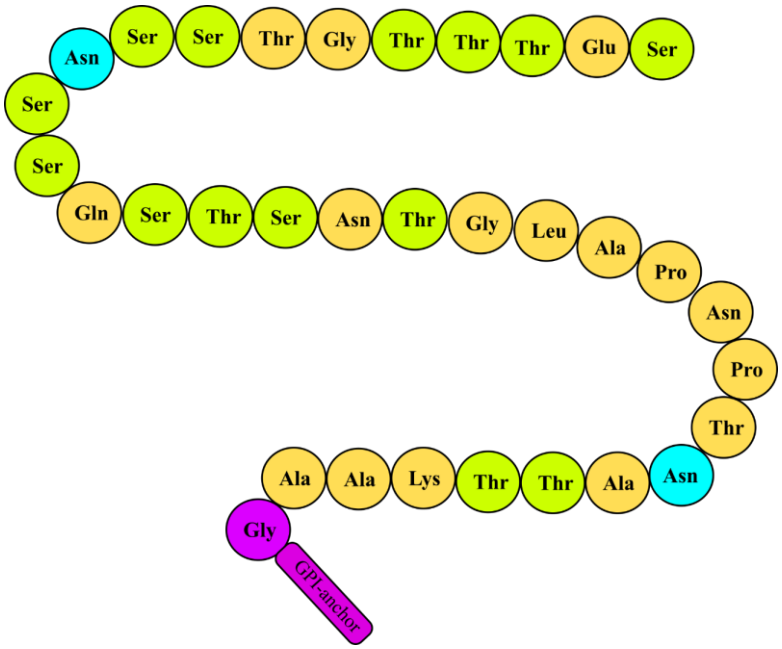

Fig. 1: CD24 structure and possible glycosylation
CD24 protein structure, amino acid sequence (3 letter code), possible glycosylation sites (green: O-glycosylation site, blue: N-glycosylation site, yellow: no glycosylation) and Glycosylphosphatidylinositol-anchor (GPI-anchor: purple). Figure modified from Eyvazi et al. (Eyvazi et al., 2018).

Even though CD24 does not have an intracellular domain it still functions as a signal molecule (Fisher et al., 1990). This is achieved via the GPI-anchor in a glycolipid-enriched membrane (GEM) / detergent-resistant membrane domain (DRM) also called lipid raft, which acts as a signal transduction platform through its enrichment with signal transducing molecules like Src family protein tyrosine kinases (PTKs), G proteins and Ras (Štefanová et al., 1991; Suzuki et al., 2001; Zarn et al., 1996). CD24 expression also seems to influence the composition of proteins in the lipid raft as the presence of CD24 excluded CXCR4 from lipid rafts and in different experiments showed recruitment of β1-integrin (Runz et al., 2008; Schabath et al., 2006).

In attempts to further understand CD24's function, several binding partners of CD24 have been identified. L1CAM (CD171) interacts with CD24 in the mouse brain and inhibits neurite outgrowth of dorsal root ganglion neurons, while it promotes neurite outgrowth of cerebellar neurons and alters L1CAM signaling. This process is dependent on α2,3-linked sialic acid residues present in some CD24 glycoforms (Kadmon et al., 1995; Kleene et al., 2001). Furthermore, CD24 seems to be a ligand of selectins in mouse and human cells and tumor cells, specifically P-selectin and E-selectin (Aigner et al., 1995, 1997; Myung et al., 2011). This enables the rolling of tumor cells on endothelial cells, cell adhesion and might enhance metastatic spread of tumor cells (Aigner et al., 1998; Friederichs et al., 2000; Myung et al., 2011). Another type of general interaction partner of CD24 are sialic acid-binding immunoglobulin (Ig)-like nectins also known as Siglecs. Specifically,

experiments in mice showed CD24 to form a trimolecular complex with Siglec-10 and HMGB1, which plays an important role in dampening immune response to danger-associated molecular patterns (DAMPs) and helps differentiate between DAMPs and pathogen-associated molecular patterns (PAMPs) (G. Y. Chen et al., 2009). Other associated DAMPs included heat shock protein (HSP)70, HSP90, and Nucleolin. Glycosylation of CD24 also seems to influence which type of Siglec it can interact with. For example, CD24 derived from human tumor cell lines binds to Siglec-5, and CD24 from human placenta binds to Siglec-10. (Kristiansen et al., 2010; Sammar et al., 2017).

In addition to the often-investigated membrane-bound fraction of CD24, more research indicates that cytosolic CD24 might also play a major role in tumorigenesis and can be a marker of poor prognosis (Duex et al., 2017). Weichert et al (Weichert et al., 2005) showed cytoplasmatic CD24 to correlate with shortened patient survival and an investigation by Wang et al showed cytoplasmatic and nuclear fractions of CD24 to be sufficient for tumor cell proliferation in PC. Wang et al (L. Wang et al., 2015) investigated three PC cell lines PC-3, DU-145, LNCaP, and showed mRNA expression in line with previous results of our research. PC-3 and DU-145 were $CD24^+$ and LNCaP was $CD24^-$, but only DU-145 expressed CD24 on the cell surface. Interestingly this did not diminish the growth reduction upon CD24 silencing. They found this effect to be caused by competitive inhibition of ARF binding to NPM by intracellular CD24, which downstream led to a decrease of TP53 tumor suppressor and tumor progression in DU-145 cells. Intracellular CD24 also seems to play a role in drug resistance acquisition in breast cancer as shown by Huth et al. (Huth et al., 2021). Upon drug treatment cytosolic CD24 translocated to the cell membrane leading to a phenotypic change with phosphorylation of p38 MAPK and overexpression of Bcl-2 which slowed down the cell cycle. These studies show that research into intracellular CD24 has much potential and is required to further solidify CD24s role in tumorigenesis and as a target for therapy.

CD24 is highly expressed in a variety of tumor types like non-Hodgkin B cell lymphoma and leukemia, neurological malignancies (Senner et al., 1999), RCC (Droz et al., 1990)(Droz et al., 1990), ovarian cancer (Kristiansen et al., 2002), breast cancer (Kristiansen, Winzer, et al., 2003; Sorbello et al., 2003), lung cancer (Jackson et al., 1992; Kristiansen, Schlüns, et al., 2003), PC (Kristiansen et al., 2004; A. Y. Liu & True, 2002), pancreatic cancer (Kristiansen et al., 2004), hepatocellular carcinoma (L. R. Huang & Hsu, 1995) and cancers of the gastrointestinal tract (Sagiv & Arber, 2008). This is most likely a result of its immune evasive, proliferation enhancing and tumor invasion enhancing properties (Fig. 2) (Barkal et al., 2019; Baumann et al., 2005; Smith et al., 2006). These effects do not seem to be limited to surface CD24 but are also found in cells with nuclear fractions of CD24 (Duex et al., 2017). These properties are most often found in tumors with poor prognosis and lead to CD24 being a marker of malignancy and poor prognosis (Duex et al., 2017; Lee et al., 2009; P. Zhang et al., 2019).

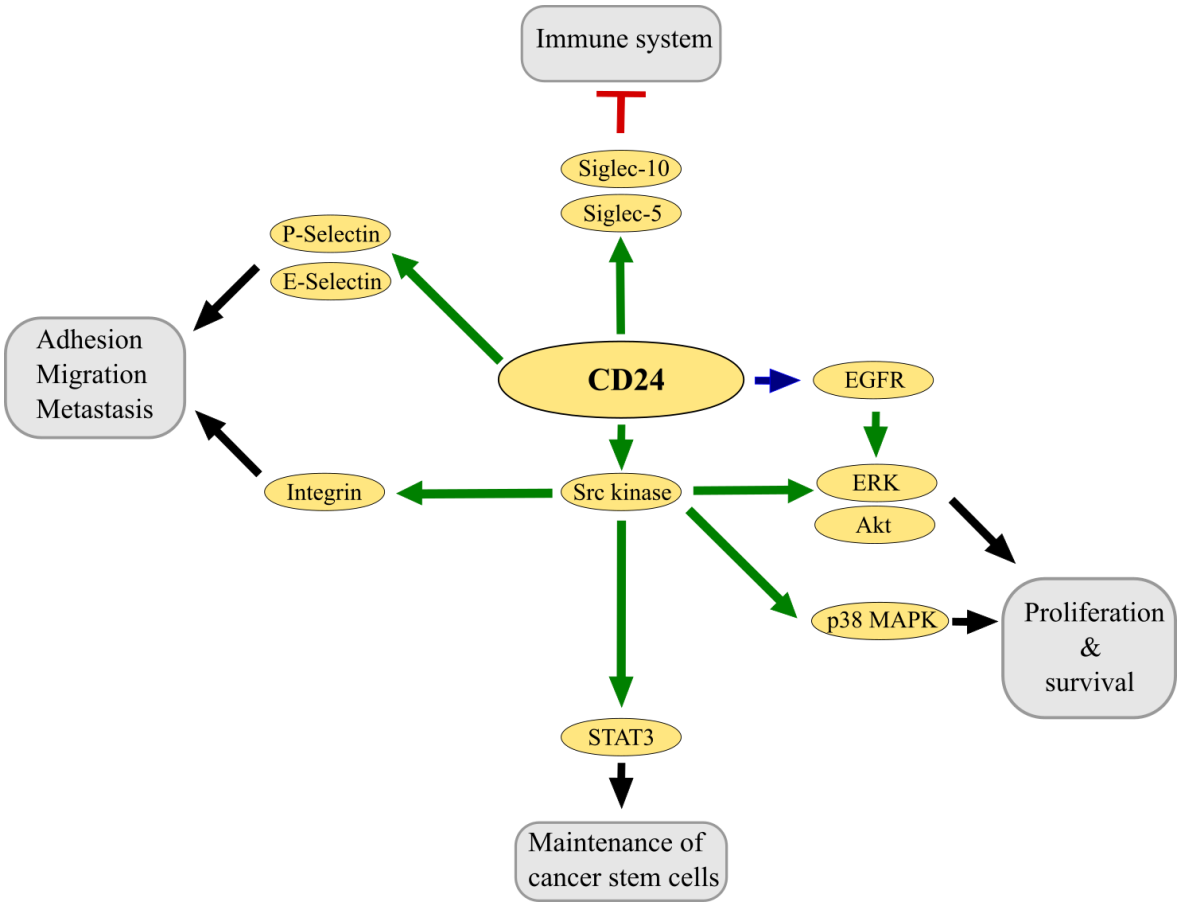

Fig. 2: Summary of CD24 signaling and biological function
CD24 is involved in a variety of different biological processes. Direct interaction of CD24 with Siglecs and Selectins lead to immune evasion and adhesion, migration, and invasion. Indirect upregulation of EGFR and signaling through Src kinase activate the ERK/Akt/MAPK pathways and lead to cell proliferation and tumor survival. Signaling via Src kinases also interacts with integrins to influence adhesion, migration, and metastasis, and activation of STAT3 pathways lead to the maintenance of cancer stem cells. These processes are not found in every $CD24^{+}$ tissue, as glycosylation and therefore interaction vary highly. Green arrow: interaction/induction. Blue arrow: indirect upregulation. Black arrow: induction of resulting process. Red "T": inhibition

The human *CD24* gene is found on chromosome 6q21 and three intronless pseudogenes are found on chromosomes 15q21, 15qq22 and Yq11 (Hough et al., 1994). Additionally, two homologs exist and were mapped to chromosome 1p36 and chromosome 20 (Hough et al., 1994). Genetic polymorphisms of *CD24* were identified and play a part in immune response modification (Jiang et al., 2015; L. Wang et al., 2007) it was thus investigated if they play a role in cancer incidence and progression, but results remain ambiguous (Marmé et al., 2012; Yan et al., 2014; Zhou, 2014).

Genetic regulation of *CD24* expression seems to be a highly variable mechanism depending on the type of tissue or cell. Firstly, expression seems to be regulated by gonadocorticoids, as androgen treatment in UC led to increased promotor activity (Overdevest et al., 2012) and estrogen downregulated *CD24* in breast cancer (Kaipparettu et al., 2008). Secondly, a variety of factors

regulated *CD24* expression in different tumor entities. As such, Twist suppressed CD24 in breast cancer (Vesuna et al., 2009), truncated glioma-associated oncology homolog 1 upregulated *CD24* gene expression (Cao et al., 2012), and SOX2 transactivated *CD24* in melanoma and TGCTs (Hüser et al., 2018; Skowron et al., 2022). Thirdly, *CD24* is epigenetically regulated in breast cancer and TGCTs and responds to epidrug treatment (Kwon et al., 2015; Skowron et al., 2022).

1.2.1 CD24 in TGCT

A recent study sheds new light on the function, gene regulation, and therapy potential of CD24 in TGCTs. CD24 is often used as a marker for cancer stem cell (CSC) populations (C. Li et al., 2007; H. Liu et al., 2016; M. Wang et al., 2011; Yeung et al., 2010; C. Zhang et al., 2011; J. Zhang et al., 2019) except in breast cancer where the CSCs seem to be $CD44^{+}/CD24^{-}$ (Al-Hajj et al., 2003). Skowron et al. showed this to be true for TGCTs as well and *CD24* was especially upregulated in ECs, which show similarities to embryonal pluripotent stem cells. They also showed *CD24* expression to be correlated with the expression of other stem cell markers like *GDF3*, *CD44,* and *CD133/PROM1* and that it was involved in cellular differentiation processes like blocking mesodermal and endodermal differentiation while pushing EC cells toward ectodermal differentiation (Skowron et al., 2022). Regarding the relevance of CD24 in potential future treatments of TGCTs Skowron et al. showed an increase in sensitivity to cisplatin-based chemotherapy in combination with anti-CD24-mAB which marks CD24 as a target for further investigation in TGCTs (Skowron et al., 2022).

1.3 CD24-based treatment and immunotherapy

The exact functions and interactions of CD24 still remain to be sufficiently explored. Nevertheless, its known role as an antiphagocytic surface protein that works as a “don’t eat me" signal similar to PD-L1, its involvement in cell proliferation and migration and its high expression in a variety of tumor entities mark it as an interesting cancer target (Altevogt et al., 2021; Barkal et al., 2019). The long-term goal will be to test CD24s potential as a target for therapy by using antibodies, antibody–drug conjugates, or cell-based immune therapy.

1.3.1 Immunotherapy

In the last one and a half centuries, cancer treatment has made huge advances from the first use of radiation to treat cancer in 1899, the discovery of the first antimetabolites in 1947, the approval of the first antibody treatment in 1997, cancer vaccine discovery like sipaleucel-T, to cell-based therapy with chimeric antigen receptor (CAR) T-cells (*Milestones in Cancer Research and Discovery - NCI*,

n.d.). Successes in treatment with classical chemotherapy stand in contrast to severe side effects due to off-target effects, long-term chemotherapy-associated damages, relapses, and resistances. For this reason and cancers worldwide relevance with almost 10 million deaths per year (Sung et al., 2021) interest in the development of novel treatments with better effectiveness and fewer side- and off-target effects remains high (Schirrmacher, 2019). The goal of further development will be to not only increase effectiveness but to prolong patient survival with increased quality of life and fewer side effects.

Most of the novel treatment discoveries in the last century were based on new insights into molecular biology, virology, and immune biology. One of those discoveries was a higher rate of cancer in people with autoimmune diseases and patients undergoing immunosuppressive treatment (Gutierrez-Dalmau & Campistol, 2007; Reid et al., 2018), another was the discovery of a variety of immune escape strategies tumors use to evade the immune system leading to the conclusion that the immune system and cancer development are tightly connected. These mechanisms include processes like antigenic variation, antigen shedding, secretion of immunosuppressive molecules, or evading T-cell immune response via programmed cell death protein-1 (PD-1) or cytotoxic T-lymphocyte-associated protein 4 (CTLA-4) (Khong & Restifo, 2002). Immunotherapy focuses not on the direct treatment of tumors but aims at activating the immune system of the host to deal with the tumor, which is often a more physiological and tolerated process (Schirrmacher, 2019). These therapies can be separated into small molecule inhibitors, monoclonal antibodies (mAB), oncolytic viruses (OV), tumor vaccines, and cell-based therapies like CAR-carrying T- or NK-cells. In recent years, especially mABs against immune checkpoint inhibitors have integrated themselves into clinical practice even as first-line therapies.

In recent years advances in the field of cell-based therapies utilizing CAR-T and CAR-NK cell therapies have delivered promising results. CARs are synthetic receptors carrying a single chain variable fragment (scFv) which enables immune cells to target a tumor-associated antigen (TAA). This scFv is contained in the ectodomain, a spacer or hinge region that connects the scFv to the transmembrane domain and is in most cases CD8α, CD28, or immunoglobulin G (IgG) based. Next up is the transmembrane domain (TMD) linking the CAR to the intracellular signaling domains, the most used TMD are adapted from CD3ζ, CD8, and CD28. Last up is the activation domain, where the amount of intracellular activation signals determines the CAR “generation” (Fig. 3), with the CD3ζ signal and costimulatory molecules from the CD28 family, tumor necrosis factor receptor, or signaling lymphocytic activation molecule (Y. Gong et al., 2021). Almost all first-generation CAR use the CD3ζ domain, most second-generation CAR add either a 4-1BB (CD137) or CD28 and third-generation CAR usually combine CD3ζ, 4-1BB, and CD28. There are even CARs including cytokines labeled as fourth-generation CARs (Y. Gong et al., 2021), and possible to add safety switches to the stimulatory domains which can swiftly eliminate the cells upon adverse reactions (Di

Stasi et al., 2011). A CAR-T cell configuration using the CD3ζ chain signaling domain generates three immunoreceptor tyrosine-based activation motifs (ITAMs), recruiting and activating Syk or ZAP70 tyrosine kinase or PI3-kinase (Y. Gong et al., 2021). Considering CAR-NK cells use similar domains similar signaling is suspected, but first studies show that NK-specific domains might lead to greater cytotoxicity (Y. Gong et al., 2021; Y. Huang et al., 2020; Xu et al., 2019). Overall, a perfect CAR configuration remains to be found and as different stimulatory domains lead to different levels of cytotoxicity, toxicity survival, proliferation, cytokine production, and longevity there might not be a universal CAR, but disease-specific CARs will have to be found (Sterner & Sterner, 2021).

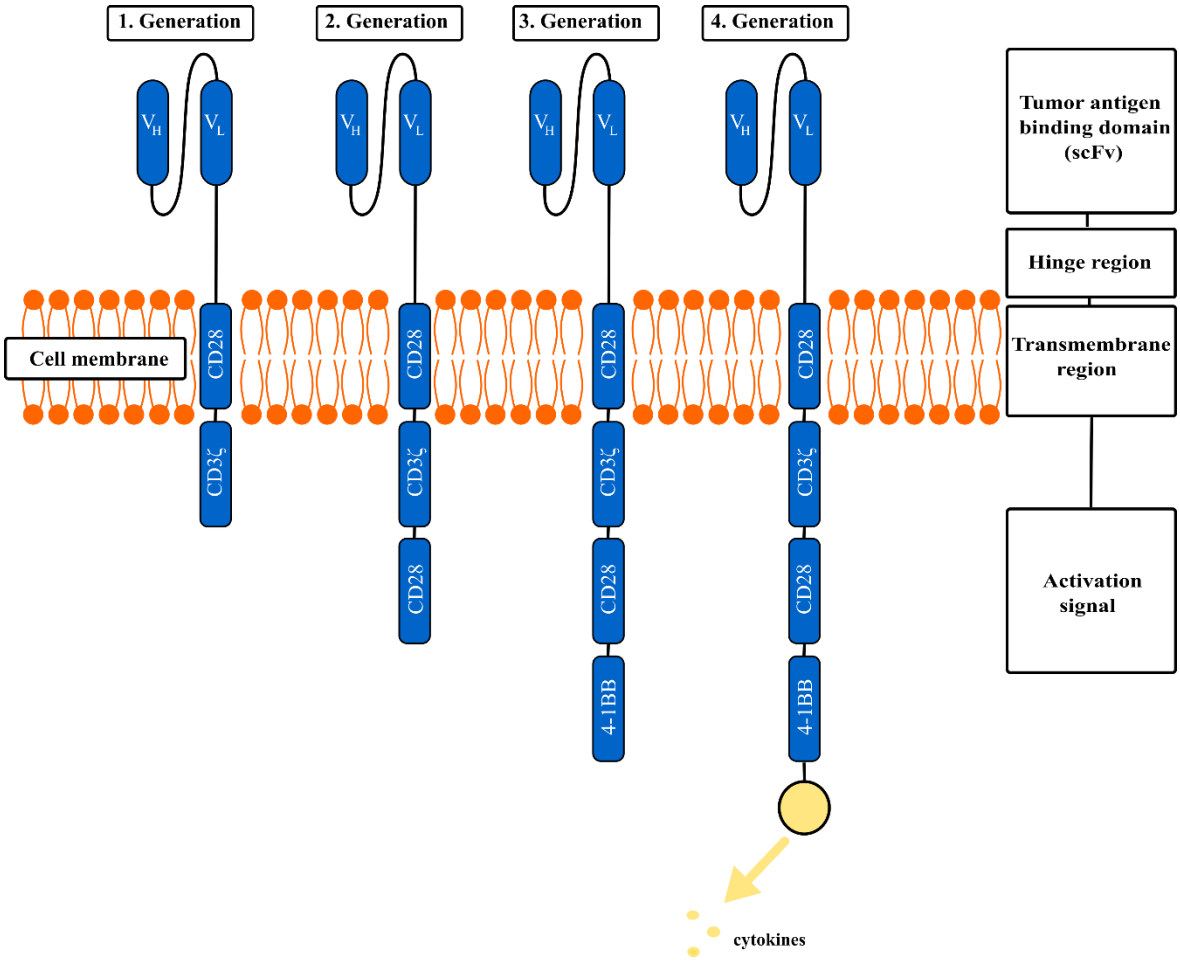

Fig. 3: Design of chimeric antigen receptors
The chimeric antigen receptor (CAR) is built from four different segments. The tumor antigen binding domain carries the small variable chain fragments (scFv) built from a light (VL) and a heavy (VH) immunoglobulin chain, defining the target antigen. It is connected to the transmembrane region via a hinge region and the transmembrane domain is most often derived from CD28. The transmembrane domain connects to the activation signal which is depending on the CAR generation built from one to three stimulatory domains. These domains most often are a combination of CD3ζ, CD28, and 4-1BB (CD137). The fourth generation adds cytokines for better tumor infiltration. This graphic is based on a figure from Gong et al.(Y. Gong et al., 2021).

The first Food and Drug Administration (FDA) and European Medicines Agency (EMA) approved CAR-T cell-based therapy is called tisagenlecleucel (Kymriah) and is a CD19-CAR-T cell produced

by Novartis. Kymriah is approved for the treatment of advanced or relapsing acute lymphoblastic leukemia (ALL) and diffuse large B-cell lymphoma especially as a salvage therapy (Ali et al., 2020; Schuster et al., 2019). Although this success in treating resistant or recurring hematologic malignancies is impressive, major limitations, especially the application of CAR cells for solid tumors remain difficult for a multitude of reasons. Firstly, tumors can change their presented antigens and evade elimination, for this reason, multiple trials are ongoing with either a dual CAR therapy or a tandem CAR displaying two scFv (Dai et al., 2020; Sterner & Sterner, 2021). Secondly, antigens in solid tumors are often not exclusively expressed on tumor cells but also healthy tissues. This can lead to severe on-target, but off-tumor toxicity. A solution could be the targeting of tumor-specific posttranslational modifications (Murad et al., 2018). Thirdly, tumor stroma and microenvironment often limit the infiltration of CAR-T cells into solid tumors, solution approaches include local application or tumor-specific chemokine receptors on CAR-T cells (Sterner & Sterner, 2021; Whilding et al., 2019). Lastly, the immunosuppressive tumor microenvironment limits CAR-T cell persistence and expansion, but the combination of CAR therapy and immune checkpoint inhibition seems to be a promising but probably insufficient approach to this problem (Grosser et al., 2019; Srivastava et al., 2021). In parallel to further research in the field of CAR-T cells research into CAR-NK cells began. They offer the unique advantage of not having to match the HLA or killer Ig-like receptor (KIR) which makes it possible to treat with mass-produced patient- or non-patient-derived CAR-NK cells, while also having reduced toxicity and no risk of cytokine release syndrome(E. Liu et al., 2020; Wrona et al., 2021). NK cells can be derived from peripheral blood, umbilical cord blood, stimulated immunocompetent progenitor stem cells, or even the stable NK-92 extranodal NK cell lymphoma cell line (Wrona et al., 2021). Additionally, NK cells have strong innate tumor-killing abilities like antibody-dependent cell cytotoxicity (ADCC), and antibody-independent mechanisms like natural cytotoxicity receptors (NCRs), KIRs, Natural Killer Group 2D (NKG2D), and DNAX accessory molecule (DNAM-1) (Wrona et al., 2021). These receptors also enable NK cells to kill CSCs and heterogenous tumors which evade T cell recognition and elimination. CSCs also differentiate under IFN-γ and TNFα, which are produced by NK cells, losing their renewal and resistance abilities (Wrona et al., 2021). Overall, CAR-NK cells are a promising alternative or improvement to CAR-T cells especially in the treatment of T-cell malignancies and hematological malignancies, and may provide ways to also treat solid tumors.

1.3.2 CD24-based therapy

Since the upregulation of *CD24* is associated with poor prognosis and its general presence in a variety of cancers qualifies it as an interesting target in tumor immunotherapy and raises the question if CD24 also invokes resistance to commonly used therapeutic strategies (Panagiotou et al., 2022). Studies show that resistance to vincristine in retinoblastoma might be due to activation of PTEN / AKT / mTORC1 pathways by CD24 (J. Sun et al., 2020). Furthermore, resistances to cisplatin were

seen in $CD24^+$ head and neck squamous cell carcinoma (HNSCC) (Modur et al., 2016), doxorubicin and cisplatin in $CD24^+$ ovarian cancer (Koh et al., 2012) as well as a CD24 positivity of gemcitabine resistant cells in pancreatic cancer (Jia et al., 2019). Inhibition of CD24 by antibody also led to a partial reversal of these resistance mechanisms (Modur et al., 2016; Skowron et al., 2022). Resistance associated with CD24 positivity was not only seen in DNA damaging agents but also targeted therapies like BRAF inhibitor resistance in $CD24^+$ melanoma (Hüser et al., 2018) and resistance to sorafenib in HCC (Lu et al., 2018).

As a result of this, a multitude of preclinical studies on the effect of CD24 inhibition in tumor proliferation or therapy modulation have been made and are summarized in **Error! Reference source not found.**.

Table 1: Preclinical studies for CD24 targeting treatment

Anti-CD24 therapy	Tumor entity / cell line	Additional drugs	Result	Reference
Anti-CD24 mAb[1] SWA11	Cisplatin-resistant embryonal carcinoma (NCCIT, 2102EP, NT2/D1)	Cisplatin	Increased cisplatin sensitivity	(Skowron et al., 2022)
Anti-CD24 mAb SN3b	Pancreatic adenocarcinoma (Colo357, Panc1)	/	Tumor growth inhibition	(Sagiv et al., 2006)
Anti-CD24 mAb SWA11	Colorectal adenocarcinoma	Irinotecan, paclitaxel, oxaliplatin, doxorubicin, 5-flourouracil	Enhanced killing effect	(Sagiv et al., 2008)
Anti-CD24 mAb ALB9	Urothelial carcinoma (UM-UC-1), lung metastases	/	Reduced tumor growth prolonged survival	(Overdevest et al., 2011)
Anti-CD24 mAb SWA11	Lung cancer (A549),	/	Reduced tumor growth	(Bretz et al., 2012)
	Pancreatic cancer (BxPC3)			
Anti-CD24 mAb SWA11	Lung cancer (A549 xenograft),	Gemcitabine	Increased infiltration with immune cells, altered cytokine microenvironment, increased gemcitabine sensitivity	(Salnikov et al., 2013)
	Ovarian carcinoma (SKOV3ip xenograft)			
Anti-CD24 mAb SN3b	Breast cancer (MCF-7	/	Increased phagocytosis	(Barkal et al., 2019)
	Pancreatic adenocarcinoma (APL1, Panc1)			
	Lung cancer (U-87-MG)			
Anti-CD24 mAB G7mAb	Lung adenocarcinoma (A549 xenograft)	Cetuximab	Improved survival, tumor growth inhibition	(Z. Chen et al., 2017)
	HCC[2] (Huh-7 xenograft)			
	Colorectal adenocarcinoma (HT-29 xenograft)			
Fusion protein rG7S-MICA	HCC (MDA-MB-231, Hat-29, HCT-116,	/	Tumor growth inhibition	(T. Wang et al., 2016)

Anti-CD24 therapy	Tumor entity / cell line	Additional drugs	Result	Reference
	BEL-7402, Huh-7, all in xenografts)			
ADC[3] SWAII-SPDB-dg.ricin A chain	Small cell lung cancer (SW2) in SCID[3] mice	/	Tumor growth inhibition	(Zangemeister-Wittke et al., 1993)
ADC SWA11.dgA	Burkitt lymphoma (BL-38) in SCID[4] mice	/	Durable complete remission	(Schnell et al., 1996)
ADC SWA11-ZZ-PE38	Colorectal adenocarcinoma (HT-29, COLO320)	/	Tumor growth inhibition	(Shapira et al., 2011)
ADC hG7-BM3-VcMMAE	HCC (BEL-7402 xenograft)	/	Tumor growth inhibition	(F. Sun et al., 2017)
ADC G7mAb-DOX	HCC (Huh7 xenograft)	/	Tumor growth inhibition improved survival	(Ma et al., 2017)
ADC HN-01	HCC (Huh7, BEL-7402 xenograft)	/	Tumor growth inhibition improved survival	(F. Sun et al., 2019)
CD24-CAR[5]-T-cells (SWA11-scFv)	Pancreatic adenocarcinoma (patient-derived) in SCID[3] mice	/	Tumor elimination, tumor growth inhibition, improved survival	(Maliar et al., 2012)
NK92-CD24-CAR (SWA11-scFv)	Ovarian carcinoma (SKOV3, OVCAR3)	/	Selective killing of $CD24^+$ tumor cells	(Klapdor et al., 2019)

[1] mAb = monoclonal antibody, [2] HCC = Hepatocellular cancer, [3] ADC = antibody-drug conjugate, [4] SCID = severe combined immunodeficiency, in vivo model of immunodeficient mice, [5] CAR = chimeric antigen receptor. Table of finished preclinical studies with CD24 as a target. The table is modified from Panagiotou et al. (Panagiotou et al., 2022)

1.4 Aim of this dissertation

The aim of this study is to further characterize the molecular properties of CD24 by identifying direct interaction partners of CD24 in the urological malignancies TGCT, UC, PC, and RCC. Additionally, we will investigate the oncological relevance of CD24 by evaluating its influence as a therapy-modulating factor and as a direct target for immunotherapy. Identification of interaction partners will help us to further decipher the molecular mechanisms of CD24 and how it increases proliferation, migration, and immune evasion in urological malignancies. We hypothesize that CD24 inhibition or targeted therapy will prove to be an alternative to standard chemotherapy or already established immunotherapy, especially in tumor entities that require viable cisplatin alternatives. The project will be divided into three parts and three research questions.

1. Does CD24 have a modulating role in the tumor response to a variety of promising immunotherapeutic drugs in TGCTs?

    a. We will answer this by conducting cell viability assays after treatment in CD24 wild-type cells and their respective CRISPR/Cas9 generated *CD24*-deficient subclones (Δ*CD24*) and comparing the cell survival. This should show us if the blockade of CD24 might be a promising mechanism to increase treatment response in TGCTs.

2. Is CD24 a promising target for cell-based treatment with NK-92-CD24-CAR cells in TGCTs?

a. Here we will test cell viability after treatment with transduced and untransduced NK-92 cells in wild-type and Δ*CD24* TGCT cell lines as well as healthy control cells. Positive results will show us that CD24 is a viable target for CAR-NK-based therapy and we will also see if the response is specific to $CD24^+$ cell lines.

3. What are the direct interaction partners of CD24 in urological malignancies?

   a. There are a few known interaction partners of CD24, but studies in TGCT and other urological malignancies like UC, PC, and RCC are still lacking, so the goal is to identify CD24 interaction partners via co-immunoprecipitation followed by mass spectrometry and gain further insight into the molecular function of CD24 in these tumor entities. Furthermore, we will be able to compare found interaction partners with already known ones and identify new processes that CD24 might be involved in.

2 Material and Methods

2.1 Material

2.1.1 Human TGCT and control cell lines

Table 2: Human TGCT and control cell lines

Cell line	Origin	Gender
2102EP WT (wild type)	Embryonal carcinoma	Male
2102EP-R	Embryonal carcinoma	Male
2102EP Δ*CD24* #9	Embryonal carcinoma	Male
2102EP Δ*CD24*#20	Embryonal carcinoma	Male
2102EP Δ*CD24* #59	Embryonal carcinoma	Male
2102EP Δ*CD24*#100	Embryonal carcinoma	Male
NCCIT WT	Embryonal carcinoma	Male
NCCIT-R	Embryonal carcinoma	Male
NCCIT Δ*CD24*#7	Embryonal carcinoma	Male
NCCIT Δ*CD24*#8	Embryonal carcinoma	Male
NCCIT Δ*CD24*#16	Embryonal carcinoma	Male
NCCIT Δ*CD24*#53	Embryonal carcinoma	Male
NT2/D1 WT	Embryonal carcinoma (metastatic site: lung)	Male
NT2/D1-R	Embryonal carcinoma	Male
NT2/D1 Δ*CD24*#106	Embryonal carcinoma	Male
TCam-2	Seminoma	Male
TCam-2-R	Seminoma	Male
HVHF2	Foreskin fibroblasts	Male
PC-3	Caucasian prostate adenocarcinoma	Male
LNCaP	Prostate carcinoma	Male
DU-145	Prostate carcinoma (metastatic site: brain)	Male
Caki-1	Clear cell renal cell carcinoma (metastatic site: skin)	Male
786-O	Renal cell carcinoma	Male
RT112	Bladder carcinoma	Female
SW1710	Bladder carcinoma	Female
SCABER	Bladder carcinoma	
NK-92	Natural killer cell lymphoblastic leukemia/lymphoma	Male
NK-92-CD24-CAR	Natural killer cell lymphoblastic leukemia/lymphoma	Male

2.1.2 Cell culture media and supplements

Table 3: Cell culture media and supplements

	Supplements	Cell lines	Manufacturer	Company address
Alpha MEM Medium	12.5 % FBS 12.5 % Horse Serum 1 % Pen / Strep 5 ng / ml IL2	NK-92-CD24-CAR NK-92	Gibco	Schwerte, Germany
RPMI Medium 1640 (1x)	10 % FBS 1 % Pen / Strep 1 % L-Glutamine	NCCIT TCam-2 PC-3 DU-145 786-0	Gibco	Schwerte, Germany
DMEM (1X) + GlutaMAX™-I	10 % FBS 1 % Pen / Strep 1 % L-Glutamine	2102EP NT2/D1	Gibco	Schwerte, Germany
DMEM (1X) + GlutaMAX™-I	10 % heat-inactivated FBS 1 % Pen / Strep	RT112 SW1710 Caki-1	Gibco	Schwerte, Germany
DMEM (1X) + GlutaMAX™-I	10 % FBS 1 % Pen / Strep 1 % L-Glutamine 1 % NEAA	HVHF2	Gibco	Schwerte, Germany

2.1.3 Cell culture and basic equipment

Table 4: Cell culture and basic equipment

Chemical/ Material	Manufacturer	Company Address
6-well culture plate	Greiner BIO-ONE	Frickenhausen, Germany
96-well culture plate	Greiner BIO-ONE	Frickenhausen, Germany
Cell culture dish 145 mm²	Greiner BIO-ONE	Frickenhausen, Germany
T25 -, T75 - Flask	CELLSTAR/Greiner Bio One	Frickenhausen, Germany
Combitips advanced®	Eppendorf AG	Hamburg, Germany
Conical bottom tube	Greiner Bio-One	Frickenhausen, Germany
Counting Slides	Bio-Rad Laboratories	Feldkirchen, Germany
Dimethyl sulfoxide	Sigma-Aldrich/MERCK	Taufkirchen, Germany
DMEM (1X) + GlutaMAX™-I	Gibco/Thermo Fisher Scientific	Schwerte, Germany
Dulbecco's Phosphate Buffered Saline (PBS)	Sigma-Aldrich/MERCK	Taufkirchen, Germany
Eppendorf tubes	Eppendorf AG	Hamburg, Germany
Fetal Bovine Serum	BIOCHROME GmbH/MERCK	Darmstadt, Germany
Filter Tips 10 µl, 100 µl, 1000 µl	Greiner BIO-ONE	Frickenhausen, Germany
Ham's F-12 Nutrient Mix, GlutaMAX™ Supplement	Gibco/Thermo Fisher Scientific	Schwerte, Germany
L-Glutamin (100x)	Gibco/Thermo Fisher Scientific	Schwerte, Germany
MEM Non-Essential Amino Acids Solution (100X)	Gibco/Thermo Fisher Scientific	Schwerte, Germany
Minisart® syringe filter 0.2 µm	SARTORIUS	Göttingen, Germany
Omnifix Luer Lock Solo Syringe 10 ml	B. Braun	Melsungen, Deutschland

Chemical/ Material	Manufacturer	Company Address
Multiply®-µStrip Pro 8-strip	Sarstedt AG & Co. KG	Nümbrecht, Germany
Penicillin / Streptomycin (P/S)	Gibco/Thermo Fisher Scientific	Schwerte, Germany
Pipettes 10 µl, 100 µl, 1000 µl, 5000 µl	Eppendorf AG	Hamburg, Germany
Pipette tips 10 µl, 100 µl, 1000 µl	Nerbe plus GmbH	Winsen/Luhe, Germany
Reagent Reservoir	Corning Incorporated	Wiesbaden, Germany
Round-bottom polystyrene tubes	VWR Chemicals	Langenfeld, Germany
RPMI Medium 1640 (1X)	Gibco/Thermo Fisher Scientific	Schwerte, Germany
Stripettes 2 ml, 5ml, 10ml, 25ml	Corning Incorporated	Wiesbaden, Germany
Syringes	B. Braun Melsungen AG	Melsungen, Germany
Trypan blue 0.4 %	Sigma-Aldrich/MERCK	Taufkirchen, Germany
Trypsin-EDTA 0.05 %, 0.25 %	Gibco/Thermo Fisher Scientific	Schwerte, Germany
IL-2	Peprotech/Thermo Fisher Scientific	Schwerte, Germany
Horse Serum	Sigma-Aldrich/MERCK	Taufkirchen, Germany

2.1.4 XTT cell viability assay

Table 5: Materials for XTT cell viability assay

Chemical/Material	Manufacturer	Company Address
Cisplatin 1 mg / ml	Accord Healthcare GmbH	Munich, Germany
Phenazinemethosulfate (PMS)	Sigma-Aldrich/MERCK	Taufkirchen, Germany
XTT sodium salt	BIOFROXX	Einhausen, Germany
Xplorer plus electronic multichannel pipette	Eppendorf	Hamburg, Germany
iMark™ Microplate Absorbance Reader	Bio-Rad Laboratories	Feldkirchen, Germany

2.1.5 AnnexinV / PI apoptosis assay

Table 6: Materials for AnnexinV / PI apoptosis assay

Chemical/Material	Manufacturer	Company Address
Annexin V-FITC	Miltenyi Biotech	Bergisch Gladbach, Germany
Annexin V Binding Buffer (20x Stock Solution)	Miltenyi Biotech	Bergisch Gladbach, Germany
Cisplatin 1 mg / ml	Accord Healthcare GmbH	Munich, Germany
Propidium iodide (PI)	Sigma-Aldrich/MERCK	Taufkirchen, Germany

2.1.6 DNA isolation

Table 7: Materials used for DNA isolation

Chemical/ Material	Manufacturer	Company Address
Rotiphenol	CARL ROTH GmbH+Co. KG	Karlsruhe, Germany
Low TE-Buffer	AppliChem GmbH	Darmstadt, Germany

Chemical/ Material	Manufacturer	Company Address
Sodiumacetat	Merck KGaA	Darmstadt, Germany
Ethanol	VWR International GmbH	Langenfeld, Germany
Centrifuge Allegra 2IR	Beckman and Coulter Life Sciences	Krefeld, Germany
Nanodrop2000	Thermo Fisher Scientific	Schwerte, Germany

Table 8: Materials used for DNA lysis buffer

Chemical/Material	Manufacturer	Company Address
Sodium Chloride	Merck KGaA	Darmstadt, Germany
Tris (Trisaminomethan, NH2C(CH2OH)3)	VWR International GmbH	Langenfeld, Germany
EDTA (Dinatrium-ethylenediamine-tetraacetat, C10H16N2O8)	Sigma-Aldrich/MERCK	Taufkirchen, Germany
SDS (Dodecylsulfat, C12H25NaO4S)	CARL ROTH GmbH+Co. KG	Karlsruhe, Germany
Proteinase K	CARL ROTH GmbH+Co. KG	Karlsruhe, Germany

The DNA-lysis buffer consists of 5 M NaCl, 1 M Tris-HCL (pH 8), 0.5 M EDTA (pH 8), 10% SDS, and Millipore Water.

2.1.7 Protein extraction

Table 9: Materials used for protein extraction

Chemical/Material	Manufacturer	Company Address
PBS	Sigma-Aldrich/MERCK	Taufkirchen, Germany
Protease-Inhibitor	Sigma-Aldrich/MERCK	Taufkirchen, Germany
Phosphatase-Inhibitor	Sigma-Aldrich/MERCK	Taufkirchen, Germany
Conical bottom tube 15ml	Greiner Bio-One	Kremsmünster, Austria
Trypsin-EDTA 0.05 % Phenolred	Gibco, Thermo Fisher Scientific	Schwerte, Germany
Centrifuge Allegra 2IR	Beckman and Coulter Life Sciences	Krefeld, Germany

Table 10: Materials used in RIPA buffer

Chemical/ Material	Manufacturer	Company Address
DOC (Sodium Deoxycholat, $C_{24}H_{39}NaO_4$)	Sigma-Aldrich/MERCK	Taufkirchen, Germany
Sodium Chloride	VWR International GmbH	Langenfeld, Germany
SDS (Dodecylsulfat, $C_{12}H_{25}NaO_4S$)	CARL ROTH GmbH+Co. KG	Karlsruhe, Germany
Tris (Trisaminomethan, $NH_2C(CH_2OH)_3$)	VWR International GmbH	Langenfeld, Germany
Triton X-100	Sigma-Aldrich/MERCK	Taufkirchen, Germany

The RIPA buffer consists of 110nM NaCl, 1 % Triton X-100, 0.5 % DOC, 0.1 % SDS, 50 mM Tris and is adjusted to a pH of 8.

The phosphatase and protease inhibitors were added to the RIPA Buffer up to a concentration of 1 % (V/V).

2.1.8 BCA protein assay

Table 11: Materials used in BCA protein assay

Chemical/Material	Manufacturer	Company Address
96-well plate	Greiner Bio-One	Kremsmünster, Austria
Albumin standard	Thermo Fisher Scientific	Schwerte, Germany
Pierce BCA Protein Assay Reagent A/B	Thermo Fisher Scientific	Schwerte, Germany
iMark Microplate reader	Bio-Rad Laboratories	Feldkirchen, Germany
ThermoMixer Comfort	Eppendorf	Hamburg, Germany
Minispin Tischzentrifuge	Eppendorf	Hamburg, Germany

Additionally, RIPA buffer was used here see Table 10.

2.1.9 SDS-PAGE and Western blot

Table 12: Materials used in polyacrylamide gel

Chemical/Material	Manufacturer	Company Address
Acrylamid (C_3H_5NO)	CARL ROTH GmbH+Co. KG	Karlsruhe, Germany
APS (Ammoniumperoxodisulfat, $(NH_4)_2S_2O_8$)	Sigma-Aldrich/MERCK	Taufkirchen, Germany
SDS (Dodecylsulfat, $C_{12}H_{25}NaO_4S$)	CARL ROTH GmbH+Co. KG	Karlsruhe, Germany
TEMED (Tetramethylethylendiamin, $C_6H_{16}N_2$)	Sigma-Aldrich/MERCK	Taufkirchen, Germany
Tris (Trisaminomethan, $NH_2C(CH_2OH)_3$)	VWR International GmbH	Langenfeld, Germany

Table 13: Formula for the separation gel 12 %

Chemical/Material	ml
H_2O	3.3
Acrylamide 30 %	4
1.5 M Tris pH 8.8)	2.5
10 % SDS pH 7.2	0.1
10 % APS	0.1
TEMED	0.005

Table 14: Formula for collection gel 12 %

Chemical/Material	ml
H_2O	3.4
Acrylamide 30 %	0.83
1 M Tris pH 6.8)	0.63
10 % SDS pH 7.2	0.05
10 % APS	0.05
TEMED	0.005

Table 15: Materials used in SDS-PAGE

Chemical/Material	Manufacturer	Company Address
BSA (Bovine Serum Albumin)	PAN-Biotech GmbH	Aidenbach, Germany
Chemiluminescent Substrate SuperSignal™ West Pico PLUS	Thermo Fisher Scientific	Schwerte, Germany
Clarity™ Western ECL Substrate	Bio-Rad Laboratories	Feldkirchen, Germany
Immobilon®-P PVDF Transfer Membranes	Merck GmbH	Darmstadt, Germany
Methanol	VWR International GmbH	Langenfeld, Germany
Milk powder, blotting grade	CARL ROTH GmbH+Co. KG	Karlsruhe, Germany
Mini-PROTEAN Tetra Cell	Bio-Rad Laboratories	Feldkirchen, Germany
Page Ruler™ Prestained Protein Ladder (stored at -20°C)	Thermo Fisher Scientific	Schwerte, Germany
Ponceau S Solution	Sigma-Aldrich/MERCK	Taufkirchen, Germany
Coomassie Brilliant Blue R 250	CARL ROTH GmbH+Co. KG	Karlsruhe, Germany
PowerPac™ Basic Power Supply	Bio-Rad Laboratories	Feldkirchen, Germany
Trans-Blot® Turbo™ Transfer System	Bio-Rad Laboratories	Feldkirchen, Germany
Whatman™ Gel Blot Paper	GE Healthcare	Schwerte, Germany
Roti®-Load 4x	CARL ROTH GmbH+Co. KG	Karlsruhe, Germany

Table 16: Chemicals used in electrophoresis buffer

Tris/Glycine/SDS buffer (10x)	Bio-Rad Laboratories	Feldkirchen, Germany

Table 17: Chemicals used in blotting buffer

Tris/Glycin buffer (10x)	Bio-Rad Laboratories	Feldkirchen, Germany
Methanol	VWR International GmbH	Langenfeld, Germany

Table 18: Chemicals used in PBS-T washing buffer

PBS 10x	VWR International GmbH	Langenfeld, Germany
Tween20	Sigma-Aldrich/MERCK	Taufkirchen, Germany

Table 19: Chemicals used in stripping buffer

SDS ultra-pure (Dodecylsulfat, $C_{12}H_{25}NaO_4S$)	CARL ROTH GmbH+Co. KG	Karlsruhe, Germany

β-Mercaptoethanol	Sigma-Aldrich/MERCK	Taufkirchen, Germany
Tris (Trisaminomethan, $NH_2C(CH_2OH)_3$)	VWR International GmbH	Langenfeld, Germany
H_2O	Sigma-Aldrich/MERCK	Taufkirchen, Germany

Table 20: Coomassie Staining solution

225 ml H2O (Millipore)	Sigma-Aldrich/MERCK	Taufkirchen, Germany
225 ml Methanol	Sigma-Aldrich/MERCK	Taufkirchen, Germany
50 ml acetic acid	Sigma-Aldrich/MERCK	Taufkirchen, Germany
1.25g Coomassie Brilliant Blue R 250	CARL ROTH GmbH+Co. KG	Karlsruhe, Germany

2.1.10 Antibodies used in Western blot

Table 21: List of antibodies used in western blot

Antibody	Catalog Number	Manufacturer	Company Address	Blocking Buffer	Concentration for western blot
SWA11		Peter Altevogt	Heidelberg, Germany	5 % Milk in PBS-T	1:5000
Normal mouse IgG2a	Sc-3878	Santa Cruz	Dallas, Texas, USA	5 % Milk in PBS-T	
Anti-β-Actin	A5441	Sigma-Aldrich/MERCK	Taufkirchen, Germany	5 % Milk in PBS-T	1:5000
Anti-Vinculin		Sigma-Aldrich/MERCK		5 % Milk in PBS-T	
Rabbit Anti-Mouse IgG (H+L)-HRP Conjugat	P0260	Agilent/Dako	Santa Clara, CA, USA	5 % Milk in PBS-T	1:1000

2.1.11 Co-Immunoprecipitation

Table 22: Materials and equipment used in co-immunoprecipitation

Chemical/Material	Manufacturer	Company Address
Dynal MPC-S magnetic particle concentrator	Thermo Fisher Scientific	Schwerte, Germany
Dynabeads M-270 Epoxid	Thermo Fisher Scientific	Schwerte, Germany
Hula Mixer Sample Mixer	Thermo Fisher Scientific	Schwerte, Germany
Milk powder, blotting grade	CARL ROTH GmbH+Co. KG	Karlsruhe, Germany
Triton-X-100	Sigma-Aldrich/MERCK	Taufkirchen, Germany
PBS	Sigma-Aldrich/MERCK	Taufkirchen, Germany
NP40 cell lysis buffer	Thermo Fisher Scientific	Schwerte, Germany
Protease-inhibitor	Sigma-Aldrich/MERCK	Taufkirchen, Germany
PMSF (0.3M stock)	Sigma-Aldrich/MERCK	Taufkirchen, Germany

Table 23: Chemicals used in Buffer A

Sodium phosphate monobasic monohydrate ($NaH_2PO_4 \cdot H_2O$)	Merck GmbH	Darmstadt, Germany

Sodium phosphate dibasic dihydrate ($Na_2HPO_4 \cdot 2H_2O$)	Merck GmbH	Darmstadt, Germany

0.1 M sodium phosphate buffer consists of 2.62 g $NaH_2 PO_4 \times H_2O$ (MW 137.99) 14.42 g $Na_2 HPO_4 \times 2H_2O$ (MW 177. 99) Dissolve in distilled water, adjust pH to 7.4 if necessary, and adjust to 1 liter.

Table 24: Chemicals used in Buffer B

Ammonium sulfate ($(NH_4)_2SO_4$)	Merck GmbH	Darmstadt, Germany

39.6 g (NH_4) 2 SO_4 (MW 132.1) dissolved in buffer A (0.1 M sodium phosphate buffer (pH 7.4)) and adjusted to 100 ml.

Table 25: Chemicals used in elution buffer

SDS (Dodecylsulfat, $C_{12}H_{25}NaO_4S$)	CARL ROTH GmbH+Co. KG	Karlsruhe, Germany
Glycerol ($C_3H_8O_3$)	Merck GmbH	Darmstadt, Germany
Tris (Trisaminomethan, $NH_2C(CH_2OH)_3$)	VWR International GmbH	Langenfeld, Germany

The buffer consists of 30 % Glycerol, 12 % SDS, 150 mM Tris base in water, adjust pH to 7.0

Table 26: Chemicals used in washing buffer for co-immunoprecipitation

PBS	Sigma-Aldrich/MERCK	Taufkirchen, Germany
Triton-X-100	Sigma-Aldrich/MERCK	Taufkirchen, Germany

2.1.12 List of drugs and diluents

Table 27: List of all drugs and diluents used in this study

Chemical/Material	Lösungsmittel	Manufacturer	Company Address
Dimethylsulfoxide (DMSO)		Sigma-Aldrich/MERCK	Taufkirchen, Germany
Ethanol		VWR Chemicals	Darmstadt, Germany
DMF		Sigma-Aldrich/MERCK	Taufkirchen, Germany
H_20		Sigma-Aldrich/MERCK	Taufkirchen, Germany
PU-HU-71	DMSO	Selleckchem	Berlin, Deutschland
17-AAG	DMSO	Selleckchem	Berlin, Deutschland
GSK343	DMF	Selleckchem	Berlin, Deutschland
Romidepsin	DMSO	Selleckchem	Housten, Texas, USA
Quisinostat	DMSO	Selleckchem	Berlin, Deutschland
Olaparib	DMSO	Cayman/Biomol	Ann Arbor, MICH, USA
Palbociclib	H_20 pH 3	Pfizer Ltd.	New York, USA

2.1.13 Technical devices

Table 28: List of technical devices used

Technical device	Manufacturer	Company Address
Chemidoc Imaging System	Bio-Rad Laboratories, Inc.	Feldkirchen, Germany

CO_2-incubator 150i	ThermoFisher Scientific	Oberhausen, Germany
MACSQuant® Flow Cytometer	Miltenyi Biotech	Bergisch Gladbach, Germany
NanoDrop™ 2000 Spectrophotometer	ThermoFisher Scientific	Oberhausen, Germany
PowerPac™ Basic Power Supply	Bio-Rad Laboratories, Inc.	Feldkirchen, Germany
S1000™ Thermal Cycler	Bio-Rad Laboratories, Inc.	Feldkirchen, Germany
TC20™ Automated Cell Counter	Bio-Rad Laboratories, Inc.	Feldkirchen, Germany
Ts2 Inverted Routine Microscope	Nikon Instruments Europe	Düsseldorf, Germany
Wallac Victor2 Perkin Elmer 1420 Multilabel Counter	Perkin Elmer	Rodgau, Germany
iMark™ Microplate Absorbance Reader	Bio-Rad Laboratories, Inc.	Munich, Germany

2.1.14 Software and online tools

Table 29: List of software and online tools used in this study

Technical device	Manufacturer / website	Company Address / citation
NanoDrop 2000 V 1.6	Thermo Fisher Scientific	Schwerte, Germany
CFX Maestro Software	Bio-Rad Laboratories	Feldkirchen, Germany
Microplate Manager 6	Bio-Rad Laboratories	Feldkirchen, Germany
GraphPad Prism V8	GraphPad Software, Inc	San Diego, CA, USA
MACSQuantify V 2.11	Miltenyi Biotech	Bergisch Gladbach, Germany
DAVID Bioinformatics Resources 2021	https://david.ncifcrf.gov/	(D. W. Huang et al., 2009b, 2009a)
STRING database	https://string-db.org	(Szklarczyk et al., 2019)
Microsoft Word (Version 2019)	Microsoft 365, Microsoft Corporation	Redmond, WA, USA
Microsoft Excel (Version 2019)	Microsoft 365, Microsoft Corporation	Redmond, WA, USA
Inkscape 1.3.2	https://inkscape.org/	GNU General Public License
INTAS GDS 2010 Windows	INTAS	Göttingen, Germany
cBioportal	https://www.cbioportal.org/	(Cerami et al., 2012; Gao et al., 2013)
Venny 2.1.0	https://bioinfogp.cnb.csic.es/tools/venny/	(*Venny 2.1.0*, n.d.)
Matplotlib	https://matplotlib.org/stable/	(Hunter, 2007)
PCAGO	https://pcago.bioinf.uni-jena.de/	(Gerst & Olzer, 2019)

2.2 Methods

2.2.1 TGCT and Control Cell Cultivation

TGCT, as well as all their respective cisplatin-resistant and Δ*CD24*, cell lines and tumor microenvironment control cells were cultured inside a CO_2-incubator 150i at 37°C with a carbon dioxide percentage of 7.5 %.

UC, RCC, and PC cell lines as well as NK-92 and NK-92-CD24-CAR cell lines were cultured inside a CO_2-incubator 150i at 37°C with a carbon dioxide percentage of 5 %.

All cell lines were routinely seeded into T75 flasks with 15ml of medium for adherent cells and 30ml of medium for suspension cells. As mentioned previously, different media were used to provide the best conditions for each cell line. All cell culture-related experiments were performed under sterile conditions.

Cells were passaged twice per week. For passaging into a new T75-flask the medium was removed, cells were washed with a minimum of five ml of PBS and cells were detached from the bottom of the flask with one ml of trypsin followed by incubation at 37°C until no more cells were attached to the bottom of the flask. The trypsinization was stopped by the addition of at least four times the amount of medium containing 10 % fetal bovine serum (FBS) as trypsin was used. A fraction of the cells were transferred to a new T75-flask, distributed equally, and then returned to the incubator. Since suspension cells were not trypsinized, the medium containing these cells was mixed thoroughly by shaking or pipetting followed by transferring a part of the medium to a new T75-flask.

2.2.2 Cell counting

Cells were counted by usage of the TC20 automated cell counter. For this, 20 microliters (µl) of trypan blue were mixed with 20 µl of cell suspension, and 10 µl of this mixture was then transferred to a cell counting slide. The automated cell counter calculates the number of cells per ml as well as their viability in percent.

2.2.3 Cell thawing and freezing

For cell freezing, the cells were harvested as described above and centrifuged to remove all supernatant. The cell pellet was resuspended in three ml of freezing medium (FBS + 10 % DMSO) and divided into three cryo-tubes. These tubes were stored at -70°C for 24 hours (h) and transferred to the liquid nitrogen tank afterward.

For cell thawing, the cells were thawed on ice. After thawing the cells were transferred into a T75 flask containing 15 ml of medium and 24 h later attachment to the bottom of the flask was evaluated. Upon attachment, a medium exchange was performed.

2.2.4 XTT cell viability assay

The XTT viability assay is a colorimetric assay in which the number of viable cells in comparison to a control is measured. Specifically, the activity of mitochondrial dehydrogenases, which are only active in viable cells, is measured. The activity of mitochondrial enzymes is inactivated shortly after cell death.

The chemical reaction of the XTT assay is the reduction of yellow XTT (2,3-Bis-(2-Methoxy-4-Nitro-5-Sulfophenyl)-2*H*-Tetrazolium-5-Carboxanilide) to orange formazan by the mitochondrial dehydrogenases. Formazan is soluble in aqueous solutions and can be quantified by using a UV / Vis spectrometer, in this case, the iMark-Microplate-absorbance-reader. Furthermore, PMS (N-methyl diabenzopyrazine methyl sulfate) is used as an electron coupling agent which speeds up the reaction.

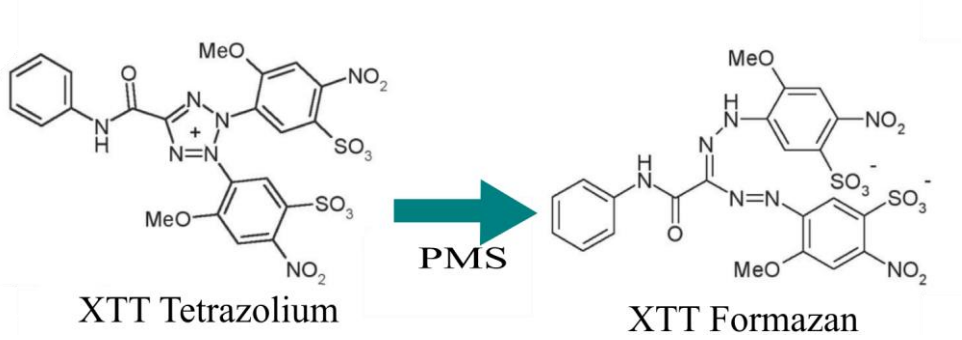

Fig. 4: Transformation of yellow XTT tetrazolium salt into orange formazan

XTT viability assays were used to evaluate the difference in cell survival between EC cell lines and their respective Δ*CD24* cell lines upon treatment with a variety of drugs and CAR-NK-cell-based immunotherapy.

2.2.4.1 Drug response

For this assay cells were seeded into 96-well plates. Per drug to be tested one plate of EC WT and 3 different Δ*CD24*clones were prepared. In each well 3000 cells in 50 µl of their respective medium were plated. After 24h, cells were treated with twice the amount of the drug in question in 50 µl of medium to achieve the target concentration in the 100 µl total volume. Every condition was plated in quadruplicates.

Table 30: Drug concentrations

Chemical/Material	Condition 1 (concentration)	Condition 2	Condition 3	Condition 4
Palbociclib	2.5 µM	5 µM	10 µM	20 µM
17-AAG	1 µM	2 µM	3 µM	5 µM
GSK343	5 µM	7.5 µM	10 µM	12.5 µM
Olaparib	5 µM	10 µM	15 µM	20 µM
PU-HU-71	75 nM	125 nM	250 nM	500 nM
Romidepsin	0.5 nM	1 nM	2.5 nM	5 nM
Quisinostat	2.5 nM	10 nM	25 nM	50 nM

Fig. 5: Seeding conditions for XTT cell viability assay
For every 24h increment measurement quadruplicates of a Blank without any cells, a control without treatment, and four concentrations were seeded.

2.2.4.2 CAR-NK-cell treatment

Cells were seeded into 96 well plates. Per cell line, two plates were prepared and 3000 cells in 100 µl of their respective media per well were plated. After 24 h, 1 plate per cell line was treated with different effector / target (E / T) ratios of 1:1, 3:1, 5:1, and 10:1 of NK-92 cells in 100 µl of medium and 1 plate per cell line was treated with NK-92-CD24-CAR-cells in the same E / T ratios. In some experiments, this treatment was repeated 48 hours after the first treatment. For this, a medium exchange was performed and the newly added 200 µl of medium contained the respective number of NK cells. Each condition was plated in quadruplicates.

2.2.4.3 XTT application

24, 48, 72, and 96 h after treatment, 50 µl of XTT (stock: 1 mg / ml) and 0.5 µl of PMS (stock: 1.25 millimolar (mM)) were added to the cells and viability was measured after 4 h of incubation with the iMark-Microplate-absorbance-reader. For the NK-cell treatment before XTT addition, the medium was pipetted off to remove the NK cells and exchanged for 100 µl of the new medium. Absorption was measured at a wavelength of 450 nanometers (nm) which detected the orange formazan and at 655 nm to detect background absorption of the cell culture medium.

2.2.4.4 Viability calculation

Cell viability was calculated by subtracting the mean blank value from the other wells for 655 nm and 450 nm values. Afterwards, the 655 nm value was subtracted from the 450 nm value to remove background absorption of the culture medium. A mean value of the four control wells was formed and afterwards, each treated well was divided by this mean control. The resulting value was then multiplied by 100 to gain the percentage of cell viability per well. A mean value and standard deviation of the quadruplicates were calculated and present the final value as viability in percent.

Additionally, the lethal dose $(LD)_{50}$ values were calculated with GraphPad Prism 8. The fold change (FC) between the LD_{50} values of WT cells and a pool of 3 Δ*CD24* cell lines was calculated by dividing the WT value by the Δ*CD24* pool value.

$$\mathrm{FC} = \mathrm{LD}_{50}(\mathrm{WT})/\mathrm{LD}_{50}(CD24\mathrm{KO\ pool})$$

2.2.5 Protein extraction

For the isolation of protein, the cell suspension was gathered in a 15 ml tube and centrifuged for 5 min at 700 rpm / 99 x g. The supernatant was discarded, and the cell pellet was resuspended and washed in 1 ml of PBS. This suspension was transferred to a 1.5 ml Eppendorf tube and centrifuged for another 5 minutes (min) at 1000 rounds per minute (rpm). After discarding the supernatant 50 - 75 µl of RIPA Buffer (according to cell pellet size) or 200 µl NP40-lysis-buffer were added and incubated for 30 min on ice. Afterward, the lysed suspension was centrifuged for 10 min at 13000 rpm at 4° C to separate cell debris from the released proteins. The supernatant was then transferred to a new 1.5 ml Eppendorf reaction tube and either used directly or stored at -20° C.

2.2.6 Determining protein concentration via BCA assay

To quantify protein concentration, the “Pierce BCA Protein Assay-Kit” was used. This assay combines the reduction of Cu^{2+} ions to Cu^{1+} by alkaline proteins and the highly sensitive and specific detection of Cu^{1+} bicinchoninic acid (BCA). The BCA Cu^{1+} protein complex is soluble and should

be measured at 562 nm. The kit includes a BSA Standard with protein concentrations ranging from 2000 µg - 20 µg. The Standard range was pipetted for every Protein-quantification in duplicates (10 µl / well) on a 96-well plate to generate a regression curve for the evaluation of the samples in question.

The samples were diluted 1 :10 in H_20 and plated in duplicates (sometimes higher dilutions were required). The BCA-Reagent-Mix is prepared by mixing reagent A and reagent B, both contained in the kit, in a proportion of 1 : 50. 200 µl of the reagent mix were then added to each well and the plate was incubated for 30 min at 37°C. After the incubation period, the absorption at 495 nm was measured using the iMark-Microplate-absorbance-reader. The concentrations of the samples were then calculated and presented in ng/µl.

2.2.7 SDS-polyacrylamide gel electrophoresis (SDS-PAGE) and western blot

Polyacrylamide gel electrophoresis is a biochemical detection method for proteins. The proteins are separated by applying a voltage. Dependent on size and molecular weight proteins can be differentiated by their migration distance and speed. The polyacrylamide gel consists of two separate parts. The very fine-meshed separating gel was poured into a gel casting module and sealed with isopropanol for polymerization. The less finely meshed stacking gel was poured on top of the separating gel and a comb was inserted. The samples were pipetted in the resulting chambers. The gel together with the glass plates was then inserted into the running chamber and the chamber was filled with 1x gel electrophoresis buffer. The sample consisted of 20 µg protein and was adjusted to 12.5 µl with H_20 and 4 µl of 4x RotiLoad. The sample mix was heated to 95 °C for 5 min and then pipetted into the chambers or stored at -20° C. To compare the sizes of the samples a protein ladder was added into one chamber. The separation of proteins was then achieved by first running the gel at a voltage of 70 V until the samples entered the separation gel upon which the voltage was raised to 99 V.

The detergent SDS has a strong protein-denaturation effect and binds to the protein backbone. The presence of SDS and 2-mercaptoethanol, which cleaves disulfide bonds, unfold proteins into linear chains where the negative charge is proportional to the polypeptide chain length.

The transfer of the separated proteins to a PVDF-membrane was done via a “Semidry Blotter”. In preparation for the blotting, four Whatman-Papers were soaked in blotting buffer. The PVDF-membrane was activated in methanol for 2 min, washed in Millipore water, and then incubated for at least five minutes in blotting buffer. For the transfer a stack of two Whatman-Papers / Gel /

Membrane / two Whatman-Paper was built in the blotting chamber and the transfer was performed at a voltage of 25 V for 20 min.

Protein transfer was then confirmed by staining the PVDF-membrane in Ponceau S Solution until red protein bands were visible or in Coomassie blue solution. For Ponceau S de-staining was achieved by shaking in Millipore water until the background was de-stained followed by washing of the membrane in PBS-T. Coomassie was de-stained by using Coomassie de-stain (Coomassie staining solution without Coomassie) followed by washing in PBS-T.

Afterwards, membranes were blocked using five ml of 5 % milk in PBS-T for one hour under constant shaking at room temperature. This was followed by the primary antibody, which was diluted in five ml of blocking buffer, incubation of the primary antibody was performed overnight under constant shaking at 4° C. Subsequently the membrane was washed thrice for 5 min in PBS-T after which the secondary antibody, also diluted in 5 ml PBS-T was incubated with the membrane for 2 h at room temperature under constant shaking. This was again followed by three washing steps of 5 min in PBS-T.

The detection was performed with the “Pierce ECL Western Blotting Substrate Set”. The two reagents were mixed in a 1:1 ratio and then used to cover the membrane followed by five minutes of incubation in the dark. The chemiluminescence detection was performed using the Chemidoc Imaging System. Additionally, a colorimetric picture was taken to visualize the protein ladder.

Detection of multiple proteins per membrane was enabled by stripping the already bound antibodies of the membrane. For this, the membrane was incubated for 30 min with stripping buffer at 60 °C in a shaking water bath and subsequently washed thrice for 5 min in PBS-T. After that, the protocol could be restarted with the blocking of the membrane.

2.2.8 Co-Immunoprecipitation of CD24

Co-immunoprecipitation is a technique to identify important protein-protein interactions by using target-specific antibodies to directly capture the target and indirectly any bound protein. This protein complex can then be analyzed to identify interaction partners and the function of the target protein.

For each reaction, 3 mg of lyophilized beads were weighed out and resuspended in 600 µl of sodium phosphate buffer (buffer A). Afterward, each sample was vortexed for 30 seconds (sec) and incubated under tilting and rotation on a “HulaMixer” for 10 min. Subsequently, samples were placed on a magnetic rack for 1 minute and the supernatant was discarded. The tubes were then removed from

the magnet and the beads were resuspended in 600 µl of buffer A and mixed by vortexing for 30 sec followed by one minute in the magnetic rack. Supernatants were again discarded.

To couple the magnetic beads to the antibody 6 µg of antibody per 1mg of magnetic beads was used. The volume of the antibody solution had to be adjusted to at least 180 µl to maintain the reaction balance of 1 / 3 ligand solution, buffer A, and Buffer B (3 M ammonium sulfate).

The beads were then resuspended in the same volume of buffer A as calculated for the ligand and mixed by vortexing. This was followed by the addition of the antibody solution, vortexing, and addition of an equal amount of buffer B. The whole reaction was then incubated for 24 h at 37 °C on a HulaMixer with a slow tilt rotation.

After 24 h, the beads were placed on the magnetic rack and the supernatant was removed. This was followed by three washing steps with PBS where the supernatant was discarded after 2 min on the magnetic rack. Physically adsorbed ligand could be removed by washing for 10 min in 0.5 % Triton-X-100 in PBS. This step was performed in between the second and third washing steps. Afterward, beads were resuspended in 600 µl of PBS and 1 mg of protein, which was lysed with NP40 lysis buffer and quantified via BCA assay(2.2.6), was added to each sample. Samples were incubated on a HulaMixer with tilting and rotation overnight at 4 °C.

Incubation was followed by a collection of beads at the tube wall on the magnetic rack for four min and removal of the supernatant. Beads were washed three times using 600 µl PBS each time. Elution of the target for mass spectrometry was achieved by adding 22 µl of SDS buffer, mixing via pipetting up and down (not vortexing), and incubation at 37 °C under slight shaking. For further processing by Western Blot, beads were resuspended in 22 µl SDS buffer and incubated for five min at 95 °C. After the incubation, samples were placed on the magnetic rack for two minutes and the purified target supernatant was transferred to a new reaction tube. Samples for mass spectrometry were stored at -80 °C and samples for Western Blot analyses were either used directly or stored at -20 °C.

2.2.9 Mass spectrometry analysis

Liquid chromatography-mass spectrometry (LC-MS) was performed by Dr. Anja Stefanski (Biologisch-Medizinisches Forschungszentrum, Molecular Proteomics Laboratory, director Prof. Kai Stühler, HHU). Samples were separated by a 4–12% polyacrylamide gel. After Coomassie brilliant blue staining, the protein-containing bands were excised and processed as described elsewhere (Poschmann et al., 2014). Briefly, bands were destained, washed, reduced with dithiothreitol, alkylated with iodoacetamide, and digested with trypsin (Serva, Heidelberg, Germany) in 50 mm NH4HCO3 overnight at 37 °C. Tryptic peptides were extracted with 0.1% trifluoroacetic

acid and subjected to MS-coupled liquid chromatography. For peptide separation over a 180-minute LC-gradient with 300 nL/min, an Ultimate 3000 Rapid Separation liquid chromatography system (Thermo Scientific, Bremen, Germany) equipped with an Acclaim PepMap 100 C18 column (75 µm inner diameter, 25 cm length, 2 mm particle size from Thermo Scientific, Bremen, Germany) was used. MS analysis was carried out on an Orbitrap Lumos mass spectrometer (Thermo Scientific, Bremen, Germany) operating in positive mode and equipped with a nano electrospray ionization source. Capillary temperature was set to 250°C and source voltage to 1.5 kV. Survey scans were carried out over a mass range from 200-2,000 m/z at a resolution of 120,000. The target value for the automatic gain control was 250,000 and the maximum fill time was 60 ms. Within a cycle time of 2 s the most intense peptide ions (excluding singly charged ions) were selected for fragmentation. Peptide fragments were analyzed in the ion trap using a maximal fill time of 50 ms and automatic gain control target value of 10,000 operating in rapid mode. Already fragmented ions were excluded for fragmentation for 60 seconds.

Acquired spectra were searched using Sequest HT within Proteome Discoverer version 2.4.1.15 against a human Swissprot database (Download: 23.01.2020) applying a precursor mass tolerance of 20 ppm and a mass tolerance of 0.5 Da for fragment spectra. Methionine oxidation was considered as variable modification, carbamidomethylation as static modification as well as tryptic cleavage specificity with a maximum of two missed cleavage sites. Post-processing, peptides were ungrouped and filtered to 1% FDR on protein and peptide levels and to all proteins identified with ≥ 2 peptides. Quantification was performed using standard parameters within the predefined LFQ workflow.

2.2.10 Online analysis tools

The Cancer Genome Atlas (TCGA) cohorts and datasets were analyzed using the “cBioPortal” online tool (https://www.cbioportal.org/) (Cerami et al., 2012; Gao et al., 2013). The molecular function of LC-MS analyzed proteins was predicted using the DAVID Functional Annotation Tool (https://david.ncifcrf.gov) (Dennis et al., 2003). Interaction predictions were analyzed and visualized using the STRING algorithm (https://string-db.org) (Szklarczyk et al., 2019). LC-MS data was visualized in Venn diagrams using “Venny” (*Venny 2.1.0*, n.d.). Figures in this work were designed using “Inkscape”. Some of the diagrams were created using the Matplotlib add-on for Python (Hunter, 2007)

3 Results

3.1 Effect of CD24 on immunotherapeutic treatments and targetability via NK-92-CD24-CAR cells

3.1.1 Effect of CD24 on response to immunotherapeutic treatments

The role of CD24 regarding treatment response and resistance mechanisms is still vague. Earlier research showed that CD24 was associated with resistance to certain drugs and a direct targeting of CD24 via the SWA11 antibody led to an increased sensitivity to cisplatin-based therapy. This showed CD24 to be a target of interest in cancer therapy. In a more thorough investigation, we tested a variety of drugs in Δ*CD24* cell lines to evaluate if the presence of CD24 sensitizes or desensitizes cells to treatment with these drugs. We chose drugs with targets that were previously associated with CD24 or are being investigated as cisplatin alternative treatments in TGCTs. We applied concentrations of CDK4/6-(Palbociclib), HSP90-(PU-H71, 17-AAG), histone deacetylase-(Romidepsin, Quisinostat), methyltransferase-(GSK343), and PARP-Inhibitors (Olaparib) in an XTT cell viability assay compared to the WT cells. XTT cell viability assays were performed in the two EC cell lines 2102EP and NCCIT as well as three different clones of their respective Δ*CD24* sublines. Drug response varied and depended on drug concentration, except for treatment with Olaparib and 17-AAG which showed mostly identical responses in all concentrations (Fig. 6).

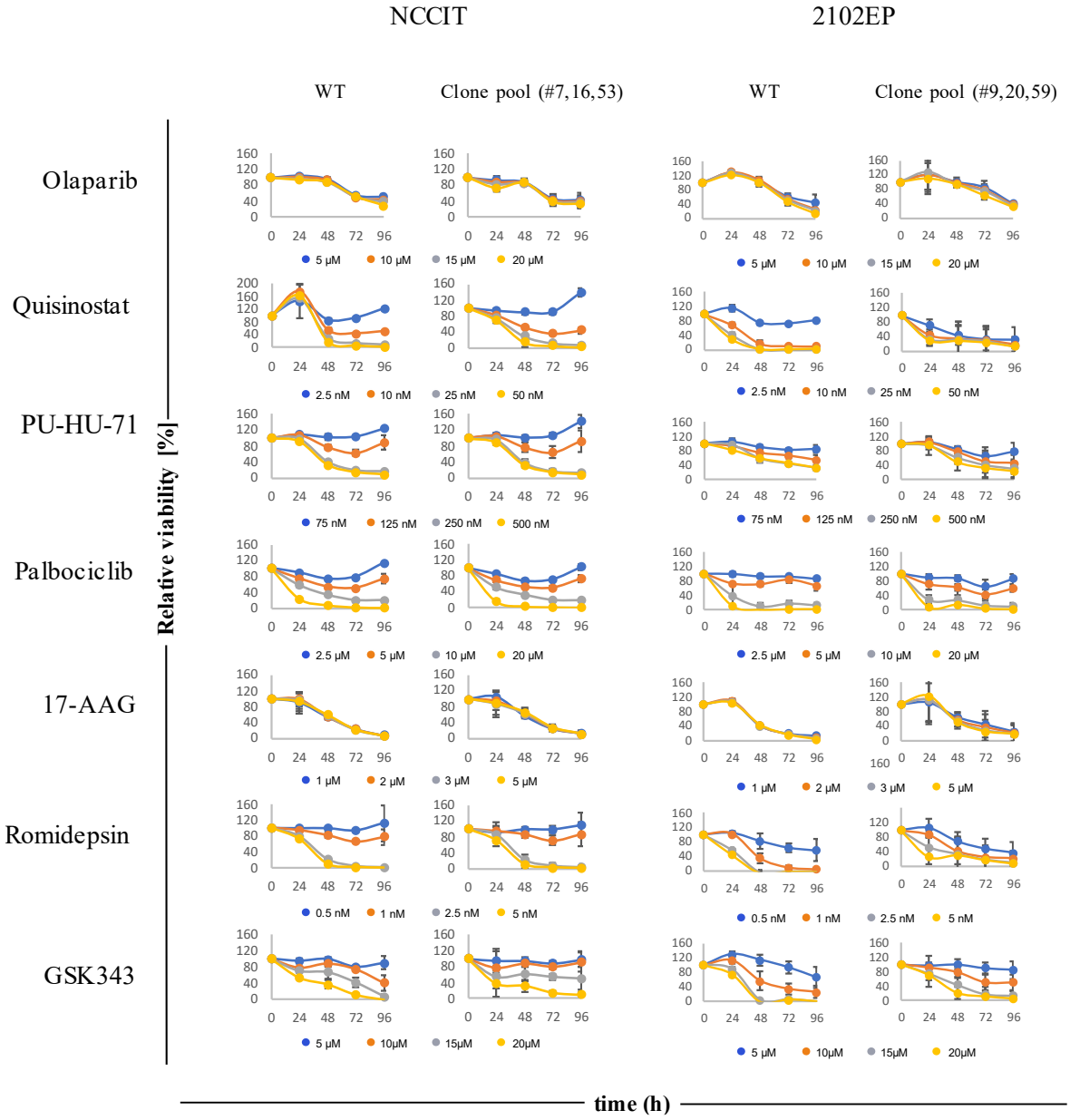

Fig. 6: Drug response in WT and Δ*CD24* EC cell lines
The cell survival of EC cell lines NCCIT and 2102EP after drug treatment in comparison to their respective Δ*CD24* sublines was evaluated via XTT assay. Every drug was applied in four concentrations, Olaparib (5 µM, 10 µM, 15 µM, 20 µM), Quisinostat (2.5 nM, 10 nM, 25 nM, 50 nM), PU-H71 (75 nM, 125 nM, 250 nM, 500 nM), Palbociclib (2.5 µM, 5 µM, 10 µM, 20 µM), 17-AAG (1 µM, 2 µM, 3 µM, 5 µM), Romidepsin (0.5 nM, 1 nM, 2.5 nM, 5 nM), GSK343 (5 µM, 7.5 µM, 10 µM, 12.5 µM). Cell viability was measured every 24 h until 96 h after treatment was reached. Every sample was seeded in quadruplicates and compared to solvent-treated control cells.

Comparing the relative cell viability of the WT cells to their respective clone pools we observed little to no difference in drug response (Fig. 7), which could be explained by the heterogeneous response between the Δ*CD24* sublines. We also determined LD_{50} values and determined fold changes of LD_{50} values of treated WT and Δ*CD24* clones (Fig. 7). We only found relevant differences above the cut-

off values (+ / - 1.5) in Quisinostat in 2102EP cells. LD_{50} values for Olaparib and 17-AAG could not be determined because no visible difference in response between the concentrations could be seen.

	Target	Drug	LD50 WT	LD50 clone pool (n=3)	Fold change (cut off 1,5)
2102EP	EZH2	GSK343	7.57 µM	9.59 µM	1.267
	CDK 4/6	Palbociclib	4.39 µM	5.15 µM	1.173
	HSP-90	PUHU71	>500 nM	456.9 µM	-1.279
		17-AAG	N/A	N/A	N/A
	HDAC	Quisinostat	3.16 nM	0.41 µM	-7.657
		Romidepsin	0.81 nM	1.013 µM	1.250
	PARP	Olaparib	N/A	N/A	N/A
NCCIT	EZH2	GSK343	11.3 µM	10.88 µM	-1.039
	CDK 4/6	Palbociclib	5.46 µM	4.86 µM	-1.123
	HSP-90	PUHU71	256.4 nM	244.9 nM	-1.047
		17-AAG	N/A	N/A	N/A
	HDAC	Quisinostat	11.95 nM	11.35 nM	-1.053
		Romidepsin	1.65 nM	1.75 nM	1.060
	PARP	Olaparib	N/A	N/A	N/A

Fig. 7: Difference in LD_{50} values between WT and Δ*CD24* EC cell lines
The fold change was determined by the LD50 values of cells treated with the various drugs. Fold changes over +/- 1.5 were considered relevant changes in drug response. The LD50 values for Δ*CD24* cells were determined for the pooled results of three different Δ*CD24* clones. Values for 17-AAG and Olaparib could not be determined and are marked N/A (not available)

3.1.2 Treatment with natural killer cells equipped with a chimeric antigen receptor targeting CD24

Previous molecular characterization of *CD24* showed high mRNA and protein levels of *CD24* / CD24 in a variety of urological malignancies, especially in the EC cell lines. As previously described CD24 seems a promising target for an immunotherapeutic or cell-based therapeutic approach. To verify this, we used NK92-CD24-CAR effector cells which contain a third-generation chimeric antigen receptor (CAR) established by Klapdor et al (Klapdor et al., 2019) to evaluate the effect on cell viability in a co-culture model with $CD24^+$-EC cell lines and their respective cisplatin-resistant clones. Controls consisted of untransduced NK-92 cells without a CAR, CD24-negative seminoma cell line TCam-2, CRISPR/CAS9-generated Δ*CD24* cell lines, and healthy fibroblasts. As a means to evaluate the effect of this co-culture treatment on GCT cells, we used XTT cell viability assays.

To thoroughly investigate the effect of CAR-NK we treated $CD24^+$ EC cell lines, their respective cisplatin- and Δ*CD24*-clones, $CD24^-$ cells, and healthy fibroblasts with NK-92-CD24-CAR cells and NK-92 cells. Expected results in $CD24^+$ cell lines were an increasing toxicity with increasing effector-target-ratio, as well as time, passed due to the accumulating and lasting cytotoxic effect of activated NK-92-CD24-CAR cells (Fig. 8).

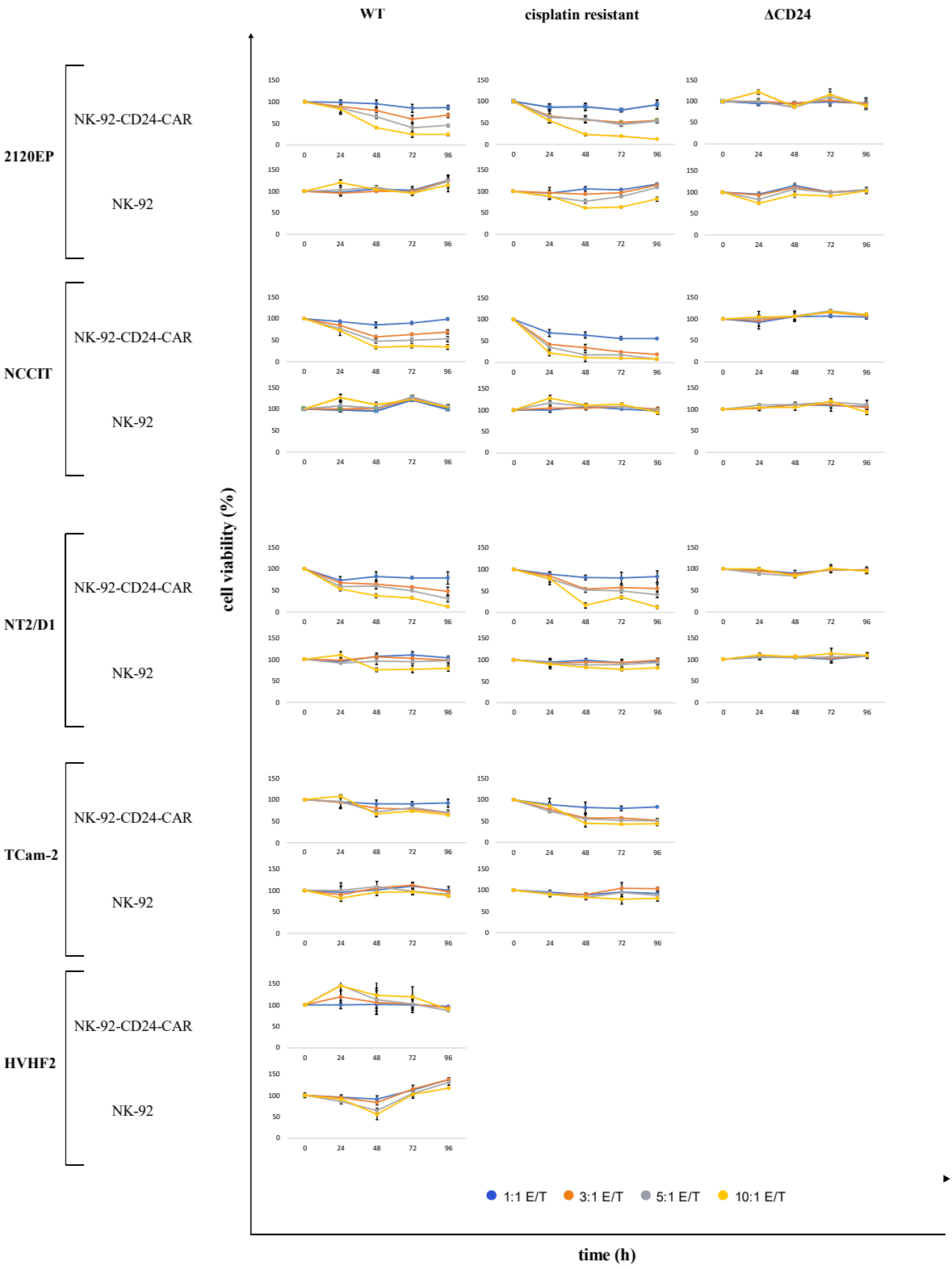

Fig. 8: NK-92-CD24-CAR treatment in XTT assays
Cell survival, in an XTT assay, of SE, fibroblast, and EC cell lines with their respective cisplatin-resistant and CD24 deficient (Δ*CD24*) cell lines after treatment with NK-92-CD24-CAR. Treatment with untransduced NK-92 cells and in Δ*CD24* cell lines served as controls. The treatment was applied in different effector-target-ratios (E / T) of 1:1, 3:1, 5:1, and 10:1. Measurements were made in 24 h intervals up to 96 h after drug application. All samples were seeded in quadruplicates and cell viability was compared to solvent-treated control cells.

As expected, the XTT cell viability assay showed a reduction of cell viability in $CD24^+$ cell lines in this exemplary data after 48 h a reduction in the cell viability to around 60 % in the 5:1 ratio, and a reduction to 44 % in the 10:1 ratio can be observed. This effect was even more pronounced in the cisplatin-resistant cells with viability reductions to under 18 % after 48h in the 5:1 ratio and under 11 % in the 10:1 ratio. In contrast, the cell viability of Δ*CD24* cells fluctuated around 100 % as expected. Treatment with untransduced NK-92 cells also showed no reduction in cell viability with measurements varying around the 100 % cell viability mark. This led us to the conclusion, that, firstly, a higher ratio of effector cells to target cells leads to an increased toxicity and, secondly, NK-92-CD24-CAR cells specifically target cells presenting CD24 and are not activated by tumor cells lacking CD24.

A comparison and compilation of all tested cell lines treated with an effector target ratio of 5:1 after 48h of treatment is shown in Fig. 9. Cell viability was sorted into 3 different categories and presented graphically.

Entity	Cell line	CD24	NK-92	CD24-CAR NK92
EC	2102EP WT	+	●	●
	2102EP-R	+	●	●
	2102EP Δ*CD24*	-	●	●
	NCCIT WT	+	●	●
	NCCIT-R	+	●	●
	NCCIT Δ*CD24*	-	●	●
	NT2/D1 WT	+	●	●
	NT2/D1 -R	+	●	●
	NT2/D1 Δ*CD24*	-	●	●
Seminoma	TCam-2	-	●	●
	TCam-2-R	-	●	●
Fibroblasts	HVHF2	-	●	●

Tumor cell viability in comparison to untreated control cells
Cohort: 48 h, effector target ratio of 5:1

● > 66 %
● 66 % - 33%
● < 33 %

Fig. 9: Summary of NK-92-CD24-CAR treatment in XTT assays
A summary of the results of XTT cell viability assays after NK-92-CD24-CAR treatment compiling the data of the 48 h measurement in the 5:1 effector-target-ratio. Cell viability was color-coded into three categories

(green dots over 66 % viability, orange dots between 33 % and 66 % viability, red dots under 33 % viability). This experiment covered 3 different EC cell lines and their cisplatin-resistant sublines. Controls consisted of CD24-cell line TCam-2 and cisplatin-resistant subline, healthy fibroblasts HVHF2, and ΔCD24 sublines of the 3 EC cell lines.

The compilation of the results showed that the specific elimination of $CD24^+$ tumor cells by NK-92-CD24-CAR treatment was not limited to the NCCIT cell line but was observed in all three different EC cell lines. After 48 h, all EC WT cell lines showed a viability reduction under 66 % in the 5:1 ratio, this effect was even more pronounced in the cisplatin-resistant clones as all showed viabilities under 60 %. Similar to the previous observations, treatment with untransduced NK-92 cells led to little to no reduction in cell viability, while cell viability in the control cell lines HVHF2 and Δ*CD24* remained unchanged. The cisplatin-resistant $CD24^-$ cell line TCam-2 showed reductions in cell viability up to 57 % after 48 h of treatment. In summary, all three EC cell lines NCCIT, 2102EP, NT2/D1, and their respective cisplatin-resistant clones showed a medium to high vitality reduction after CD24-CAR-NK-92 treatment. Additionally, the cytotoxic effect specifically targeted cells presenting CD24, as our fibroblast and $CD24^-$ controls showed little to no reduction in cell viability.

3.2 Identification of direct interaction partners of CD24 in urologic malignancies

To identify the interaction partners of CD24 we performed co-immunoprecipitations (Co-IP) using magnetic beads. The resulting isolated proteins were further analyzed by mass spectrometry. Our goal was to identify proteins that interact with CD24 and investigate their function and involvement in biological processes to gain further insights into the role of CD24 in urological tumors.

We performed these experiments in EC cell lines to further build on our previous understanding of CD24 in GCTs and expanded the experiments to other urological tumors like UC, PC, and RCC.

After the bead-antibody coupling process, using the CD24 antibody SWA11 or an unspecific IgG_{2a} antibody, 1mg of protein was added to each sample. In EC cell lines controls consisted of Co-IP performed with the unspecific IgG_{2a} antibody in WT cells and the SWA11 antibody in CRIPSR/CAS9-generated *CD24* deficient EC cell lines (Δ*CD24*), whereas controls in other urological tumor cell lines only consisted of the unspecific IgG_{2a} antibody and WT cells.

3.2.1 Identification of $CD24^+$ cell lines in UC, PC and RCC

It is known that *CD24* is frequently expressed in a variety of tumor cell lines. In order to gain an overview of *CD24* mRNA expression in urological malignancies we checked the TCGA cohorts of TGCTs, UC, PC, and ccRCC for mRNA expression using cBioPortal. We found high expression of

CD24 in all urological tumor entities with already known low values in seminoma (Fig. 10, [A]). To check for *CD24* expression on mRNA level in urological tumor cell lines Dr. Margaretha Skowron and Dr. med. Gamal Wakileh (Söhngen et al., 2023) (Söhngen,Master thesis, 2022) qRT-PCR to check for *CD24* expression in UC, PC and RCC cell lines. We found high expression in EC cell lines NCCIT, 2102EP, and NT2/D1, in UC cell lines SW1710 and RT112, and in RCC cell line Caki-1. Medium expression was seen in RCC cell line 786-O and PC cell line PC-3 (Fig. 10, [B]). In the next step, we checked a panel of UC (VM-CUB-1, SCABER, RT112, SW1710), RCC (Caki-1, 786-O, ACHN), and PC (DU-145, PC-1, LNCaP) cell lines for CD24 protein levels.

Using the western blot analysis, we could confirm multiple cell lines per tumor entity translating CD24 protein (Fig. 10, [C], [D]). The cell lines RT112, SW1710, Caki-1, 786-O, DU-145, and PC-3 were identified as $CD24^{+}$, and we chose cell lines RT112 for UC, Caki-1 for RCC and PC-3 for PC for our further analysis. The appearance of CD24 protein bands in a Western Blot varied in different cell lines. This is a product of varying molecular weight depending on glycosylation. While the center of the band was found around the 35 kDa mark in most cell lines, different CD24 proteins fell into the ranges between 23 kDa to 55 kDa (Fig. 10, [C], [D]).

A

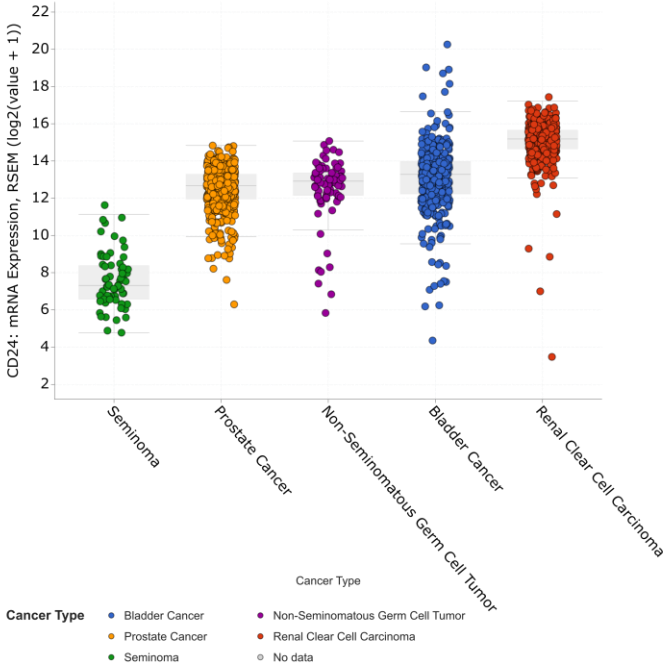

B

Entity	Cell line	mRNA	Protein
EC	NCCIT	++	++
	2102EP	++	++
	NT2/D1	++	++
Seminoma	TCam-2	-	-
UC	SW1710	++	++
	RT-112	++	++
	VM-CUB-1	-	-
	UM-UC-3	-	-
	T24	-	-
RCC	Caki-1	++	++
	786-O	+	+
	ACHN	-	-
PC	PC-3	+	+
	DU-145	+	++
	LNCaP	-	-

C

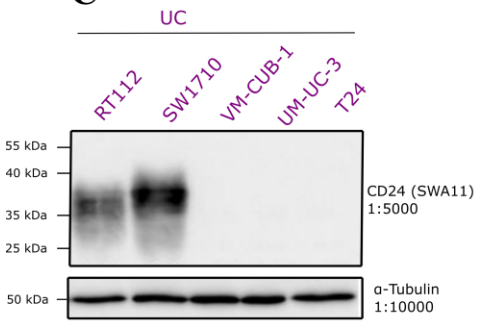

D

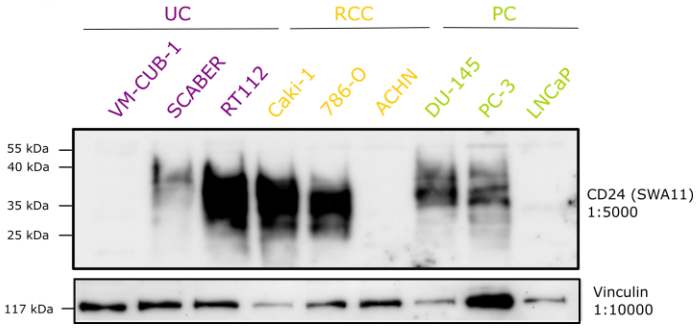

Fig. 10: *CD24* mRNA and CD24 protein levels in urological tumor entities
[A] TCGA analysis of mRNA expression in urological malignancies using cBioPortal for Cancer Genomics, [B] Summary of mRNA and protein levels in urological malignancies, qPCR and some of the western blots were performed by Gamal Wakileh and Margaretha Skowron, ((Skowron et al., 2022), (Söhngen et al., 2023)), [C] Western Blots for UC cell lines performed by Christian Söhngen, 20 µg of protein were separated via SDS-PAGE, transferred to PVDF-membrane, and stained with the CD24 antibody SWA11 (dilution 1:5000). α-Tubulin (dilution 1:10000) served as a loading control, [D] CD24 protein levels in UC (VM-CUB-1, SCABER, RT112), RCC (Caki-1, 786-O, ACHN) and PC (DU-145, PC-3, LNCaP) were analyzed via Western Blot assay.

20 µg of protein were separated via SDS-PAGE, transferred to PVDF-membrane, and stained with the CD24 antibody SWA11 (dilution 1:5000). Vinculin (dilution 1:10000) served as a housekeeper.

3.2.2 Confirmation of successful Co-IP via Western blot

Since CD24 itself is not identifiable in an LC-MS analysis, due to its extensive and varying glycosylation as well as posttranslational modification, we performed western blot analysis of co-immunoprecipitation samples to confirm their success (Fig. 11).

The different input controls showed us the extensive and varying glycosylation of CD24 leading to the typical CD24 band between 25 and 55 kDa. In the controls, we mainly saw the heavy and light chains of the used antibodies at 25 kDa and 55 kDa respectively although a small amount of protein

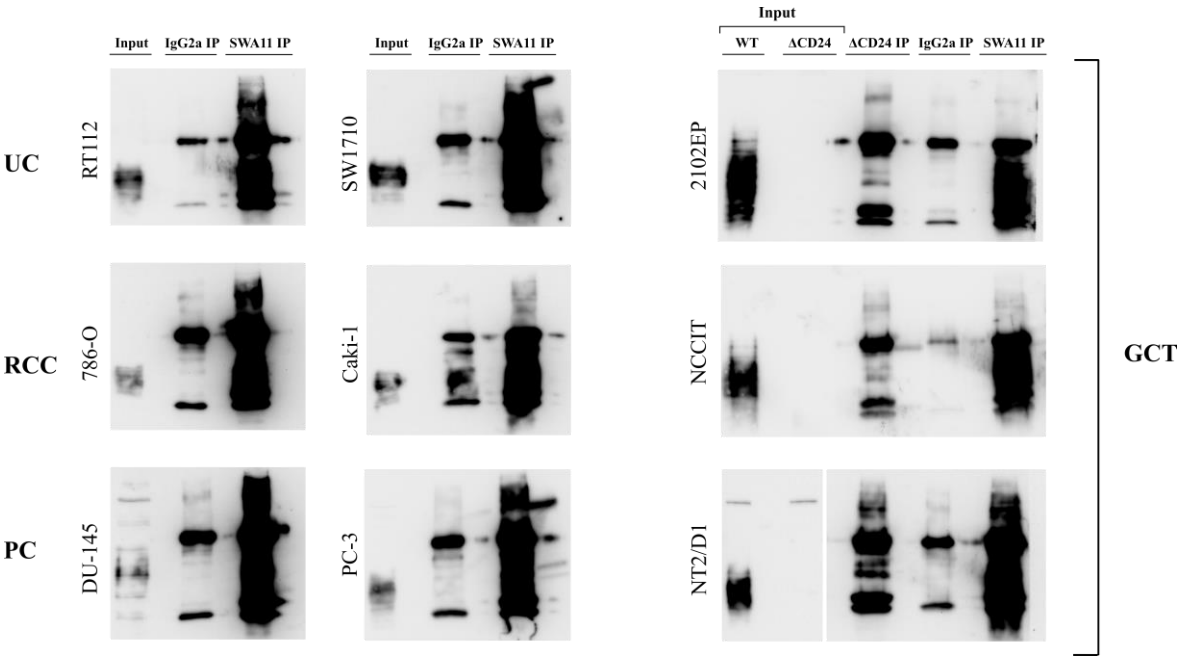

Fig. 11: Western blot analysis of protein lysates upon co-immunoprecipitation with CD24
Confirmation of successful co-immunoprecipitation via western blot in protein lysates of EC cell lines, their Δ*CD24* sublines, UC, RCC, and PC upon co-immunoprecipitation with CD24 or IgG2a isotype control. For comparison an input control (2 %, 20 µg) was added. SWA11 (dilution 1:5000) antibody was used for staining.

seemed to have precipitated in the Δ*CD24* SWA11 Co-IP. CD24 itself did not seem to precipitate. Contrarily a large amount of CD24 and associated proteins was isolated in the WT SWA11 Co-IPs leading to over-saturation due to the high amount of protein used. Because of these Western blots, we concluded that our Co-IP of CD24 in the respective cell lines was successful. Our samples were sent to the Molecular Proteomics Laboratory at the Biologisch-Medizinisches Forschungszentrum (Biologisch-Medizinisches Forschungszentrum (BMFZ), Lab Proteomics, director Prof. Dr. Kai

Stühler, HHU) for LC-MS. Further analyses were performed by Dr. Anja Stefanski (BMFZ-Molecular Proteomics Laboratory).

3.2.3 Characterization of CD24 interaction partners by LC-MS analysis

The subsequent LC-MS analysis was carried out to accurately identify which proteins precipitated with CD24 in the varying tumor entities. This was especially important as this study aimed to further understand the role of CD24 in urological tumor entities and a common interaction partner could deliver new starting points for further investigation. In an initial analysis, all detected proteins were sorted regarding signal intensity we initially only included proteins with a log_2 transformed signal intensity of over 22. First, we compared the co-immunoprecipitated proteins of all three EC cell lines NCCIT, NT2/D1, and 2102EP, normalized against the IgG_{2a} isotype and Δ*CD24* controls (Fig. 12). We found 94 out of 547 proteins which precipitated in all three EC cell lines which corresponded to 16.37 % of all proteins above the cutoff threshold. To further generalize possible interaction partners, we correlated the 94 proteins found in ECs with the co-immunoprecipitated proteins of the UC cell line RT112, the PC cell line PC-3, and the RCC cell line Caki-1. Only 2 out of 254 proteins co-immunoprecipitated with CD24 in all cell lines. These two proteins were CKAP4 and MYO1C. Nevertheless, we identified multiple interesting interaction partners of CD24 that were previously reported and were present in multiple urological tumor entities. These proteins were NPM1, HSP70, HSP90, HMGB1, RalA and RalB.

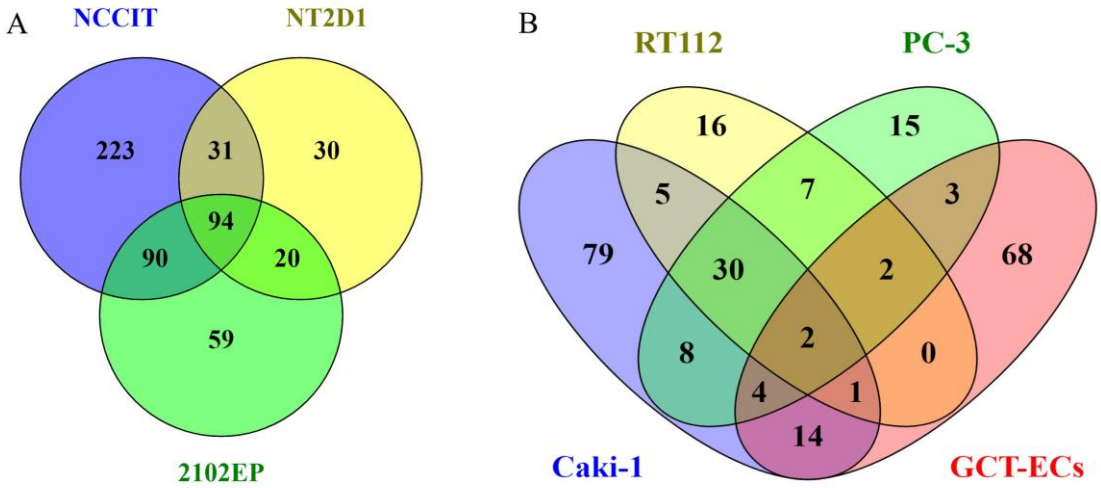

Fig. 12: Comparison of immunoprecipitated proteins in ECs, UC, RCC, and PC
[A] A Venn diagram showing commonly interacting proteins in EC cells after normalization to the IgG2a and ΔCD24 EC cell controls, the cutoff threshold was a log2 transformed signal intensity of over 22. Proteins were identified through Co-IP followed by LC-MS. [B] Venn diagram showing commonly interacting proteins between UC, RCC, and PC after Co-IP and LC-MS cutoff threshold was a log2 transformed signal intensity of over 22.

Upon further analysis and in reaction to the large quantity of identified targets we chose to raise the stringency to abundance ratios above 10 and a p-value of <0.05. Results of this more stringent analysis can be found in Fig. 13[A,B] where firstly we compared the co-immunoprecipitated proteins of the pan-urological cell lines Caki-1, PC-3, and RT112. We found 25 commonly precipitated proteins in RCC, UC, and PC cell lines and some overlap of up to 80 proteins between two out of three cell lines in this case PC-3 and Caki-1 (Fig. 13, [A], Table 31). In comparison in (Fig. 13, [B], Table 32) we compared the precipitated proteins of the three EC cell lines NCCIT, NT2/D1 and 2102EP, normalized against the IgG_{2a} isotype and Δ*CD24* controls. We found 8 out of 422 proteins precipitated in all three EC cell lines which corresponds to 1.89 % of all proteins above the cutoff threshold. These proteins were ACHE, C6orf120, CNTFR, GDE1, MFSD10, RAPA2A, STX10 and TRABD. The same was done for immunoprecipitated proteins in our three panurological cell lines and here we found 25 common proteins between the RCC, PC, and UC cell lines (Fig. 13, [B], Table 31). Again, we correlated the 8 proteins found in ECs with the co-immunoprecipitated proteins of the UC cell line RT112, the PC cell line PC-3, and the RCC cell line Caki-1. Here we found no overlapping proteins that precipitated in all cell lines. In addition, a principal component analysis (PCA) of the results was performed (Fig. 13, [C]). It showed clusters of CD24 Co-IP using the SWA11 antibody separated from the controls using the IgG_{2a} isotype control. Co-IPs of Δ*CD24* cells using the SWA11 antibody also clearly clustered apart from the WT cells further validating the successful Co-IP.

A

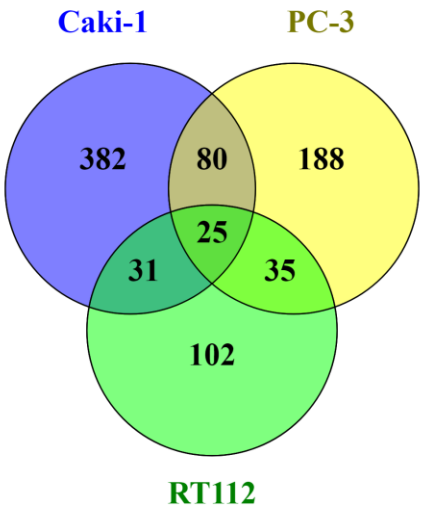

B

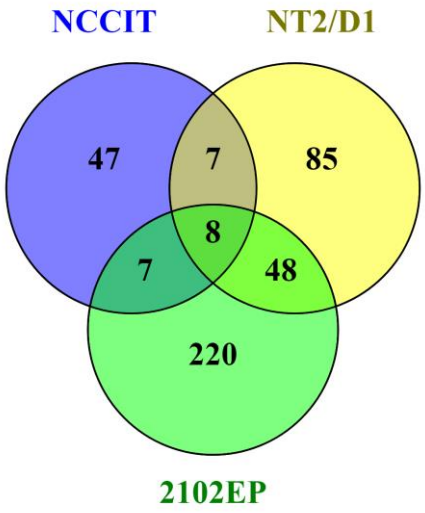

C

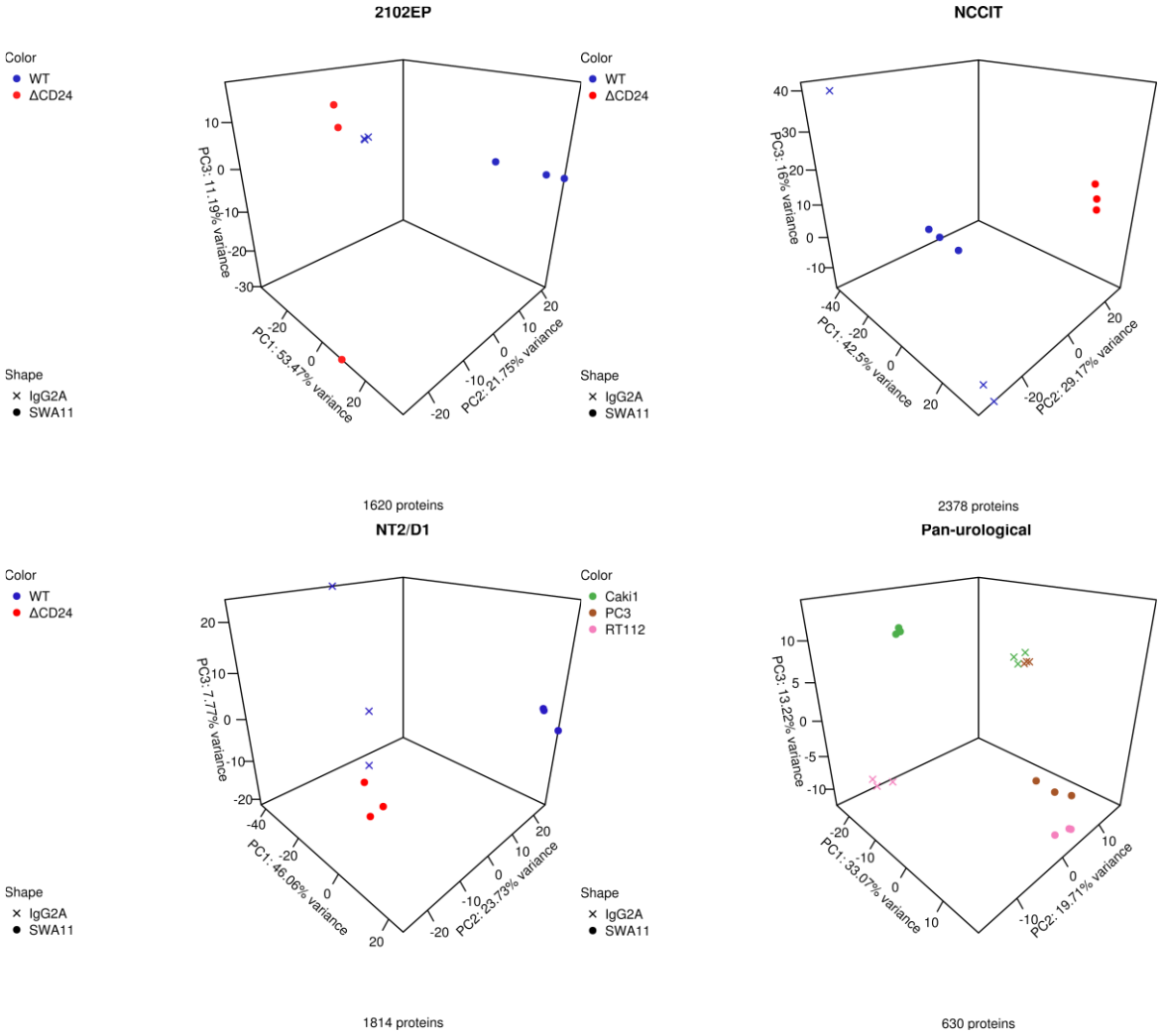

Fig. 13: Overlap of protein interaction partners and principal component analysis in Co-IPs of EC cell lines and other urological malignancies

[A] A Venn diagram showing commonly interacting proteins in EC cells after normalization to the IgG_{2a} and Δ*CD24* EC cell controls. Proteins were identified through Co-IP followed by LC-MS. [B] Venn diagram

showing commonly interacting proteins between UC, RCC, and PC after Co-IP and LC-MS. [C] Principal component analysis (PCA) plots of MC-LS after Co-IP using the CD24 antibody SWA11 or an IgG2a isotype control in three EC cell lines and Δ*CD24* sublines (2102EP, NCCIT, NT2/D1), RCC (Caki-1), PC (PC-3) and UC (RT-112) cell lines (n = 3).

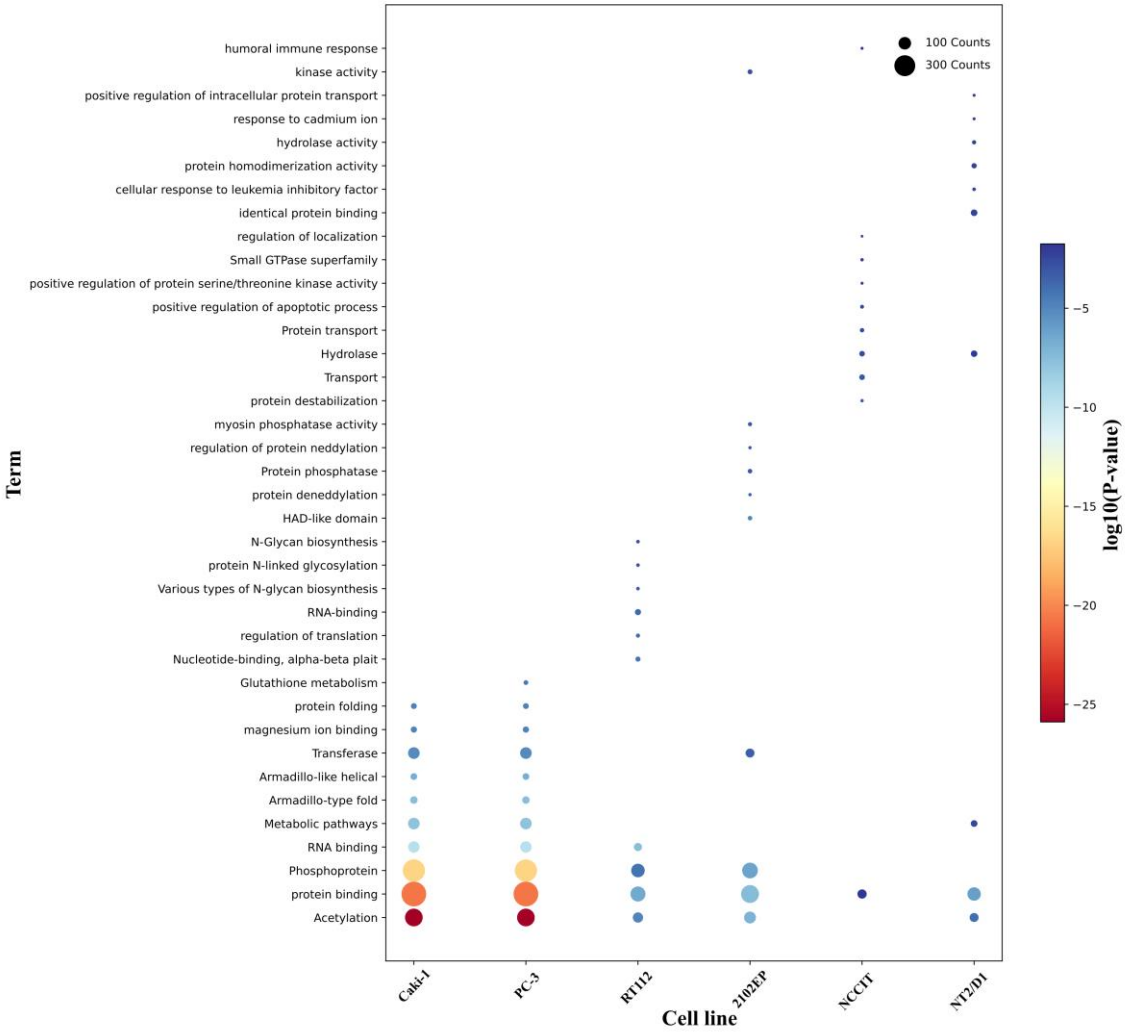

Fig. 14: DAVID gene ontology analysis of immunoprecipitated proteins
Co-immunoprecipitated proteins were further analyzed via mass spectrometry analysis. For each entity proteins with an abundance ratio of over 10 and a p-value <0.05 were analyzed via DAVID Gene Ontology with the categories UP_KW_biological process, UP_KW_molecular function, UP_KW_PTM, GOTERM_BP_DIRECT, GOTERM_MF_DIRECT, KEGG_PATHWAY and INTERPRO. The top 10 results for each tumor entity are displayed here. Terms are presented on the Y-axis, cell lines on the X-axis, counts are presented by dot size, and the p-value is color-coded from blue to red.

However, since the goal of this study was to gain insights into the function of CD24, not only the amount and names of precipitated proteins but also their involvement in biological processes and interactions was of great interest to us. Therefore, STRING and DAVID (GO) analysis of the precipitated proteins with an abundance ratio of over 10 and a p-value <0.05were performed to

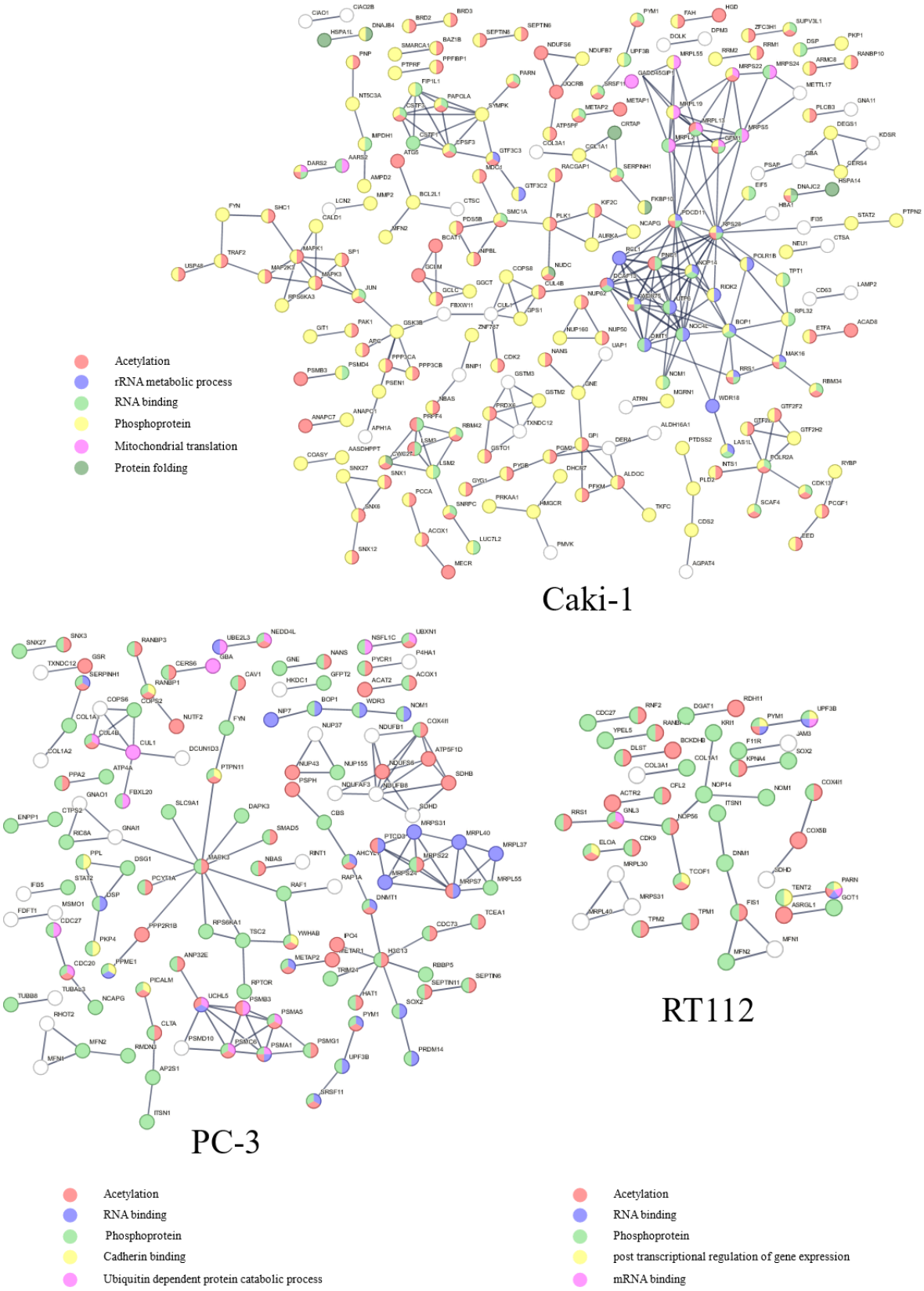

Fig. 15: STRING analysis of CD24 interaction partners in UC, RCC, and PC
For each entity proteins with an abundance ratio of over 10 and a p-value <0,05 were analyzed via STRING analysis. Proteins in the network are further color-coded for biological functions previously found in the DAVID gene ontology analysis.

identify clusters or common pathways interaction partners of CD24 are involved in, per respective tumor entity (Fig. 14, Fig. 15, appendix Fig. 17, Table 33-38). For DAVID gene ontology analysis, we searched UP_KW_biological process, UP_KW_molecular function, UP_KW_PTM, GOTERM_BP_DIRECT, GOTERM_MF_DIRECT, KEGG_PATHWAY and INTERPRO. DAVID gene ontology analysis for the proteins identified in GCTs revealed the involvement of the interaction partners in protein binding, protein transport, phosphoprotein binding, and most importantly post-translational modifications for example histone acetylation and protein folding. Although, as described earlier, the interaction partners of CD24 were highly variable in different urological tumor entities DAVID gene ontology analysis under the same parameters showed CD24 interaction partners in UC, RCC, and PC to be involved in highly similar biological processes of protein binding, RNA binding and post-translational modifications like acetylation and protein binding and folding. Similar DAVID and STRING analyses performed for the 25 common proteins in the panurological cell lines and the respective 8 proteins commonly found in all EC cell lines showed little to no involvement in the aforementioned biological processes (Fig. 16).

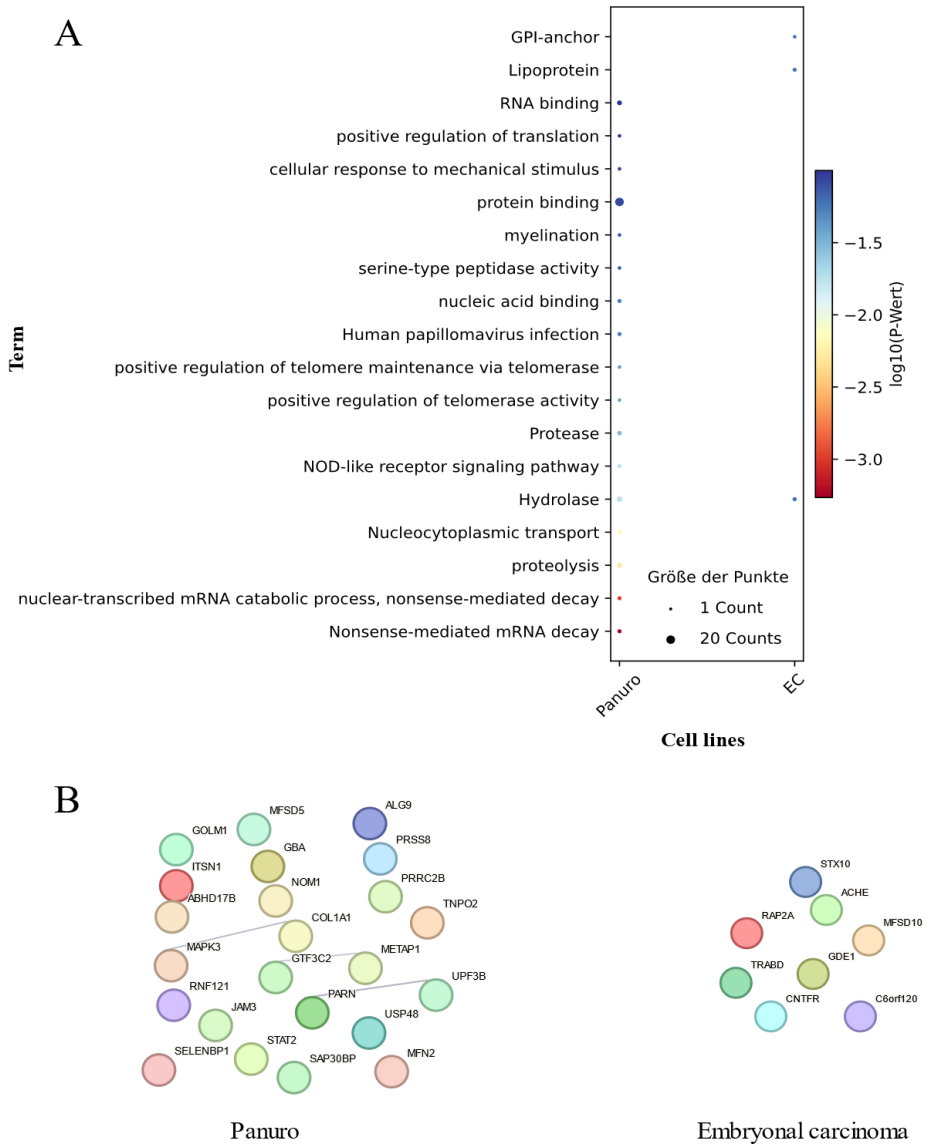

Fig. 16: DAVID and STRING Analysis of common interaction partners in embryonal carcinoma and panurologically

[A] Co-immunoprecipitated proteins were further analyzed via mass spectrometry analysis. Proteins with an abundance ratio of over 10 and a p-value <0.05 were compared for each cell line. Common proteins in EC cell lines (n=8, Table 32) and panurological cell lines (n=25, Table 31) were then analyzed via DAVID Gene Ontology with the categories UP_KW_biological process, UP_KW_molecular function, UP_KW_PTM, GOTERM_BP_DIRECT, GOTERM_MF_DIRECT, KEGG_PATHWAY and INTERPRO. Terms are presented on the Y-axis, cell lines on the X-axis, counts are presented by dot size, and the p-value is color-coded from blue to red. [B] STRING analysis was performed for these proteins.

4 Discussion and Conclusion

In this study, we were able to gain new insights into interaction partners of CD24 and therefore its molecular function in especially TGCTs and urological malignancies overall. We showed that *CD24* was expressed in at least one cell line of every urological tumor entity on mRNA and protein levels. Additionally, we showed CD24 to be a promising target for immune cell-based therapy with therapeutic NK-92-CD24-CAR *in vitro*. The relevance of these results and discoveries will now be discussed regarding their therapeutic and biological implications.

4.1 Presence of CD24 and its influence on therapy response in TGCTs

The results of our cell viability assays indicate that CD24 does not have a major influence on drug response in the two different EC cell lines NCCIT and 2102EP. Upregulation of *CD24* is associated with poor patient prognosis because of enhanced immune evasive, invasive, proliferative, and migratory capabilities. Additionally, blockade of CD24 using the SWA11 antibody led to increased cisplatin sensitivity in TGCTs, and CD24 was shown to modulate treatment responses in certain tumor types. As cisplatin alternative treatments in especially recurring and cisplatin-resistant TGCTs are still lacking and these tumors are often at least partially comprised of CD24+ EC cells we tested a catalog of drugs for their treatment effects in WT, cisplatin-resistant, and Δ*CD24* EC cell lines. Of special interest was a potential modulating effect of the presence of CD24 on drug response. The drugs we used were all selected either for their target being associated with CD24 or they were previously shown to be successful in TGCT treatment in previous works in our research group (Kurz et al., 2020; Müller et al., 2022; Skowron et al., 2020, 2022). The first group of drugs were HSP90 inhibitors (PU-H71, 17-AAG) a drug mainly used in breast cancer and melanoma research. HSP90 is a protein tightly associated with CD24 and tumor angiogenesis while also being recruited into lipid rafts by CD24 (X. Wang et al., 2016). Treatment with an HSP90 inhibitor shows a significant dose-dependent reduction in cell viability but the hypothesized reduction of HSP90 in Δ*CD24* cells shows no therapy-modulating effect. This is in line with HSP90 inhibitor studies in $CD24^-$ breast cancer stem cells that inhibited tumor growth, because extracellular HSP90 was targeted that is not influenced by the presence of CD24 (Stivarou et al., 2016). The second group was epigenetic drugs that were previously shown to be effective in TGCTs like histone deacetylase inhibitors (Quisinostat, Romidepsin) and polycomb-repressive complexes (GSK343) (Müller et al., 2022) but also might interfere with CD24 function as CD24 utilizes epigenetic mechanisms (Skowron et al., 2022). Treatment with these drugs showed some difference in response in the 2102EP cell line but not the NCCIT cells. These results in – 2102EP-Δ*CD24*most likely result from the inhomogeneous behavior of the Δ*CD24* clones, as each clone showed vastly different drug response and the results were shown

as a pool of the clone results. The third group was PARP inhibitors which also are believed to be promising targets in TGCTs (Cavallo et al., 2012). The presence of *CD24* does not show any influence on PARP inhibitor response in our results although a newer study found PARP1 to attenuate the transcription of *CD24* and *PARP*- and CD24 inhibition were recently shown to have a synergistic effect in pancreatic cancer by Chen et al. (K. Chen et al., 2023). The last drug was a CDK4/6 inhibitor that was also shown as a promising target in TGCT treatment (Skowron et al., 2020). Again, our results do not indicate any difference in drug response which was to be expected since literature research showed no connection between CD24 and CDK4/6.

4.2 Relevance of CD24 expression levels in urological malignancies

An important step in the evaluation of CD24 as an immunotherapeutic target is an investigation into the expression levels of *CD24* to evaluate its fitness as a tumor-associated antigen. This includes not only the antigen localized on the cell surface but also mRNA levels and cytoplasmatic protein levels. To identify interaction partners of CD24 in urological tumors and test a cell-based therapy in EC we tested multiple cell lines per tumor entity for *CD24* gene expression and CD24 protein levels.

Results of qRT-PCR analysis to determine *CD24*-mRNA levels performed in our lab (CD24 therapy paper) show varying results in urological malignancies. *CD24*-mRNA levels seem to be cell-line specific and suggest different expressions of *CD24* in different tumor subtypes. In TGCTs, the EC group was shown by Skowron et al. to be highly *CD24* positive and this effect was consistent in different EC cell lines (Skowron et al., 2022). UC cell lines show very different levels of *CD24* expression with RT-112 and SW1710 reaching mRNA levels comparable to EC cell lines and other cell lines showing little *CD24* mRNA expression (CD24 therapy paper). This is in concordance with studies into UC subtyping which describe *CD24* as a marker for luminal phenotypes in bladder cancer (Guo et al., 2020) and meta-analysis showing CD24 to be associated with advanced clinical stages and lymphovascular invasion (Lee et al., 2009). Thus, tumor stage and type upon generation of the cell line most likely determines *CD24* status in UC cell lines. In RCC Söhngen et al. (Söhngen et al., 2023) show differing levels of *CD24* mRNA with Caki-1 showing high levels, 786-O intermediate levels, and ACHN showing low *CD24* levels. *CD24* expression is again cell line dependent, Caki-1 and 786-O are clear cell RCC and were both *CD24* positive in contrast to the *CD24* negative papillary RCC cell line ACHN. This may look like *CD24* expression might be again subtype-specific, but previously performed research by Arik et al. (Arik et al., 2017) showed that *CD24* expression is heterogeneous with close to 50 % fractions in the clear cell and papillary / chromophobe RCCs. In RCC cell lines, *CD24* expression seems to correlate more with differentiation and prognosis than tumor type. PC shows only low *CD24* mRNA levels in both cell lines DU-145 and PC-3 and a recent publication by Tolkach et al. suggests that CD24 expression might be most dependent on molecular

events like TMPRSS2-ERG fusion or PTEN deletion (Tolkach et al., 2021). In summary, the expression of *CD24* is regulated by a variety of mechanisms that might be tumor entity-specific, but the function and processes CD24 is involved in, as well as its association with poorer prognosis, seem to be generally applicable in urological malignancies.

We also checked CD24 protein levels with Western Blot analysis in the most promising urological cell lines and compared protein and mRNA levels. Our results show a high correlation of mRNA and protein levels with cell lines with high *CD24* mRNA levels also having a significantly larger amount of CD24 protein (Söhngen et al., 2023). Our urological cell lines showed CD24 molecular weights between 23 and 54 kDa and were not only entity but also cell line specific. A wide range of molecular weights is in line with CD24s varying extensive glycosylation making up most of its molecular weight. This fits with research in a variety of tumor entities where even molecular weights of up to 70 kDa were described, furthermore, glycosylation may also be different in membrane-bound CD24 and secreted or cytosolic CD24 (Altevogt et al., 2021).

In summary, this study evaluated the CD24 expression in the main urological malignancies of TGCTs, UCs, PCs, and RCCs and showed CD24 expression to be cell line specific. This is in line with other studies that showed CD24 expression to be very heterogeneous in urological malignancies and to mainly correlate with advanced tumors or to be associated with molecular tumor subtypes for example in bladder cancer. This establishes an important baseline for further research into CD24 especially for therapeutic approaches targeting CD24.

4.3 CD24 interaction partners in urological malignancies

CD24 plays an important role in tumor progression and immune evasion and although some interaction partners of CD24 have been identified, not all molecular mechanisms of CD24 have been unraveled yet. In this study, we identified CD24 interaction partners in the highly CD24-positive EC, UC, RCC, and PC cell lines to understand CD24 molecular function in urological malignancies. We identified 94 common interaction partners in three EC cell lines but comparison to the interaction partners of UC, RCC, and PC only showed two proteins found in all entities, CKAP4 and MYO1C. We predicted protein processes in a pool of three EC cell lines and DAVID gene ontology analysis showed CD24 to interact with proteins involved in protein binding, phosphoprotein binding, RNA binding, GPI-anchorage, and post-translational modifications like acetylation. Identical analysis of the identified interaction partners in UC, RCC, and PC revealed predicted interactions highly similar to the results of the EC analysis leading us to the conclusion that CD24 seems to play a similar role in all urological malignancies. As our initial analysis revealed a lot of interaction partners with questionable reliability in the next step, we raised the stringency of our analysis by including a p-value and an abundance ratio above 10. After this increase of stringency, the number of common

interaction partners in GCT and pan-urological cell lines dropped by a significant amount and no common interaction partners between all cell lines could be identified. Literary Research into the 8 commonly found proteins in EC cell lines and the 25 commonly found proteins in UC, RCC, and PC revealed no previously known or researched associations of these Proteins with CD24. Nonetheless, analysis of these more stringent interaction partners still showed them to be mainly involved in the previously mentioned processes in ECs, as well as pan-urologically. These results are in line with our previous research that showed CD24 to suppress mesodermal and endodermal differentiation via homeobox, glycol- and phosphoproteins influencing transcription, protein processing, extracellular signaling, and potassium transport, while also promoting ectodermal differentiation via glycol- and phosphoproteins that influence G-coupled receptors and cytokine-mediated signaling (Skowron et al., 2022) The two commonly found interaction partners CKAP4 and MYOC1 can also be of interest and were not previously described to interact with CD24. CKAP4 was shown to be an important target in cancer and especially in some urological malignancies (S. X. Li et al., 2020). Shanjee et al (Shahjee et al., 2010) showed CKAP4 to enhance the antiproliferative activity of APF in UC cells leading to upregulation of TP53, activation of AKT / GSK3β / β-catenin and phosphorylation, and downregulation of MMP2 expression. In ccRCC Sun et al (C. M. Sun et al., 2017) showed CKAP4 overexpression to promote cell proliferation, invasion, and migration by modulating cell cycle through CCNB signaling and to be associated with advanced tumor stage and Fuhrmann grade, although overexpressed CKAP4 is only found in 5 % of ccRCC patients. Overall CKAP4 seems to play an important role in cancer although it is not certain if it is a pro-cancer or anticancer protein and this might depend on specific circumstances or tumor entity (S. X. Li et al., 2020). MYO1C, on the other hand, was found to be a suspect for a tumor suppressor gene by Hedberg et al. (Hedberg Oldfors et al., 2015), further research by Visuttijai et al.(Visuttijai et al., 2016) then found evidence for a negative correlation of MYO1C and cell proliferation, migration and adhesion in endometrial cancer and ascribed this to MYO1C playing a role in the PI3K pathway by binding PIP2. After binding to PIP2 MYO1C also becomes associated with lipid rafts where it might interact with CD24. In contrast, studies in PC cell lines showed the MYO1C isoform A to function as a driver of invasion and metastasis by driving secretion of exosomes enabling invasion across extracellular matrix barriers (Maly et al., 2017). According to Saidova et al (Saidova et al., 2021) it might also serve as a marker for PC and is associated with $CD24^-$ PC phenotypes. In summary, these two ambiguous proteins might fulfill entity-specific roles in cancer and their interaction with CD24 should be an interesting target for further research in the near future. Before further research can be conducted, we would have to confirm and validate these two proteins though, since they fell out of the analysis after raising the stringency.

We also identified other interesting interaction partners that were not necessarily found in every urological tumor entity, namely NPM1, RalA/B, and DAMPs like HSP90, HSP70, and HMGB1. NPM1 was found in GCTs, PC-3, and Caki-1 which validates Wang et al (L. Wang et al., 2015) who

showed that CD24 immunoprecipitated with NPM and inhibited ARF binding to NPM. This decreased ARF, increased MDM2 levels, and led to a decrease of TP53. Our results show that this process might not be exclusive to PC, but further testing is required to ensure this. Another interactor of interest we found is RalA and RalB supporting Smith et al. who showed CD24 to be regulated by Ral GTPases in cervical carcinoma and UC cells (UM-UC-3). CD24s role in repressing tissue damage-induced immune response is mainly dependent on its interaction with Siglecs and DAMPs and we could validate Chen et al.(G. Y. Chen et al., 2009) data showing the association of CD24 with HSP90, HSP70, and to a lesser degree HMGB1. HSP90 interaction with CD24 is especially interesting as this interaction was previously found to play a role in cancer angiogenesis that might also be of interest in urological malignancies (X. Wang et al., 2016). The difference in interaction partners of CD24 in different tumor entities might be due to a difference in glycosylation between the cell lines investigated and the limitation of only one cell line being investigated in UC, RCC, and PC each.

In summary, we validated a lot of already known CD24 interaction partners to also interact with CD24 in urological malignancies. Although no common interaction partners could be found in all cell lines after increasing the stringency, and the commonly found 25 in panurological cell lines and the 8 in EC cell lines had little involvement with CD24-associated processes. We still identified proteins in each cell line that were involved in similar aforementioned CD24 characteristic biological processes, although mediated by different proteins. We also found new potential interaction partners of CD24 that require further investigation into the actual results of these interactions. Here we must be careful still because many of these targets require further validation prior to deeper research. These interactions are all promising targets for further research to find out if the involved processes lead to similar outcomes as in the already-known tumor entities. Confirmation of this would help us to unite and generalize these functions of CD24 to better understand its role in cancer.

4.4 CD24 as a putative target for immunotherapy

One goal of this study was to establish whether CD24 is a membrane protein that might be a viable immunotherapeutic target in $CD24^+$ tumor entities and in this case specifically TGCTs and ECs. The therapy of choice in this study was a cell-based approach utilizing a third-generation NK-92-CD24-CAR. CD24 antibody SWA11 was utilized as a scFv and these cells were previously shown to be effective in vitro and in patient-derived cells by Klapdor et al. (Klapdor et al., 2019).

In a first step, we validated if contact with CD24 led to an activation of NK92-CD24-CAR. Christian Söhngen utilized an IFN-γ-ELISA assay to check for IFN-γ secretion upon co-culture of $CD24^+$ and NK-92-CD24-CAR cells. This showed concentrations of 400 pg / ml in Ecs and RCCs and 1000 pg / ml in PC cell lines confirming activation of the CARs (Söhngen et al., 2023) IFN-γ secretions in

this magnitude are in line with the observations of Klapdor et al. (Klapdor et al., 2019) who showed concentrations between 500 pg / ml and 2000 pg / ml confirming that the CARs seemed to work as intended. Afterward, we began testing of the efficacy of NK-92-CD24-CARs to efficiently kill highly CD24-positive tumor cells. We began cell viability assays in the three EC cell lines, their Δ*CD24* and cisplatin-resistant clones, and $CD24^-$ and healthy control cells (Fig. 8, Fig. 9). Results show a highly selective elimination of $CD24^+$ tumor cells and no off-target toxicity. This exclusive targeting confirms the results of Klapdor et al. (Klapdor et al., 2019 Fig. 2) and is important for future applications *in vivo* or even in humans. We observed little cell viability reduction in TCam-2 to no cell viability reduction in EC cell lines after untransduced NK-92 cell treatment, although one might suspect some viability reduction due to their intrinsic tumor-killing capabilities. Here our results are in contrast to Klapdor et al. (Klapdor et al., 2019, Fig. 3C) who observed killing capabilities of NK-92 in some primary ovarian carcinoma cells. This lack of toxicity by the untransduced NK cells is caused by multiple factors. Firstly NK-92 cells are NK cells of malignant origin lacking their CD16 domain and therefore being incapable of one of their cancer-killing mechanisms antibody dependent cell cytotoxicity (ADCC) (J. H. Gong et al., 1994). Secondly, other receptors like KIRs, NKG2D, or DNAM-1 lead to caspase-mediated apoptosis of cancer cells but they and their ligands are not expressed to similar levels or at all on all tumor cells (Wrona et al., 2021).We analyzed previous TGCT RNA-seq data by Skowron, Müller and Burmeister et al. (GSE168646 (Skowron et al., 2022), GSE195794, GSE190022 (Burmeister et al., 2022), GSE190792 (Skowron et al., 2020), GSE189472 (Müller et al., 2022) for expression of NK activating receptor ligands and found expression of DNAM ligands like CD112 / Nectin-2 and CD155 / PVR, but low expression of NKG2D ligands like MICA, MICB and ULBP 1-3. Especially DNAM-1 ligands and MICB showed higher expression in seminoma cell line TCam-2 than in EC cell lines which might explain their slightly higher vulnerability to untransduced NK-92 cells. Additionally, IFN-γ secretion should lead to the recruiting of macrophages and dendritic cells which are naturally lacking in an *in vitro* setting. In summary, our results show that the NK-92-CD24-CAR therapy to be a promising new treatment and the SWA11-scFv-CAR to be a suitable recognition domain to specifically target CD24 positive tissues as was previously also shown in other studies (Table-1)

The study was limited by only being performed in EC and seminoma cell lines and not *in vivo,* but due to the positive results we expanded our testing to other urological malignancies positive for CD24 like UC, RCC, and PC. Testing in these cell lines by Christian Söhngen showed similar successful results and showed a significant effect in cells with lower levels of CD24 than EC cell lines (Söhngen et al., 2023). We also found some cytotoxic activity in NK-92 cells as observed by Klapdor et al.(Klapdor et al., 2019; Söhngen et al., 2023). Overall, *in vitro* NK-92-CD24-CAR cells are effective in killing $CD24^+$ tumor cells and seem to be an alternative in cisplatin-resistant tumors. In general, CD24 seems to be a viable target for therapy and if the NK-92-CD24-CARs can overcome the innate challenges of CAR cell therapies of solid tumors, like the immunosuppressive tumor

microenvironment, lowered immune cell invasion, cell persistence, expansion, immune evasion and off-target toxicity *in vivo* remains to be seen. Expanding these experiments into an *in vivo* setting will be the next step in the journey of CD24-targeted therapy in urological malignancies.

5 Reference list / Bibliography

Aigner, S., Ramos, C. L., Hafezi-Moghadam, A., Lawrence, M. B., Friederichs, J., Altevogt, P., & Ley, K. (1998). CD24 mediates rolling of breast carcinoma cells on P-selectin. *FASEB Journal : Official Publication of the Federation of American Societies for Experimental Biology*, *12*(12), 1241–1251. https://doi.org/10.1096/fasebj.12.12.1241

Aigner, S., Ruppert, M., Hubbe, M., Sammar, M., Sthoeger, Z., Butcher, E. C., Vestweber, D., & Altevogt, P. (1995). Heat stable antigen (mouse CD24) supports myeloid cell binding to endothelial and platelet P-selectin. *International Immunology*, *7*(10), 1557–1565. https://doi.org/10.1093/intimm/7.10.1557

Aigner, S., Sthoeger, Z. M., Fogel, M., Weber, E., Zarn, J., Ruppert, M., Zeller, Y., Vestweber, D., Stahel, R., Sammar, M., & Altevogt, P. (1997). CD24, a mucin-type glycoprotein, is a ligand for P-selectin on human tumor cells. *Blood*, *89*(9), 3385–3395.

Albers, P., Albrecht, W., Algaba, F., Bokemeyer, C., Cohn-Cedermark, G., Fizazi, K., Horwich, A., Laguna, M. P., Nicolai, N., & Oldenburg, J. (2015). Guidelines on Testicular Cancer: 2015 Update. *European Urology*, *68*(6), 1054–1068. https://doi.org/10.1016/J.EURURO.2015.07.044

Al-Hajj, M., Wicha, M. S., Benito-Hernandez, A., Morrison, S. J., & Clarke, M. F. (2003). Prospective identification of tumorigenic breast cancer cells. *Proceedings of the National Academy of Sciences of the United States of America*, *100*(7), 3983–3988. https://doi.org/10.1073/PNAS.0530291100

Ali, S., Kjeken, R., Niederlaender, C., Markey, G., Saunders, T. S., Opsata, M., Moltu, K., Bremnes, B., Grønevik, E., Muusse, M., Håkonsen, G. D., Skibeli, V., Kalland, M. E., Wang, I., Buajordet, I., Urbaniak, A., Johnston, J., Rantell, K., Kerwash, E., … Pignatti, F. (2020). The European Medicines Agency Review of Kymriah (Tisagenlecleucel) for the Treatment of Acute Lymphoblastic Leukemia and Diffuse Large B-Cell Lymphoma. *The Oncologist*, *25*(2), e321–e327. https://doi.org/10.1634/THEONCOLOGIST.2019-0233

Altevogt, P., Sammar, M., Hüser, L., & Kristiansen, G. (2021). Novel insights into the function of CD24: A driving force in cancer. *International Journal of Cancer*, *148*(3), 546–559. https://doi.org/10.1002/IJC.33249

Arik, D., Can, C., Dündar, E., Kabukçuoğlu, S., & Paşaoğlu, Ö. (2017). Prognostic Significance of CD24 in Clear Cell Renal Cell Carcinoma. *Pathology Oncology Research : POR*, *23*(2), 409–416. https://doi.org/10.1007/s12253-016-0128-8

Bancroft, E. K., Page, E. C., Castro, E., Lilja, H., Vickers, A., Sjoberg, D., Assel, M., Foster, C. S., Mitchell, G., Drew, K., Mæhle, L., Axcrona, K., Evans, D. G., Bulman, B., Eccles, D., McBride, D., Van Asperen, C., Vasen, H., Kiemeney, L. A., … Eeles, R. A. (2014). Targeted Prostate Cancer Screening in BRCA1 and BRCA2 Mutation Carriers: Results from the Initial Screening Round of the IMPACT Study. *European Urology*, *66*(3), 489. https://doi.org/10.1016/J.EURURO.2014.01.003

Barkal, A. A., Brewer, R. E., Markovic, M., Kowarsky, M., Barkal, S. A., Zaro, B. W., Krishnan, V., Hatakeyama, J., Dorigo, O., Barkal, L. J., & Weissman, I. L. (2019). CD24 signalling through macrophage Siglec-10 is a new target for cancer immunotherapy. *Nature*, *572*(7769), 392. https://doi.org/10.1038/S41586-019-1456-0

Bibliography

Baumann, P., Cremers, N., Kroese, F., Orend, G., Chiquet-Ehrismann, R., Uede, T., Yagita, H., & Sleeman, J. P. (2005). CD24 Expression Causes the Acquisition of Multiple Cellular Properties Associated with Tumor Growth and Metastasis. *Cancer Research*, *65*(23), 10783–10793. https://doi.org/10.1158/0008-5472.CAN-05-0619

Bretz, N. P., Salnikov, A. V., Perne, C., Keller, S., Wang, X., Mierke, C. T., Fogel, M., Erbe-Hofmann, N., Schlange, T., Moldenhauer, G., & Altevogt, P. (2012). CD24 controls Src/STAT3 activity in human tumors. *Cellular and Molecular Life Sciences*, *69*(22), 3863–3879. https://doi.org/10.1007/S00018-012-1055-9/FIGURES/8

Burger, M., Catto, J. W. F., Dalbagni, G., Grossman, H. B., Herr, H., Karakiewicz, P., Kassouf, W., Kiemeney, L. A., La Vecchia, C., Shariat, S., & Lotan, Y. (2013). Epidemiology and Risk Factors of Urothelial Bladder Cancer. *European Urology*, *63*(2), 234–241. https://doi.org/10.1016/J.EURURO.2012.07.033

Burmeister, A., Stephan, A., Alves Avelar, L. A., Müller, M. R., Seiwert, A., Höfmann, S., Fischer, F., Torres-Gomez, H., Hoffmann, M. J., Niegisch, G., Bremmer, F., Petzsch, P., Köhrer, K., Albers, P., Kurz, T., Skowron, M. A., & Nettersheim, D. (2022). Establishment and Evaluation of Dual HDAC/BET Inhibitors as Therapeutic Options for Germ Cell Tumors and Other Urological Malignancies. *Molecular Cancer Therapeutics*, *21*(11), 1674–1688. https://doi.org/10.1158/1535-7163.MCT-22-0207

Cao, X., Geradts, J., Dewhirst, M. W., & Lo, H. W. (2012). Upregulation of VEGF-A and CD24 Gene Expression by the tGLI1 Transcription Factor Contributes to the Aggressive Behavior of Breast Cancer Cells. *Oncogene*, *31*(1), 104. https://doi.org/10.1038/ONC.2011.219

Cavallo, F., Graziani, G., Antinozzi, C., Feldman, D. R., Houldsworth, J., Bosl, G. J., Chaganti, R. S. K., Moynahan, M. E., Jasin, M., & Barchi, M. (2012). Reduced Proficiency in Homologous Recombination Underlies the High Sensitivity of Embryonal Carcinoma Testicular Germ Cell Tumors to Cisplatin and Poly (ADP-Ribose) Polymerase Inhibition. *PLoS ONE*, *7*(12). https://doi.org/10.1371/JOURNAL.PONE.0051563

Cerami, E., Gao, J., Dogrusoz, U., Gross, B. E., Sumer, S. O., Aksoy, B. A., Jacobsen, A., Byrne, C. J., Heuer, M. L., Larsson, E., Antipin, Y., Reva, B., Goldberg, A. P., Sander, C., & Schultz, N. (2012). The cBio cancer genomics portal: an open platform for exploring multidimensional cancer genomics data. *Cancer Discovery*, *2*(5), 401–404. https://doi.org/10.1158/2159-8290.CD-12-0095

Chen, G. Y., Tang, J., Zheng, P., & Liu, Y. (2009). CD24 and Siglec-10 Selectively Repress Tissue Damage-Induced Immune Responses. *Science (New York, N.Y.)*, *323*(5922), 1722. https://doi.org/10.1126/SCIENCE.1168988

Chen, K., Dai, M., Luo, Q., Wang, Y., Shen, W., Liao, Y., Zhou, Y., & Cheng, W. (2023). PARP1 controls the transcription of CD24 by ADP-ribosylating the RNA helicase DDX5 in pancreatic cancer. *The International Journal of Biochemistry & Cell Biology*, *155*, 106358. https://doi.org/10.1016/J.BIOCEL.2022.106358

Chen, Z., Wang, T., Tu, X., Xie, W., He, H., Wang, M., & Zhang, J. (2017). Antibody-based targeting of CD24 enhances antitumor effect of cetuximab via attenuating phosphorylation of Src/STAT3. *Biomedicine & Pharmacotherapy = Biomedecine & Pharmacotherapie*, *90*, 427–436. https://doi.org/10.1016/J.BIOPHA.2017.03.094

Bibliography

Cheng, L., Albers, P., Berney, D. M., Feldman, D. R., Daugaard, G., Gilligan, T., & Looijenga, L. H. J. (2018). Testicular cancer. *Nature Reviews Disease Primers*. https://doi.org/10.1038/s41572-018-0029-0

Cram, D. S., McIntosh, A., Oxbrow, L., Johnston, A. M., & DeAizpurua, H. J. (1999). Differential mRNA display analysis of two related but functionally distinct rat insulinoma (RIN) cell lines: identification of CD24 and its expression in the developing pancreas. *Differentiation*, *64*(4), 237–246. https://doi.org/10.1046/J.1432-0436.1999.6440237.X

Dai, H., Wu, Z., Jia, H., Tong, C., Guo, Y., Ti, D., Han, X., Liu, Y., Zhang, W., Wang, C., Zhang, Y., Chen, M., Yang, Q., Wang, Y., & Han, W. (2020). Bispecific CAR-T cells targeting both CD19 and CD22 for therapy of adults with relapsed or refractory B cell acute lymphoblastic leukemia. *Journal of Hematology and Oncology*, *13*(1), 1–10. https://doi.org/10.1186/S13045-020-00856-8/FIGURES/5

Dennis, G., Sherman, B. T., Hosack, D. A., Yang, J., Gao, W., Lane, H. C., & Lempicki, R. A. (2003). DAVID: Database for Annotation, Visualization, and Integrated Discovery. *Genome Biology*, *4*(5), P3.

Di Stasi, A., Tey, S.-K., Dotti, G., Fujita, Y., Kennedy-Nasser, A., Martinez, C., Straathof, K., Liu, E., Durett, A. G., Grilley, B., Liu, H., Cruz, C. R., Savoldo, B., Gee, A. P., Schindler, J., Krance, R. A., Heslop, H. E., Spencer, D. M., Rooney, C. M., & Brenner, M. K. (2011). Inducible Apoptosis as a Safety Switch for Adoptive Cell Therapy. *New England Journal of Medicine*, *365*(18), 1673–1683. https://doi.org/10.1056/NEJMOA1106152/SUPPL_FILE/NEJMOA1106152_DISCLOSURES.PDF

Droz, D., Rousseau-Merck, M. F., Jaubert, F., Diebold, N., Nezelof, C., Adafer, E., & Mouly, H. (1990). Cell differentiation in Wilms' tumor (nephroblastoma): an immunohistochemical study. *Human Pathology*, *21*(5), 536–544. https://doi.org/10.1016/0046-8177(90)90011-S

Duex, J. E., Owens, C., Chauca-Diaz, A., Dancik, G. M., Vanderlinden, L. A., Ghosh, D., Leivo, M. Z., Hansel, D. E., & Theodorescu, D. (2017). Nuclear CD24 Drives Tumor Growth and Is Predictive of Poor Patient Prognosis. *Cancer Research*, *77*(18), 4858–4867. https://doi.org/10.1158/0008-5472.CAN-17-0367

EAU Guidelines. Edn. presented at the EAU Annual Congress Paris 2024. (2024). *EAU Guidelines Office, Arnhem, The Netherlands. Https://Uroweb.Org/Guidelines*.

Elghetany, M. T., & Patel, J. (2002). Assessment of CD24 expression on bone marrow neutrophilic granulocytes: CD24 is a marker for the myelocytic stage of development. *American Journal of Hematology*, *71*(4), 348–349. https://doi.org/10.1002/AJH.10176

Escudier, B., Porta, C., Schmidinger, M., Rioux-Leclercq, N., Bex, A., Khoo, V., Grünwald, V., Gillessen, S., & Horwich, A. (2019). Renal cell carcinoma: ESMO Clinical Practice Guidelines for diagnosis, treatment and follow-up. *Annals of Oncology*, *30*(5), 706–720. https://doi.org/10.1093/ANNONC/MDZ056

Eyvazi, S., Kazemi, B., Dastmalchi, S., & Bandehpour, M. (2018). Involvement of CD24 in Multiple Cancer Related Pathways Makes It an Interesting New Target for Cancer Therapy. *Current Cancer Drug Targets*, *18*(4), 328–336. https://doi.org/10.2174/1570163814666170818125036

Fang, X., Tang, J., & Liu, Y. (2010). CD24: from A to Z. *Cellular and Molecular Immunology*, *7*, 100–103. https://doi.org/10.1038/cmi.2009.119

Bibliography

Fischer, G. F., Majdic, O., Gadd, S., & Knapp, W. (1990). Signal transduction in lymphocytic and myeloid cells via CD24, a new member of phosphoinositol-anchored membrane molecules. *Journal of Immunology (Baltimore, Md. : 1950)*, *144*(2), 638–641.

Friederichs, J., Zeller, Y., Hafezi-Moghadam, A., Gröne, H. J., Ley, K., & Altevogt, P. (2000). The CD24/P-selectin binding pathway initiates lung arrest of human A125 adenocarcinoma cells. *Cancer Research*, *60*(23), 6714–6722.

Fung, C., Sesso, H. D., Williams, A. M., Kerns, S. L., Monahan, P., Zaid, M. A., Feldman, D. R., Hamilton, R. J., Vaughn, D. J., Beard, C. J., Kollmannsberger, C. K., Cook, R., Althouse, S., Ardeshir-Rouhani-Fard, S., Lipshultz, S. E., Einhorn, L. H., Fossa, S. D., Travis, L. B., Curreri, S., … Robison, L. L. (2017). Multi-Institutional Assessment of Adverse Health Outcomes Among North American Testicular Cancer Survivors After Modern Cisplatin-Based Chemotherapy. *Journal of Clinical Oncology*, *35*(11), 1211. https://doi.org/10.1200/JCO.2016.70.3108

Gao, J., Aksoy, B. A., Dogrusoz, U., Dresdner, G., Gross, B., Sumer, S. O., Sun, Y., Jacobsen, A., Sinha, R., Larsson, E., Cerami, E., Sander, C., & Schultz, N. (2013). Integrative Analysis of Complex Cancer Genomics and Clinical Profiles Using the cBioPortal. *Science Signaling*, *6*(269), pl1. https://doi.org/10.1126/SCISIGNAL.2004088

Gerst, R., & Olzer, M. H. ¨. (2019). PCAGO: An interactive tool to analyze RNA-Seq data with principal component analysis. *BioRxiv*, 433078. https://doi.org/10.1101/433078

Gkolfinopoulos, S., Psyrri, A., & Bamias, A. (2021). Clear-cell renal cell carcinoma - A comprehensive review of agents used in the contemporary management of advanced/metastatic disease. *Oncology Reviews*, *15*(1). https://doi.org/10.4081/ONCOL.2021.530

Gong, J. H., Maki, G., & Klingemann, H. G. (1994). Characterization of a human cell line (NK-92) with phenotypical and functional characteristics of activated natural killer cells. *Leukemia*, *8*(4), 652–658.

Gong, Y., Wolterink, R. G. J. K., Wang, J., Bos, G. M. J., & Germeraad, W. T. V. (2021). Chimeric antigen receptor natural killer (CAR-NK) cell design and engineering for cancer therapy. *Journal of Hematology & Oncology*, *14*(1), 73. https://doi.org/10.1186/S13045-021-01083-5

Grosser, R., Cherkassky, L., Chintala, N., & Adusumilli, P. S. (2019). Combination Immunotherapy with CAR T Cells and Checkpoint Blockade for the Treatment of Solid Tumors. *Cancer Cell*, *36*(5), 471. https://doi.org/10.1016/J.CCELL.2019.09.006

Guo, C. C., Bondaruk, J., Yao, H., Wang, Z., Zhang, L., Lee, S., Lee, J.-G., Cogdell, D., Zhang, M., Yang, G., Dadhania, V., Choi, W., Wei, P., Gao, J., Theodorescu, D., Logothetis, C., Dinney, C., Kimmel, M., Weinstein, J. N., … Czerniak, B. (2020). Assessment of Luminal and Basal Phenotypes in Bladder Cancer. *Scientific Reports*, *10*. https://doi.org/10.1038/S41598-020-66747-7

Gutierrez-Dalmau, A., & Campistol, J. M. (2007). Immunosuppressive Therapy and Malignancy in Organ Transplant Recipients A Systematic Review. *Drugs*, *67*(8), 1167–1198. http://www.ipittr.

Hah, Y. S., & Koo, K. C. (2021). Immunology and Immunotherapeutic Approaches for Advanced Renal Cell Carcinoma: A Comprehensive Review. *International Journal of Molecular Sciences*, *22*(9). https://doi.org/10.3390/IJMS22094452

Bibliography

Hedberg Oldfors, C., Dios, D. G., Linder, A., Visuttijai, K., Samuelson, E., Karlsson, S., Nilsson, S., & Behboudi, A. (2015). Analysis of an independent tumor suppressor locus telomeric to Tp53 suggested Inpp5k and Myo1c as novel tumor suppressor gene candidates in this region. *BMC Genetics*, *16*(1). https://doi.org/10.1186/S12863-015-0238-4

Higuchi, I., Kawai, H., Kawajiri, M., Fukunaga, H., Horikiri, T., Niiyama, T., Nakagawa, M., Arimura, K., & Osame, M. (1999). Statistically significant differences in the number of CD24 positive muscle fibers and satellite cells between sarcoglycanopathy and age-matched Becker muscular dystrophy patients. *Internal Medicine (Tokyo, Japan)*, *38*(5), 412–415. https://doi.org/10.2169/internalmedicine.38.412

Hoimes, C. J., Flaig, T. W., Milowsky, M. I., Friedlander, T. W., Bilen, M. A., Gupta, S., Srinivas, S., Merchan, J. R., McKay, R. R., Petrylak, D. P., Sasse, C., Moreno, B. H., Yu, Y., Carret, A. S., & Rosenberg, J. E. (2023). Enfortumab Vedotin Plus Pembrolizumab in Previously Untreated Advanced Urothelial Cancer. *Journal of Clinical Oncology*, *41*(1), 22. https://doi.org/10.1200/JCO.22.01643

Hough, M. R., Rosten, P. M., Sexton, T. L., Kay, R., & Humphries, R. K. (1994). Mapping of CD24 and Homologous Sequences to Multiple Chromosomal Loci. *Genomics*, *22*(1), 154–161. https://doi.org/10.1006/GENO.1994.1356

Hsieh, J. J., Purdue, M. P., Signoretti, S., Swanton, C., Albiges, L., Schmidinger, M., Heng, D. Y., Larkin, J., & Ficarra, V. (2017). Renal cell carcinoma. *Nature Reviews. Disease Primers*, *3*, 17009. https://doi.org/10.1038/NRDP.2017.9

Huang, D. W., Sherman, B. T., & Lempicki, R. A. (2009a). Bioinformatics enrichment tools: paths toward the comprehensive functional analysis of large gene lists. *Nucleic Acids Research*, *37*(1), 1–13. https://doi.org/10.1093/NAR/GKN923

Huang, D. W., Sherman, B. T., & Lempicki, R. A. (2009b). Systematic and integrative analysis of large gene lists using DAVID bioinformatics resources. *Nature Protocols*, *4*(1), 44–57. https://doi.org/10.1038/NPROT.2008.211

Huang, L. R., & Hsu, H. C. (1995). Cloning and expression of CD24 gene in human hepatocellular carcinoma: a potential early tumor marker gene correlates with p53 mutation and tumor differentiation. *Cancer Research*, *55*(20), 4717–4721.

Huang, Y., Zeng, J., Liu, T., Xu, Q., Song, X., & Zeng, J. (2020). *DNAM1 and 2B4 Costimulatory Domains Enhance the Cytotoxicity of Anti-GPC3 Chimeric Antigen Receptor-Modified Natural Killer Cells Against Hepatocellular Cancer Cells in vitro*. https://doi.org/10.2147/CMAR.S253565

Hubbe, M., & Altevogt, P. (1994). Heat-stable antigen/CD24 on mouse T lymphocytes: evidence for a costimulatory function. *European Journal of Immunology*, *24*(3), 731–737. https://doi.org/10.1002/eji.1830240336

Hunter, J. D. (2007). Matplotlib: A 2D graphics environment. *Computing in Science and Engineering*, *9*(3), 90–95. https://doi.org/10.1109/MCSE.2007.55

Hüser, L., Sachindra, S., Granados, K., Federico, A., Larribère, L., Novak, D., Umansky, V., Altevogt, P., & Utikal, J. (2018). SOX2-mediated upregulation of CD24 promotes adaptive resistance toward targeted therapy in melanoma. *International Journal of Cancer*, *143*(12), 3131–3142. https://doi.org/10.1002/ijc.31609

Bibliography

Huth, H. W., Castro-Gomes, T., de Goes, A. M., & Ropert, C. (2021). Translocation of intracellular CD24 constitutes a triggering event for drug resistance in breast cancer. *Scientific Reports*, *11*(1). https://doi.org/10.1038/S41598-021-96449-7

Israel, E., Kapelushnik, J., Yermiahu, T., Levi, I., Yaniv, I., Shpilberg, O., & Shubinsky, G. (2005). Expression of CD24 on CD19-CD79a+ early B-cell progenitors in human bone marrow. *Cellular Immunology*, *236*(1–2), 171–178. https://doi.org/10.1016/J.CELLIMM.2005.08.026

Jackson, D., Waibel, R., Weber, E., Bell, J., & Stahel, R. A. (1992). CD24, a signal-transducing molecule expressed on human B cells, is a major surface antigen on small cell lung carcinomas. *Cancer Research*, *52*(19), 5264–5270.

Jia, Y., Gu, D., Wan, J., Yu, B., Zhang, X., Gabriela Chiorean, E., Wang, Y., & Xie, J. (2019). The role of GLI-SOX2 signaling axis for gemcitabine resistance in pancreatic cancer. *Oncogene*, *38*, 1764–1777. https://doi.org/10.1038/s41388-018-0553-0

Jiang, L., Bai, X., Wang, Y., & Wei, M. (2015). Association between CD24-P226-C/T polymorphism and multiple sclerosis: A meta-analysis. *Immunological Investigations*, *44*(4), 321–330. https://doi.org/10.3109/08820139.2014.1003650

Kadmon, G., von Bohlen und Halbach, F., Horstkorte, R., Eckert, M., Altevogt, P., & Schachner, M. (1995). Evidence for Cis Interaction and Cooperative Signalling by the Heat-stable Antigen Nectadrin (murine CD24) and the Cell Adhesion Molecule L1 in Neurons. *European Journal of Neuroscience*, *7*(5), 993–1004. https://doi.org/10.1111/J.1460-9568.1995.TB01087.X

Kaipparettu, B. A., Malik, S., Konduri, S. D., Liu, W., Rokavec, M., Van Der Kuip, H., Hoppe, R., Hammerich-Hille, S., Fritz, P., Schroth, W., Abele, I., Das, G. M., Oesterreich, S., & Brauch, H. (2008). Estrogen-mediated down-regulation of CD24 in breast cancer cells. *International Journal of Cancer. Journal International Du Cancer*, *123*(1), 66. https://doi.org/10.1002/IJC.23480

Kamel, M. H., Moore, P. C., Bissada, N. K., & Heshmat, S. M. (2012). Potential Years of Life Lost Due to Urogenital Cancer in the United States: Trends From 1972 to 2006 Based on Data From the SEER Database. *The Journal of Urology*, *187*(3), 868–871. https://doi.org/10.1016/J.JURO.2011.10.142

Kamoun, A., de Reyniès, A., Allory, Y., Sjödahl, G., Robertson, A. G., Seiler, R., Hoadley, K. A., Groeneveld, C. S., Al-Ahmadie, H., Choi, W., Castro, M. A. A., Fontugne, J., Eriksson, P., Mo, Q., Kardos, J., Zlotta, A., Hartmann, A., Dinney, C. P., Bellmunt, J., … Weinstein, J. (2020). A Consensus Molecular Classification of Muscle-invasive Bladder Cancer. *European Urology*, *77*(4), 420. https://doi.org/10.1016/J.EURURO.2019.09.006

Karlsson, R., Aly, M., Clements, M., Zheng, L., Adolfsson, J., Xu, J., Grönberg, H., & Wiklund, F. (2014). A Population-based Assessment of Germline HOXB13 G84E Mutation and Prostate Cancer Risk. *European Urology*, *65*(1), 169–176. https://doi.org/10.1016/J.EURURO.2012.07.027

Kay, R., Rosten, P. M., & Humphries, R. K. (1991). CD24, a signal transducer modulating B cell activation responses, is a very short peptide with a glycosyl phosphatidylinositol membrane anchor. *Journal of Immunology (Baltimore, Md. : 1950)*, *147*(4), 1412–1416.

Khong, H. T., & Restifo, N. P. (2002). Natural selection of tumor variants in the generation of "tumor escape" phenotypes. *Nature Immunology*, *3*(11), 999–1005. https://doi.org/10.1038/ni1102-999

Bibliography

Klapdor, R., Wang, S., Morgan, M., Dörk, T., Hacker, U., Hillemanns, P., Büning, H., & Schambach, A. (2019). Characterization of a Novel Third-Generation Anti-CD24-CAR against Ovarian Cancer. *International Journal of Molecular Sciences*, *20*(3). https://doi.org/10.3390/IJMS20030660

Kleene, R., Yang, H., Kutsche, M., & Schachner, M. (2001). The Neural Recognition Molecule L1 is a Sialic Acid-binding Lectin for CD24, Which Induces Promotion and Inhibition of Neurite Outgrowth. *Journal of Biological Chemistry*, *276*(24), 21656–21663. https://doi.org/10.1074/JBC.M101790200

Koh, J., Lee, S. byul, Park, H., Lee, H. J., Cho, N. H., & Kim, J. (2012). Susceptibility of CD24(+) ovarian cancer cells to anti-cancer drugs and natural killer cells. *Biochemical and Biophysical Research Communications*, *427*(2), 373–378. https://doi.org/10.1016/J.BBRC.2012.09.067

Kristiansen, G., Denkert, C., Schlüns, K., Dahl, E., Pilarsky, C., & Hauptmann, S. (2002). CD24 is expressed in ovarian cancer and is a new independent prognostic marker of patient survival. *The American Journal of Pathology*, *161*(4), 1215–1221. https://doi.org/10.1016/S0002-9440(10)64398-2

Kristiansen, G., MacHado, E., Bretz, N., Rupp, C., Winzer, K. J., König, A. K., Moldenhauer, G., Marmé, F., Costa, J., & Altevogt, P. (2010). Molecular and clinical dissection of CD24 antibody specificity by a comprehensive comparative analysis. *Laboratory Investigation*, *90*(7), 1102–1116. https://doi.org/10.1038/labinvest.2010.70

Kristiansen, G., Sammar, M., & Altevogt, & P. (2004). Tumour biological aspects of CD24, a mucin-like adhesion molecule. *Journal of Molecular Histology*, *35*, 255–262.

Kristiansen, G., Schlüns, K., Yongwei, Y., Denkert, C., Dietel, M., & Petersen, I. (2003). CD24 is an independent prognostic marker of survival in nonsmall cell lung cancer patients. *British Journal of Cancer*, *88*(2), 231. https://doi.org/10.1038/SJ.BJC.6600702

Kristiansen, G., Winzer, K.-J., Mayordomo, E., Bellach, J., Schlüns, K., Denkert, C., Dahl, E., Pilarsky, C., Altevogt, P., Guski, H., & Dietel, M. (2003). CD24 expression is a new prognostic marker in breast cancer. *Clinical Cancer Research : An Official Journal of the American Association for Cancer Research*, *9*(13), 4906–4913.

Kurz, L., Miklyaeva, A., Skowron, M. A., Overbeck, N., Poschmann, G., Becker, T., Eul, K., Kurz, T., Schönberger, S., Calaminus, G., Stühler, K., Dykhuizen, E., Albers, P., & Nettersheim, D. (2020). ARID1A Regulates Transcription and the Epigenetic Landscape via POLE and DMAP1 while ARID1A Deficiency or Pharmacological Inhibition Sensitizes Germ Cell Tumor Cells to ATR Inhibition. *Cancers*, *12*(4). https://doi.org/10.3390/cancers12040905

Kwon, M. J., Han, J., Seo, J. H., Song, K., Jeong, H. M., Choi, J. S., Kim, Y. J., Lee, S. H., Choi, Y. La, & Shin, Y. K. (2015). CD24 Overexpression Is Associated with Poor Prognosis in Luminal A and Triple-Negative Breast Cancer. *PLoS ONE*, *10*(10). https://doi.org/10.1371/JOURNAL.PONE.0139112

Lawson, D. A., Xin, L., Lukacs, R. U., Cheng, D., & Witte, O. N. (2007). Isolation and functional characterization of murine prostate stem cells. *Proceedings of the National Academy of Sciences of the United States of America*, *104*(1), 181–186. https://doi.org/10.1073/pnas.0609684104

Bibliography

Lee, J.-H., Kim, S.-H., Lee, E.-S., & Kim, Y.-S. (2009). CD24 overexpression in cancer development and progression: a meta-analysis. *Oncology Reports*, *22*(5), 1149–1156. https://doi.org/10.3892/or_00000548

Li, C., Heidt, D. G., Dalerba, P., Burant, C. F., Zhang, L., Adsay, V., Wicha, M., Clarke, M. F., & Simeone, D. M. (2007). Identification of Pancreatic Cancer Stem Cells. *Cancer Research*, *67*(3), 1030–1037. https://doi.org/10.1158/0008-5472.CAN-06-2030

Li, O., Zheng, P., & Liu, Y. (2004). CD24 Expression on T Cells Is Required for Optimal T Cell Proliferation in Lymphopenic Host. *The Journal of Experimental Medicine*, *200*(8), 1083. https://doi.org/10.1084/JEM.20040779

Li, S. X., Li, J., Dong, L. W., & Guo, Z. Y. (2020). Cytoskeleton-Associated Protein 4, a Promising Biomarker for Tumor Diagnosis and Therapy. *Frontiers in Molecular Biosciences*, *7*. https://doi.org/10.3389/FMOLB.2020.552056

Li, X., Wilmanowski, R., Gao, X., Vanaernum, Z. L., Donnelly, D. P., Kochert, B., Schuessler, H. A., & Richardson, D. (2022). Precise O-Glycosylation Site Localization of CD24Fc by LC-MS Workflows. *Analytical Chemistry*, *94*(23), 8416–8425. https://doi.org/10.1021/ACS.ANALCHEM.2C01137/ASSET/IMAGES/LARGE/AC2C01137_0007.JPEG

Liu, A. Y., & True, L. D. (2002). Characterization of Prostate Cell Types by CD Cell Surface Molecules. *The American Journal of Pathology*, *160*(1), 37. https://doi.org/10.1016/S0002-9440(10)64346-5

Liu, E., Marin, D., Banerjee, P., Macapinlac, H. A., Thompson, P., Basar, R., Kerbauy, L. N., Overman, B., Thall, P., Kaplan, M., Nandivada, V., Kaur, I., Cortes, A. N., Cao, K., Daher, M., Hosing, C., Cohen, E. N., Kebriaei, P., Mehta, R., … Rezvani, K. (2020). Use of CAR-Transduced Natural Killer Cells in CD19-Positive Lymphoid Tumors. *The New England Journal of Medicine*, *382*(6), 545. https://doi.org/10.1056/NEJMOA1910607

Liu, H., Wang, Y.-J., Bian, L., Fang, Z.-H., Zhang, Q.-Y., & Cheng, J.-X. (2016). CD44+/CD24+ cervical cancer cells resist radiotherapy and exhibit properties of cancer stem cells. *European Review for Medical and Pharmacological Sciences*, *20*(9), 1745–1754.

Lu, S., Yao, Y., Xu, G., Zhou, C., Zhang, Y., Sun, J., Jiang, R., Shao, Q., & Chen, Y. (2018). CD24 regulates sorafenib resistance via activating autophagy in hepatocellular carcinoma. *Cell Death & Disease*, *9*(6). https://doi.org/10.1038/S41419-018-0681-Z

Ma, Z., He, H., Sun, F., Xu, Y., Huang, X., Ma, Y., Zhao, H., Wang, Y., Wang, M., & Zhang, J. (2017). Selective targeted delivery of doxorubicin via conjugating to anti-CD24 antibody results in enhanced antitumor potency for hepatocellular carcinoma both in vitro and in vivo. *Journal of Cancer Research and Clinical Oncology*, *143*(10), 1929–1940. https://doi.org/10.1007/S00432-017-2436-0

Magnaldo, T., & Barrandon, Y. (1996). CD24 (heat stable antigen, nectadrin), a novel keratinocyte differentiation marker, is preferentially expressed in areas of the hair follicle containing the colony-forming cells. *Journal of Cell Science*, *109*(13), 3035–3045. https://doi.org/10.1242/JCS.109.13.3035

Maliar, A., Servais, C., Waks, T., Chmielewski, M., Lavy, R., Altevogt, P., Abken, H., & Eshhar, Z. (2012). Redirected T cells that target pancreatic adenocarcinoma antigens eliminate tumors

and metastases in mice. *Gastroenterology*, *143*(5). https://doi.org/10.1053/J.GASTRO.2012.07.017

Maly, I. V., Domaradzki, T. M., Gosy, V. A., & Hofmann, W. A. (2017). Myosin isoform expressed in metastatic prostate cancer stimulates cell invasion. *Scientific Reports*, *7*(1). https://doi.org/10.1038/S41598-017-09158-5

Marmé, F., Werft, W., Walter, A., Keller, S., Wang, X., Benner, A., Burwinkel, B., Sinn, P., Hug, S., Sohn, C., Bretz, N., Moldenhauer, G., Rupp, C., Rupp, A.-K., Biakhov, M. Y., Bottini, A., Friedrichs, K., Khailenko, V. A., Manikhas, G. M., … Schneeweiss, A. (2012). CD24 Ala57Val polymorphism predicts pathologic complete response to sequential anthracycline- and taxane-based neoadjuvant chemotherapy for primary breast cancer. *Breast Cancer Research and Treatment*, *132*(3), 819–831. https://doi.org/10.1007/s10549-011-1759-9

Milestones in Cancer Research and Discovery - NCI. (n.d.). Retrieved February 1, 2023, from https://www.cancer.gov/research/progress/250-years-milestones

Modur, V., Joshi, P., Nie, D., Robbins, K. T., Khan, A. U., & Rao, K. (2016). CD24 Expression May Play a Role as a Predictive Indicator and a Modulator of Cisplatin Treatment Response in Head and Neck Squamous Cellular Carcinoma. *PLoS ONE*, *11*(6). https://doi.org/10.1371/JOURNAL.PONE.0156651

Mottet, N., van den Bergh, R. C. N., Briers, E., Van den Broeck, T., Cumberbatch, M. G., De Santis, M., Fanti, S., Fossati, N., Gandaglia, G., Gillessen, S., Grivas, N., Grummet, J., Henry, A. M., van der Kwast, T. H., Lam, T. B., Lardas, M., Liew, M., Mason, M. D., Moris, L., … Cornford, P. (2021). EAU-EANM-ESTRO-ESUR-SIOG Guidelines on Prostate Cancer-2020 Update. Part 1: Screening, Diagnosis, and Local Treatment with Curative Intent. *European Urology*, *79*(2), 243–262. https://doi.org/10.1016/J.EURURO.2020.09.042

Müller, M. R., Burmeister, A., Skowron, M. A., Stephan, A., Bremmer, F., Wakileh, G. A., Petzsch, P., Köhrer, K., Albers, P., & Nettersheim, D. (2022). Therapeutical interference with the epigenetic landscape of germ cell tumors: a comparative drug study and new mechanistical insights. *Clinical Epigenetics*, *14*(1). https://doi.org/10.1186/S13148-021-01223-1

Murad, J. P., Kozlowska, A. K., Lee, H. J., Ramamurthy, M., Chang, W. C., Yazaki, P., Colcher, D., Shively, J., Cristea, M., Forman, S. J., & Priceman, S. J. (2018). Effective targeting of TAG72+peritoneal ovarian tumors via regional delivery of CAR-engineered T cells. *Frontiers in Immunology*, *9*(NOV), 2268. https://doi.org/10.3389/FIMMU.2018.02268/FULL

Myung, J. H., Gajjar, K. A., Pearson, R. M., Launiere, C. A., Eddington, D. T., & Hong, S. (2011). Direct measurements on CD24-mediated rolling of human breast cancer MCF-7 cells on E-selectin. *Analytical Chemistry*, *83*(3), 1078–1083. https://doi.org/10.1021/AC102901E

O'Donnell, P. H., Milowsky, M. I., Petrylak, D. P., Hoimes, C. J., Flaig, T. W., Mar, N., Moon, H. H., Friedlander, T. W., McKay, R. R., Bilen, M. A., Srinivas, S., Burgess, E. F., Ramamurthy, C., George, S., Geynisman, D. M., Bracarda, S., Borchiellini, D., Geoffrois, L., Maroto Rey, J. P., … Rosenberg, J. E. (2023). Enfortumab Vedotin With or Without Pembrolizumab in Cisplatin-Ineligible Patients With Previously Untreated Locally Advanced or Metastatic Urothelial Cancer. *Journal of Clinical Oncology*, *41*(25), 4107. https://doi.org/10.1200/JCO.22.02887

Overdevest, J. B., Knubel, K. H., Duex, J. E., Thomas, S., Nitz, M. D., Harding, M. A., Smith, S. C., Frierson, H. F., Conaway, M., & Theodorescu, D. (2012). CD24 expression is important in male urothelial tumorigenesis and metastasis in mice and is androgen regulated.

Proceedings of the National Academy of Sciences of the United States of America, *109*(51), E3588. https://doi.org/10.1073/PNAS.1113960109/-/DCSUPPLEMENTAL

Overdevest, J. B., Thomas, S., Kristiansen, G., Hansel, D. E., Smith, S. C., & Theodorescu, D. (2011). CD24 Offers a Therapeutic Target for Control of Bladder Cancer Metastasis Based on a Requirement for Lung Colonization. *Cancer Research*, *71*(11), 3802. https://doi.org/10.1158/0008-5472.CAN-11-0519

Panagiotou, E., Syrigos, N. K., Charpidou, A., Kotteas, E., & Vathiotis, I. A. (2022). CD24: A Novel Target for Cancer Immunotherapy. *Journal of Personalized Medicine 2022, Vol. 12, Page 1235*, *12*(8), 1235. https://doi.org/10.3390/JPM12081235

Patel, V. G., Oh, W. K., & Galsky, M. D. (2020). Treatment of muscle-invasive and advanced bladder cancer in 2020. *CA: A Cancer Journal for Clinicians*, *70*(5), 404–423. https://doi.org/10.3322/CAAC.21631

Poschmann, G., Grzendowski, M., Stefanski, A., Bruns, E., Meyer, E., & Stühler, K. (2014). *Redox proteomics reveal stress responsive proteins linking peroxiredoxin-1 status in glioma to chemosensitivity and oxidative stress ☆*. https://doi.org/10.1016/j.bbapap.2014.11.011

Rajpert-De Meyts, E., McGlynn, K. A., Okamoto, K., Jewett, M. A. S., & Bokemeyer, C. (2016). Testicular germ cell tumours. *The Lancet*, *387*(10029), 1762–1774. https://doi.org/10.1016/S0140-6736(15)00991-5

Rebello, R. J., Oing, C., Knudsen, K. E., Loeb, S., Johnson, D. C., Reiter, R. E., Gillessen, S., Van der Kwast, T., & Bristow, R. G. (2021). Prostate cancer. *Nature Reviews Disease Primers 2021 7:1*, *7*(1), 1–27. https://doi.org/10.1038/s41572-020-00243-0

Reid, E., Suneja, G., Ambinder, R. F., Ard, K., Baiocchi, R., Barta, S. K., Carchman, E., Cohen, A., Gupta, N., Johung, K. L., Klopp, A., LaCasce, A. S., Lin, C., Makarova-Rusher, O. V., Mehta, A., Menon, M. P., Morgan, D., Nathwani, N., Noy, A., … Freedman-Cass, D. A. (2018). Cancer in People Living With HIV, Version 1.2018, NCCN Clinical Practice Guidelines in Oncology. *Journal of the National Comprehensive Cancer Network*, *16*(8), 986–1017. https://doi.org/10.6004/JNCCN.2018.0066

Runz, S., Mierke, C. T., Joumaa, S., Behrens, J., Fabry, B., & Altevogt, P. (2008). CD24 induces localization of beta1 integrin to lipid raft domains. *Biochemical and Biophysical Research Communications*, *365*(1), 35–41. https://doi.org/10.1016/J.BBRC.2007.10.139

Sagiv, E., & Arber, N. (2008). The novel oncogene CD24 and its arising role in the carcinogenesis of the GI tract: from research to therapy. *Expert Review of Gastroenterology & Hepatology*, *2*(1), 125–133. https://doi.org/10.1586/17474124.2.1.125

Sagiv, E., Kazanov, D., & Arber, N. (2006). CD24 plays an important role in the carcinogenesis process of the pancreas. *Biomedicine & Pharmacotherapy*, *60*(6), 280–284. https://doi.org/10.1016/J.BIOPHA.2006.06.006

Sagiv, E., Starr, A., Rozovski, U., Khosravi, R., Altevogt, P., & Wang, T. (2008). *Targeting CD24 for Treatment of Colorectal and Pancreatic Cancer by Monoclonal Antibodies or Small Interfering RNA*. *8*, 2803–2813. https://doi.org/10.1158/0008-5472.CAN-07-6463

Saidova, A. A., Potashnikova, D. M., Tvorogova, A. V., Paklina, O. V., Veliev, E. I., Knyshinsky, G. V., Setdikova, G. R., Rotin, D. L., Maly, I. V., Hofmann, W. A., & Vorobjev, I. A. (2021). Myosin 1C

isoform A is a novel candidate diagnostic marker for prostate cancer. *PloS One*, *16*(5). https://doi.org/10.1371/JOURNAL.PONE.0251961

Salnikov, A. V., Bretz, N. P., Perne, C., Hazin, J., Keller, S., Fogel, M., Herr, I., Schlange, T., Moldenhauer, G., & Altevogt, P. (2013). Antibody targeting of CD24 efficiently retards growth and influences cytokine milieu in experimental carcinomas. *British Journal of Cancer*, *108*(7), 1449. https://doi.org/10.1038/BJC.2013.102

Sammar, M., Siwetz, M., Meiri, H., Fleming, V., Altevogt, P., & Huppertz, B. (2017). Expression of CD24 and Siglec-10 in first trimester placenta: implications for immune tolerance at the fetal-maternal interface. *Histochemistry and Cell Biology*, *147*(5), 565–574. https://doi.org/10.1007/S00418-016-1531-7

Schabath, H., Runz, S., Joumaa, S., & Altevogt, P. (2006). CD24 affects CXCR4 function in pre-B lymphocytes and breast carcinoma cells. *Journal of Cell Science*, *119*(Pt 2), 314–325. https://doi.org/10.1242/JCS.02741

Schirrmacher, V. (2019). From chemotherapy to biological therapy: A review of novel concepts to reduce the side effects of systemic cancer treatment (Review). *International Journal of Oncology*, *54*(2), 407–419. https://doi.org/10.3892/IJO.2018.4661/HTML

Schnell, R., Katouzi, A. A., Linnartz, C., Schoen, G., Drillich, S., Hansmann, M. L., Schiefer, D., Barth, S., Zangemeister-Wittke, U., Stahel, R. A., Diehl, V., & Engert, A. (1996). Potent anti-tumor effects of an anti-CD24 ricin A-chain immunotoxin in vitro and in a disseminated human Burkitt's lymphoma model in SCID mice. *International Journal of Cancer*, *66*(4), 526–531. https://doi.org/10.1002/(SICI)1097-0215(19960516)66:4<526::AID-IJC17>3.0.CO;2-5

Schuster, S. J., Bishop, M. R., Tam, C. S., Waller, E. K., Borchmann, P., McGuirk, J. P., Jäger, U., Jaglowski, S., Andreadis, C., Westin, J. R., Fleury, I., Bachanova, V., Foley, S. R., Ho, P. J., Mielke, S., Magenau, J. M., Holte, H., Pantano, S., Pacaud, L. B., … Maziarz, R. T. (2019). Tisagenlecleucel in Adult Relapsed or Refractory Diffuse Large B-Cell Lymphoma. *New England Journal of Medicine*, *380*(1), 45–56. https://doi.org/10.1056/NEJMOA1804980/SUPPL_FILE/NEJMOA1804980_DISCLOSURES.PDF

Senner, V., Sturm, A., Baur, I., Schrell, U. H. M., Distel, L., & Paulus, W. (1999). CD24 Promotes Invasion of Glioma Cells In Vivo. *Journal of Neuropathology & Experimental Neurology*, *58*(8), 795–802. https://doi.org/10.1097/00005072-199908000-00002

Shahjee, H. M., Koch, K. R., Guo, L., Zhang, C. O., & Keay, S. K. (2010). Antiproliferative factor decreases Akt phosphorylation and alters gene expression via CKAP4 in T24 bladder carcinoma cells. *Journal of Experimental & Clinical Cancer Research : CR*, *29*(1), 160. https://doi.org/10.1186/1756-9966-29-160

Shapira, S., Shapira, A., Starr, A., Kazanov, D., Kraus, S., Benhar, I., & Arber, N. (2011). An immunoconjugate of Anti-CD24 and pseudomonas exotoxin selectively kills human colorectal tumors in mice. *Gastroenterology*, *140*(3), 935–946. https://doi.org/10.1053/J.GASTRO.2010.12.004

Shewan, D., Calaora, V., Nielsen, P., Cohen, J., Rougon, G., & Moreau, H.-V. (1996). mCD24, a Glycoprotein Transiently Expressed by Neurons, Is an Inhibitor of Neurite Outgrowth. *The Journal of Neuroscience*, *16*(8), 2624–2634.

Skowron, M. A., Becker, T. K., Kurz, L., Jostes, S., Bremmer, F., Fronhoffs, F., Funke, K., Wakileh, G. A., Müller, M. R., Burmeister, A., Lenz, T., Stefanski, A., Stühler, K., Petzsch, P., Köhrer, K.,

Bibliography

Altevogt, P., Albers, P., Kristiansen, G., Schorle, H., & Nettersheim, D. (2022). The signal transducer CD24 suppresses the germ cell program and promotes an ectodermal rather than mesodermal cell fate in embryonal carcinomas. *Molecular Oncology*, *16*(4), 982. https://doi.org/10.1002/1878-0261.13066

Skowron, M. A., Vermeulen, M., Winkelhausen, A., Becker, T. K., Bremmer, F., Petzsch, P., Schönberger, S., Calaminus, G., Köhrer, K., Albers, P., & Nettersheim, D. (2020). CDK4/6 inhibition presents as a therapeutic option for paediatric and adult germ cell tumours and induces cell cycle arrest and apoptosis via canonical and non-canonical mechanisms. *British Journal of Cancer*, *123*(3), 378–391. https://doi.org/10.1038/S41416-020-0891-X

Smith, S. C., Oxford, G., Wu, Z., Nitz, M. D., Conaway, M., Frierson, H. F., Hampton, G., & Theodorescu, D. (2006). The Metastasis-Associated Gene CD24 Is Regulated by Ral GTPase and Is a Mediator of Cell Proliferation and Survival in Human Cancer. *Cancer Research*, *66*(4), 1917–1922. https://doi.org/10.1158/0008-5472.CAN-05-3855

Söhngen, C. (2022). *Molekulare Charakterisierung des Signalproteins CD24 in urologischen Malignitäten und dessen Eignung als Ziel für Immuntherapien* [Master Thesis].

Söhngen, C., Thomas, D. J., Skowron, M. A., Bremmer, F., Eckstein, M., Stefanski, A., Driessen, M. D., Wakileh, G. A., Stühler, K., Altevogt, P., Theodorescu, D., Klapdor, R., Schambach, A., & Nettersheim, D. (2023). CD24 targeting with NK-CAR immunotherapy in testis, prostate, renal and (luminal-type) bladder cancer and identification of direct CD24 interaction partners. *The FEBS Journal*. https://doi.org/10.1111/FEBS.16880

Sorbello, V., Fuso, L., Sfiligoi, C., Scafoglio, C., Ponzone, R., Biglia, N., Weisz, A., Sismondi, P., & De Bortoli, M. (2003). Quantitative real-time RT-PCR analysis of eight novel estrogen-regulated genes in breast cancer. *The International Journal of Biological Markers*, *18*(2), 123–129. https://doi.org/10.1177/172460080301800205

Srivastava, S., Furlan, S. N., Jaeger-Ruckstuhl, C. A., Sarvothama, M., Berger, C., Smythe, K. S., Garrison, S. M., Specht, J. M., Lee, S. M., Amezquita, R. A., Voillet, V., Muhunthan, V., Yechan-Gunja, S., Pillai, S. P. S., Rader, C., Houghton, A. M. G., Pierce, R. H., Gottardo, R., Maloney, D. G., & Riddell, S. R. (2021). Immunogenic chemotherapy enhances recruitment of CAR-T cells to lung tumors and improves anti-tumor efficacy when combined with checkpoint blockade. *Cancer Cell*, *39*(2), 193. https://doi.org/10.1016/J.CCELL.2020.11.005

Štefanová, I., Hořejší, V., Ansotegui, I. J., Knapp, W., & Stockinger, H. (1991). GPI-Anchored Cell-Surface Molecules Complexed to Protein Tyrosine Kinases. *Science*, *254*(5034), 1016–1019. https://doi.org/10.1126/SCIENCE.1719635

Sterner, R. C., & Sterner, R. M. (2021). CAR-T cell therapy: current limitations and potential strategies. *Blood Cancer Journal*, *11*(4). https://doi.org/10.1038/S41408-021-00459-7

Stivarou, T., Stellas, D., Vartzi, G., Thomaidou, D., & Patsavoudi, E. (2016). Targeting highly expressed extracellular HSP90 in breast cancer stem cells inhibits tumor growth in vitro and in vivo. *Cancer Biology & Therapy*, *17*(8), 799. https://doi.org/10.1080/15384047.2016.1195041

Sun, C. M., Geng, J., Yan, Y., Yao, X., & Liu, M. (2017). Overexpression of CKAP4 is Associated with Poor Prognosis in Clear Cell Renal Cell Carcinoma and Functions via Cyclin B Signaling. *Journal of Cancer*, *8*(19), 4018. https://doi.org/10.7150/JCA.21226

Bibliography

Sun, F., Wang, T., Jiang, J., Wang, Y., Ma, Z., Li, Z., Han, Y., Pan, M., Cai, J., Wang, M., & Zhang, J. (2017). Engineering a high-affinity humanized anti-CD24 antibody to target hepatocellular carcinoma by a novel CDR grafting design. *Oncotarget*, *8*(31), 51238–51252. https://doi.org/10.18632/ONCOTARGET.17228

Sun, F., Wang, Y., Luo, X., Ma, Z., Xu, Y., Zhang, X., Lv, T., Zhang, Y., Wang, M., Huang, Z., & Zhang, J. (2019). Anti-CD24 Antibody-Nitric Oxide Conjugate Selectively and Potently Suppresses Hepatic Carcinoma. *Cancer Research*, *79*(13), 3395–3405. https://doi.org/10.1158/0008-5472.CAN-18-2839

Sun, J., Feng, D., Xi, H., Luo, J., Zhou, Z., Liu, Q., Chen, Y., & Shao, Q. (2020). CD24 blunts the sensitivity of retinoblastoma to vincristine by modulating autophagy. *Molecular Oncology*, *14*(8), 1740–1759. https://doi.org/10.1002/1878-0261.12708

Sung, H., Ferlay, J., Siegel, R. L., Laversanne, M., Soerjomataram, I., Jemal, A., & Bray, F. (2021). Global Cancer Statistics 2020: GLOBOCAN Estimates of Incidence and Mortality Worldwide for 36 Cancers in 185 Countries. *CA: A Cancer Journal for Clinicians*, *71*(3), 209–249. https://doi.org/10.3322/CAAC.21660

Suzuki, T., Kiyokawa, N., Taguchi, T., Sekino, T., Katagiri, Y. U., & Fujimoto, J. (2001). CD24 Induces Apoptosis in Human B Cells Via the Glycolipid-Enriched Membrane Domains/Rafts-Mediated Signaling System. *The Journal of Immunology*, *166*(9), 5567–5577. https://doi.org/10.4049/JIMMUNOL.166.9.5567

Szklarczyk, D., Gable, A. L., Lyon, D., Junge, A., Wyder, S., Huerta-Cepas, J., Simonovic, M., Doncheva, N. T., Morris, J. H., Bork, P., Jensen, L. J., & Von Mering, C. (2019). STRING v11: protein-protein association networks with increased coverage, supporting functional discovery in genome-wide experimental datasets. *Nucleic Acids Research*, *47*(D1), D607–D613. https://doi.org/10.1093/NAR/GKY1131

Todesursachen in Deutschland - Statistisches Bundesamt. (n.d.-a). Retrieved January 22, 2023, from https://www.destatis.de/DE/Themen/Gesellschaft-Umwelt/Gesundheit/Todesursachen/_inhalt.html

Todesursachen in Deutschland - Statistisches Bundesamt. (n.d.-b). Retrieved January 23, 2023, from https://www.destatis.de/DE/Themen/Gesellschaft-Umwelt/Gesundheit/Todesursachen/_inhalt.html#sprg235878

Tolkach, Y., Zarbl, R., Bauer, S., Ritter, M., Ellinger, J., Hauser, S., Hüser, L., Klauck, S. M., Altevogt, P., Sültmann, H., Dietrich, D., & Kristiansen, G. (2021). DNA Promoter Methylation and ERG Regulate the Expression of CD24 in Prostate Cancer. *The American Journal of Pathology*, *191*(4), 618–630. https://doi.org/10.1016/J.AJPATH.2020.12.014

Tran, L., Xiao, J. F., Agarwal, N., Duex, J. E., & Theodorescu, D. (2020). Advances in bladder cancer biology and therapy. *Nature Reviews Cancer 2020 21:2*, *21*(2), 104–121. https://doi.org/10.1038/s41568-020-00313-1

Venny 2.1.0. (n.d.). Retrieved March 9, 2023, from https://bioinfogp.cnb.csic.es/tools/venny/

Vesuna, F., Lisok, A., Kimble, B., & Raman, V. (2009). Twist Modulates Breast Cancer Stem Cells by Transcriptional Regulation of CD24 Expression. *Neoplasia (New York, N.Y.)*, *11*(12), 1318. https://doi.org/10.1593/NEO.91084

Bibliography

Visuttijai, K., Pettersson, J., Azar, Y. M., Van Den Bout, I., Örndal, C., Marcickiewicz, J., Nilsson, S., Hörnquist, M., Olsson, B., Ejeskär, K., & Behboudi, A. (2016). Lowered Expression of Tumor Suppressor Candidate MYO1C Stimulates Cell Proliferation, Suppresses Cell Adhesion and Activates AKT. *PLoS ONE*, *11*(10). https://doi.org/10.1371/JOURNAL.PONE.0164063

Wang, L., Lin, S., Rammohan, K. W., Liu, Z., Liu, J. Q., Liu, R. H., Guinther, N., Lima, J., Zhou, Q., Wang, T., Zheng, X., Birmingham, D. J., Rovin, B. H., Hebert, L. A., Wu, Y., Lynn, D. J., Cooke, G., Yu, C. Y., Zheng, P., & Liu, Y. (2007). A Dinucleotide Deletion in CD24 Confers Protection against Autoimmune Diseases. *PLOS Genetics*, *3*(4), e49. https://doi.org/10.1371/JOURNAL.PGEN.0030049

Wang, L., Liu, R., Ye, P., Wong, C., Chen, G. Y., Zhou, P., Sakabe, K., Zheng, X., Wu, W., Zhang, P., Jiang, T., Bassetti, M. F., Jube, S., Sun, Y., Zhang, Y., Zheng, P., & Liu, Y. (2015). Intracellular CD24 disrupts the ARF–NPM interaction and enables mutational and viral oncogene-mediated p53 inactivation. *Nature Communications 2015 6:1*, *6*(1), 1–15. https://doi.org/10.1038/ncomms6909

Wang, M., Xiao, J., Shen, M., Yahong, Y., Tian, R., Zhu, F., Jiang, J., Du, Z., Hu, J., Liu, W., & Qin, R. (2011). Isolation and characterization of tumorigenic extrahepatic cholangiocarcinoma cells with stem cell-like properties. *International Journal of Cancer*, *128*(1), 72–81. https://doi.org/10.1002/IJC.25317

Wang, T., Sun, F., Xie, W., Tang, M., He, H., Jia, X., Tian, X., Wang, M., & Zhang, J. (2016). A bispecific protein rG7S-MICA recruits natural killer cells and enhances NKG2D-mediated immunosurveillance against hepatocellular carcinoma. *Cancer Letters*, *372*(2), 166–178. https://doi.org/10.1016/J.CANLET.2016.01.001

Wang, X., Zhang, Y., Zhao, Y., Liang, Y., Xiang, C., Zhou, H., Zhang, H., Zhang, Q., Qing, H., Jiang, B., Xiong, H., & Peng, L. (2016). CD24 promoted cancer cell angiogenesis via Hsp90-mediated STAT3/VEGF signaling pathway in colorectal cancer. *Oncotarget*, *7*(34), 55663–55676. https://doi.org/10.18632/ONCOTARGET.10971

Weichert, W., Denkert, C., Burkhardt, M., Gansukh, T., Bellach, J., Altevogt, P., Dietel, M., & Kristiansen, G. (2005). Cytoplasmic CD24 Expression in Colorectal Cancer Independently Correlates with Shortened Patient Survival. *Clinical Cancer Research*, *11*(18), 6574–6581. https://doi.org/10.1158/1078-0432.CCR-05-0606

Whilding, L. M., Halim, L., Draper, B., Parente-Pereira, A. C., Zabinski, T., Davies, D. M., & Maher, J. (2019). CAR T-Cells Targeting the Integrin αvβ6 and Co-Expressing the Chemokine Receptor CXCR2 Demonstrate Enhanced Homing and Efficacy against Several Solid Malignancies. *Cancers*, *11*(5). https://doi.org/10.3390/CANCERS11050674

Wrona, E., Borowiec, M., & Potemski, P. (2021). CAR-NK Cells in the Treatment of Solid Tumors. *International Journal of Molecular Sciences*, *22*(11). https://doi.org/10.3390/IJMS22115899

Xu, Y., Liu, Q., Zhong, M., Wang, Z., Chen, Z., Zhang, Y., Xing, H., Tian, Z., Tang, K., Liao, X., Rao, Q., Wang, M., & Wang, J. (2019). 2B4 costimulatory domain enhancing cytotoxic ability of anti-CD5 chimeric antigen receptor engineered natural killer cells against T cell malignancies. *Journal of Hematology and Oncology*, *12*(1), 1–13. https://doi.org/10.1186/S13045-019-0732-7/FIGURES/5

Yan, S., Xu, D., Jiang, T., Wang, P., Yin, Y., Wang, X., Hua, C., Zhang, B., Li, Z., Lu, L., Liu, X., Wang, B., Zhang, D., Zhang, R., Sun, B., & Wang, X. (2014). CD24 single nucleotide polymorphisms

and cancer risk. *Tumor Biology*, *35*(9), 8927–8932. https://doi.org/10.1007/S13277-014-2127-2/FIGURES/2

Yeung, T. M., Gandhi, S. C., Wilding, J. L., Muschel, R., & Bodmer, W. F. (2010). Cancer stem cells from colorectal cancer-derived cell lines. *Proceedings of the National Academy of Sciences of the United States of America*, *107*(8), 3722–3727. https://doi.org/10.1073/pnas.0915135107

Zangemeister-Wittke, U., Lehmann, H. -P, Waibel, R., Wawrzynczak, E. J., & Stahel, R. A. (1993). Action of a CD24-specific deglycosylated ricin-A-chain immunotoxin in conventional and novel models of small-cell-lung-cancer xenograft. *International Journal of Cancer*, *53*(3), 521–528. https://doi.org/10.1002/IJC.2910530327

Zarn, J. A., Zimmermann, S. M., Pass, M. K., Waibel, R., & Stahel, R. A. (1996). Association of CD24 with the kinase c-fgr in a small cell lung cancer cell line and with the kinase lyn in an erythroleukemia cell line. *Biochemical and Biophysical Research Communications*, *225*(2), 384–391. https://doi.org/10.1006/BBRC.1996.1184

Zhang, C., Li, C., He, F., Cai, Y., & Yang, H. (2011). Identification of CD44+CD24+ gastric cancer stem cells. *Journal of Cancer Research and Clinical Oncology*, *137*(11), 1679–1686. https://doi.org/10.1007/s00432-011-1038-5

Zhang, J., Chen, X., Bian, L., Wang, Y., & Liu, H. (2019). CD44 + /CD24 +-Expressing Cervical Cancer Cells and Radioresistant Cervical Cancer Cells Exhibit Cancer Stem Cell Characteristics. *Original Article Gynecol Obstet Invest*, *84*, 174–182. https://doi.org/10.1159/000493129

Zhang, P., Zheng, P., & Liu, Y. (2019). Amplification of the CD24 gene is an independent predictor for poor prognosis of breast cancer. *Frontiers in Genetics*, *10*(JUN). https://doi.org/10.3389/FGENE.2019.00560/FULL

Zhou, X. (2014). CD24 Polymorphisms Cannot Predict Pathologic Complete Response to Anthracycline- and Taxane-Based Neoadjuvant Chemotherapy in Breast Cancer. *Clinical Breast Cancer*, *14*(2), e33–e40. https://doi.org/10.1016/J.CLBC.2013.11.001

Eidesstaatliche Erklärung

Ich versichere hiermit, dass ich die vorliegende Doktorarbeit selbständig verfasst und keine anderen als die angegebenen Quellen und Hilfsmittel verwendet habe. Ich habe die Stellen gekennzeichnet, die ich wörtlich oder inhaltlich den benutzten Quellen entnommen habe. Die Arbeit hat in gleicher oder ähnlicher Form noch keiner anderen Prüfungsbehörde vorgelegen.

Die Arbeit wurde im urologischen Forschungslabor „Translationale UroOnkologie“ der Klinik für Urologie des Universitätsklinikums Düsseldorf unter der Betreuung und Konzeption von Prof. Dr. Daniel Nettersheim angefertigt. Die vorgestellten Experimente wurden selbständig durchgeführt, mit Ausnahme der folgenden Versuche und Ergebnisse, welche von Dritten bzw. in Kooperation mit Dritten erstellt wurden:

- • Die CD24-qRT-PCR der EC-Zelllinien 2102EP, NCCIT und NT2/D1 (Fig. 10 [B] wurde von Dr. Margaretha Skowron (Wissenschaftliche Mitarbeiterin, Translationale UroOnkologie, HHU Düsseldorf) und die der Tumor-Zelllinien VM-CUB-1, RT-112, Caki-1, 786-O, ACHN, DU145 und PC-3 (Abbildung 8) von Dr. med. Gamal Wakileh (Forschungsstipendiat, Forschungslabor der Klinik für Urologie, Arbeitsgruppe „Translationale Uroonkologie“, HHU Düsseldorf) durchgeführt

- • Die massenspektrometrische Analyse der CD24-Co-immunprizipitierten Proben wurde von Dr. Anja Stefanski (Biologisch-Medizinisches Forschungszentrum (BMFZ), Arbeitsgruppe „Molecular Proteomics Laboratory“, Leitung Prof. Dr. Kai Stühler, HHU) durchgeführt

- Die XTT Assays zum Einfluss von CD24 auf die Drug Sensitivität wurden in Zusammenarbeit mit Dr. med. Gamal Wakileh (Forschungsstipendiat, Forschungslabor der Klinik für Urologie, Arbeitsgruppe „Translationale Uroonkologie“, HHU Düsseldorf) durchgeführt

Düsseldorf den 12.06.2024

David Julian Thomas

Ort, Datum

Unterschrift (David Julian Thomas)

6 Appendix

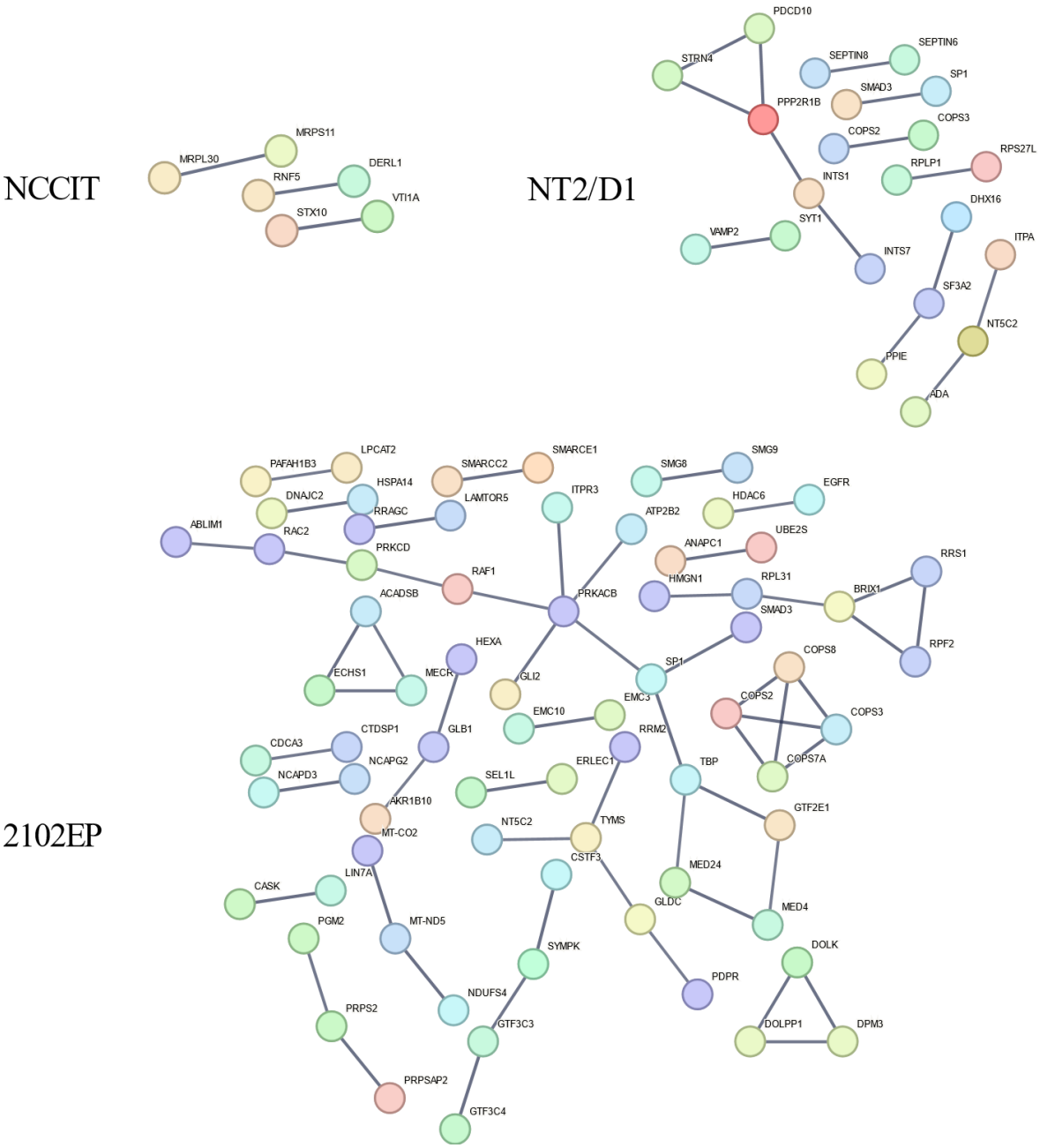

Fig. 17: STRING analysis of CD24 interaction partners in GCT
For each entity proteins with an abundance ratio of over 10 and a p-value <0,05 were analyzed via STRING analysis. Proteins in the network are further color-coded for biological functions previously found in the DAVID gene ontology analysis.

Table 31: Co-IP precipitated proteins and overlap in pan-urological cells

RT-112, PC-3, Caki-1	RT-112, PC-3	RT-112, Caki-1	PC-3, Caki-1
ABHD17B	ANKRD10	AASDHPPT	ACOX1
ALG9	BCAM	ALG11	ACSL5
COL1A1	CDC27	BAZ1B	ADAM17
ERVK-24	CLK2	BTAF1	ANP32E

Appendix

GBA	CNOT7	CAMLG	ARMC8
GOLM1	CNPY2	COL3A1	BOP1
GTF3C2	COPS2	DPPA4	C12orf10
ITSN1	COX4I1	ECI1	C9orf169
JAM3	IFITM3	ENOX2	CAPG
MAPK3	IGHG2	FAM127B	CD58
METAP1	LEMD3	FBXW11	CDC123
MFN2	LPP	HDGFRP2	CLTA
MFSD5	MFN1	HS1BP3	CLUH
NOM1	MRPL40	IGKC	COG1
PARN	MRPS31	KDM5C	CSTB
PRRC2B	PFN2	KIAA0196	CTPS2
PRSS8	PSMD10	LUC7L2	CTSA
RNF121	RBM33	MARK2	CUL1
SAP30BP	RBM4B	MMP2	CUL4B
SELENBP1	RDH11	MTAP	CWC27
STAT2	RIC8A	NOP14	DBNL
TNPO2	RINT1	NUDCD2	DHRS1
UPF3B	SDHD	PALD1	DNAJB4
USP48	SERPINB9	PTPRF	DPH2
WIBG; PYM1	SOX2	RANBP10	DSP
	SV2A	RRS1	ERGIC3
	TAF6L	SLC7A3	FYN
	TMEM87A	TOM1	GBF1
	TMOD2	TPM2	GNAO1
	TRIM24	TRIP10	GNE
	TRMT1	ZNF219	HAT1
	TUBB8		IFI35
	USP5		IPO8
	YIF1A		JMJD6
	ZNF281		KAT7
			KCTD5
			KNTC1
			LAD1
			LRRC1
			ME1
			METAP2
			MINA
			MPV17L2
			MRPL55
			MRPS22
			MRPS24
			NAA25

NANS
NBAS
NCAPG
NCDN
NDUFS6
NEDD4L
NHLRC2
OTUB1
PIP4K2C
PPIF
PRDM14
PSMB3
PSPH
PTMA
RANBP3
RIOK2
ROR1
RRM1
SEPTIN6
SERPINF1
SERPINH1
SMARCA1
SMPDL3B
SNX27
SRSF11
STXBP2
SUPV3L1
TBC1D2
TPRG1L
TPT1
TXNDC12
USP15
ZSCAN10

Table 32: Co-IP precipitated proteins and overlap in GCT cell lines

2102EP, NCCIT, NT2/D1	2102EP/NT2/D1	2102EP/NCCIT	NCCIT/NT2/D1
ACHE	ACTR1B	DOCK6	GPI
C6orf120	ANAPC1	DOLPP1	GPRC5C
CNTFR	ANO6	ERBB2IP	RNF5
GDE1	ATP1A2	GALNT14	SEPT8
MFSD10	ATP5J	ITPR3	ST6GAL1
RAP2A	ATP6V1G2	KRT36	TMEM147
STX10	C17orf49	STK39	TMEM222
TRABD	CASK		

Appendix

CCNY
COPS2
COPS3
CTDSP1
DNAJC2
DOLK
EFCAB14
EHD2
EMC10
FAM210A
GLDC
KDM5C
KIAA0196
L2HGDH
MFF
MTAP
MTFP1
MYADM
NCAPD3
NFYB
NT5C2
PDCD10
PNPLA4
PTPMT1
QRICH1
SCAF8
SH3BP4
SIDT2
SLC16A3
SLC9A6
SMAD3
SMG9
SP1
SPATA5L1
SPRY4
TMPRSS4
URB2
XPO6
ZC3H4
ZDHHC3

Appendix

Table 33: TGCT 2102EP gene ontology analysis

Category	Term	Count	PValue	Bonferroni
GOTERM_MF_DIRECT	protein binding	216	3.42E-08	1.75E-05
UP_KW_PTM	Acetylation	89	1.15E-07	2.07E-06
UP_KW_PTM	Phosphoprotein	163	5.94E-07	1.07E-05
INTERPRO	HAD-like domain	9	1.30E-05	0.0079944
GOTERM_BP_DIRECT	protein deneddylation	4	3.44E-04	0.4100494
UP_KW_MOLECULAR_FUNCTION	Transferase	47	4.09E-04	0.0266504
UP_KW_MOLECULAR_FUNCTION	Protein phosphatase	9	8.80E-04	0.056476
GOTERM_BP_DIRECT	regulation of protein neddylation	4	9.12E-04	0.7533983
GOTERM_MF_DIRECT	myosin phosphatase activity	7	9.75E-04	0.393
GOTERM_MF_DIRECT	kinase activity	11	0.0015523	0.5485886
GOTERM_MF_DIRECT	magnesium ion binding	11	0.0016534	0.5713935
GOTERM_MF_DIRECT	protein serine/threonine phosphatase activity	6	0.0016767	0.5765016
GOTERM_BP_DIRECT	dolichyl diphosphate biosynthetic process	3	0.0016805	0.9243624
GOTERM_BP_DIRECT	protein neddylation	4	0.0032832	0.9935776
UP_KW_MOLECULAR_FUNCTION	Acyltransferase	9	0.0035634	0.2099064
INTERPRO	Proteasome component (PCI) domain	4	0.0042098	0.9265677
KEGG_PATHWAY	Endocytosis	11	0.004599	0.6955554
KEGG_PATHWAY	Estrogen signaling pathway	8	0.0047111	0.7042806
UP_KW_BIOLOGICAL_PROCESS	Nucleotide biosynthesis	3	0.0052111	0.3685743
INTERPRO	NLI interacting factor	3	0.0063711	0.9808664
UP_KW_MOLECULAR_FUNCTION	Hydrolase	38	0.0068673	0.3654266
GOTERM_MF_DIRECT	ATP binding	34	0.0081488	0.9848431
GOTERM_MF_DIRECT	protein homodimerization activity	20	0.0083719	0.9864917
GOTERM_BP_DIRECT	cellular response to amino acid stimulus	5	0.0100411	0.9999998
GOTERM_MF_DIRECT	syntaxin binding	5	0.0113529	0.9971084
GOTERM_MF_DIRECT	transcription factor activity, core RNA polymerase III binding	3	0.0115345	0.997368
INTERPRO	Armadillo-type fold	12	0.0117049	0.9993163
KEGG_PATHWAY	Galactose metabolism	4	0.0122441	0.9583508
GOTERM_BP_DIRECT	cell division	12	0.0128582	1
KEGG_PATHWAY	GnRH signaling pathway	6	0.0133032	0.9684211
UP_KW_BIOLOGICAL_PROCESS	Cell division	13	0.014225	0.7165693
GOTERM_MF_DIRECT	identical protein binding	36	0.0157751	0.9997087
GOTERM_BP_DIRECT	protein localization to lysosome	3	0.0161797	1
UP_KW_MOLECULAR_FUNCTION	Kinase	19	0.0164048	0.6643522
UP_KW_MOLECULAR_FUNCTION	Isomerase	7	0.0186048	0.7104661
GOTERM_MF_DIRECT	nucleosomal DNA binding	4	0.019067	0.9999476
GOTERM_BP_DIRECT	type B pancreatic cell proliferation	3	0.0205985	1
KEGG_PATHWAY	Metabolic pathways	34	0.0218249	0.9966312
UP_KW_BIOLOGICAL_PROCESS	Mitosis	10	0.0218265	0.8565835
GOTERM_BP_DIRECT	protein dephosphorylation	6	0.0219988	1
GOTERM_BP_DIRECT	ubiquitin-dependent ERAD pathway	5	0.0221397	1
GOTERM_MF_DIRECT	magnesium ion transmembrane transporter activity	3	0.0227119	0.9999922

Category	Term	Count	PValue	Bonferroni
INTERPRO	Armadillo-like helical	9	0.0229169	0.9999994
GOTERM_BP_DIRECT	small GTPase mediated signal transduction	6	0.0234179	1
GOTERM_MF_DIRECT	palmitoyltransferase activity	3	0.0253205	0.999998
GOTERM_BP_DIRECT	osteoblast development	3	0.025458	1
GOTERM_BP_DIRECT	'de novo' cotranslational protein folding	2	0.0261473	1
KEGG_PATHWAY	Pancreatic cancer	5	0.0279605	0.9993356
GOTERM_BP_DIRECT	nucleoside metabolic process	3	0.028045	1
INTERPRO	SANT/Myb domain	4	0.0298243	1
GOTERM_BP_DIRECT	positive regulation of peptidyl-serine phosphorylation	5	0.0344432	1
KEGG_PATHWAY	Salmonella infection	9	0.0352785	0.9999054
GOTERM_BP_DIRECT	ribosomal large subunit assembly	3	0.0363969	1
GOTERM_BP_DIRECT	protein palmitoylation	3	0.0363969	1
GOTERM_BP_DIRECT	lysosome organization	4	0.0374666	1
KEGG_PATHWAY	Amino sugar and nucleotide sugar metabolism	4	0.0377994	0.9999519
GOTERM_BP_DIRECT	regulation of neurotrophin TRK receptor signaling pathway	2	0.0389645	1
GOTERM_BP_DIRECT	protein mannosylation	2	0.0389645	1
GOTERM_BP_DIRECT	spindle assembly involved in meiosis	2	0.0389645	1
GOTERM_BP_DIRECT	phosphorylation	9	0.0389973	1
INTERPRO	Smg8/Smg9	2	0.0407175	1
GOTERM_MF_DIRECT	inositol hexakisphosphate binding	2	0.0410266	1
GOTERM_MF_DIRECT	protein kinase activity	11	0.0410344	1
KEGG_PATHWAY	Colorectal cancer	5	0.0412886	0.9999811
GOTERM_BP_DIRECT	regulation of cardiac conduction	3	0.0424275	1
GOTERM_BP_DIRECT	developmental growth	3	0.0424275	1
INTERPRO	Zinc finger, DHHC-type, palmitoyltransferase	3	0.0426755	1
KEGG_PATHWAY	N-Glycan biosynthesis	4	0.0460307	0.9999948
GOTERM_MF_DIRECT	histone acetyltransferase binding	3	0.0466112	1
KEGG_PATHWAY	Terpenoid backbone biosynthesis	3	0.0468633	0.9999958

Table 34: TGCT NCCIT gene ontology analysis

Category	Term	Count	PValue	Bonferroni
GOTERM_BP_DIRECT	protein destabilization	4	6.10E-04	0.3470335
UP_KW_BIOLOGICAL_PROCESS	Transport	16	8.11E-04	0.0358539
UP_KW_MOLECULAR_FUNCTION	Hydrolase	15	0.0026453	0.1193923
UP_KW_BIOLOGICAL_PROCESS	Protein transport	8	0.0031622	0.132834
GOTERM_BP_DIRECT	positive regulation of apoptotic process	6	0.0043178	0.9514263
GOTERM_BP_DIRECT	positive regulation of protein serine/threonine kinase activity	3	0.007566	0.9950517
GOTERM_MF_DIRECT	protein binding	51	0.0115513	0.9205661
INTERPRO	Small GTPase superfamily	4	0.0119628	0.8946577
GOTERM_BP_DIRECT	regulation of localization	2	0.0126888	0.9998671
GOTERM_BP_DIRECT	humoral immune response	3	0.0177504	0.9999963
INTERPRO	Small GTP-binding protein domain	4	0.0200612	0.9773951

Appendix

Category	Term	Count	PValue	Bonferroni
UP_KW_PTM	Prenylation	4	0.0220532	0.2681651
UP_KW_BIOLOGICAL_PROCESS	Lipid metabolism	7	0.0255032	0.6873071
GOTERM_BP_DIRECT	vesicle fusion with Golgi apparatus	2	0.0283273	1
GOTERM_BP_DIRECT	NAD biosynthesis via nicotinamide riboside salvage pathway	2	0.0314256	1
GOTERM_BP_DIRECT	negative regulation of NF-kappaB transcription factor activity	3	0.0362192	1
GOTERM_BP_DIRECT	positive regulation of DNA damage response, signal transduction by p53 class mediator	2	0.0375931	1
GOTERM_BP_DIRECT	ER-associated misfolded protein catabolic process	2	0.0375931	1
GOTERM_BP_DIRECT	actin cytoskeleton organization	4	0.0378627	1
GOTERM_MF_DIRECT	GTP binding	5	0.0433738	0.9999366
GOTERM_BP_DIRECT	replicative senescence	2	0.0498124	1
GOTERM_BP_DIRECT	negative regulation of single stranded viral RNA replication via double stranded DNA intermediate	2	0.0498124	1
GOTERM_BP_DIRECT	hormone metabolic process	2	0.0498124	1

Table 35: TGCT NT2/D1 gene ontology analysis

Category	Term	Count	PValue	Bonferroni
GOTERM_MF_DIRECT	protein binding	116	9.16E-07	3.03E-04
UP_KW_PTM	Acetylation	48	1.14E-04	0.0018157
KEGG_PATHWAY	Metabolic pathways	24	0.0032698	0.443592
GOTERM_MF_DIRECT	identical protein binding	23	0.0055095	0.8393765
GOTERM_BP_DIRECT	cellular response to leukemia inhibitory factor	5	0.0062639	0.9968555
GOTERM_MF_DIRECT	protein homodimerization activity	13	0.0072548	0.9101919
GOTERM_MF_DIRECT	hydrolase activity	7	0.0104613	0.9692211
GOTERM_BP_DIRECT	response to cadmium ion	3	0.0125577	0.9999907
GOTERM_BP_DIRECT	positive regulation of intracellular protein transport	3	0.0125577	0.9999907
UP_KW_MOLECULAR_FUNCTION	Hydrolase	22	0.0126423	0.4773638
UP_KW_BIOLOGICAL_PROCESS	Nucleotide metabolism	3	0.0167925	0.6729742
GOTERM_MF_DIRECT	calmodulin binding	6	0.0172742	0.9968731
GOTERM_BP_DIRECT	liver development	4	0.0192995	1
GOTERM_BP_DIRECT	intrinsic apoptotic signaling pathway in response to DNA damage by p53 class mediator	3	0.0213308	1
UP_KW_BIOLOGICAL_PROCESS	mRNA splicing	7	0.0262237	0.8268955
INTERPRO	RNA recognition motif domain	6	0.0268093	0.9998726
UP_KW_BIOLOGICAL_PROCESS	Transport	24	0.031445	0.878604
GOTERM_BP_DIRECT	vesicle fusion	3	0.0334286	1
UP_KW_MOLECULAR_FUNCTION	RNA-binding	11	0.0388155	0.867216
UP_KW_PTM	Phosphoprotein	79	0.0436094	0.5100356

Category	Term	Count	PValue	Bonferroni
GOTERM_MF_DIRECT	phosphoprotein phosphatase activity	3	0.0441398	0.9999997
INTERPRO	Nucleotide-binding, alpha-beta plait	6	0.0463419	0.9999998
INTERPRO	SANT/Myb domain	3	0.0481867	0.9999999
GOTERM_MF_DIRECT	sphingosine-1-phosphate phosphatase activity	2	0.0487796	0.9999999
UP_KW_BIOLOGICAL_PROCESS	Protein transport	10	0.0494887	0.9649102
KEGG_PATHWAY	Choline metabolism in cancer	4	0.0497288	0.9998917

Table 36: Urothelial carcinoma RT-112 DAVID gene ontology analysis

Category	Term	Count	PValue	Bonferroni
GOTERM_MF_DIRECT	RNA binding	38	2.62E-08	9.52E-06
GOTERM_MF_DIRECT	protein binding	149	3.10E-07	1.13E-04
UP_KW_PTM	Acetylation	65	1.19E-05	2.38E-04
INTERPRO	Nucleotide-binding, alpha-beta plait	12	5.28E-05	0.0229855
UP_KW_PTM	Phosphoprotein	119	7.14E-05	0.0014278
GOTERM_BP_DIRECT	regulation of translation	7	1.78E-04	0.1930568
UP_KW_MOLECULAR_FUNCTION	RNA-binding	19	2.20E-04	0.0111766
KEGG_PATHWAY	Various types of N-glycan biosynthesis	5	7.01E-04	0.1460039
GOTERM_BP_DIRECT	protein N-linked glycosylation	5	0.0015415	0.8446367
KEGG_PATHWAY	N-Glycan biosynthesis	5	0.0016918	0.3168035
GOTERM_BP_DIRECT	mitochondrion localization	3	0.0028103	0.9665212
GOTERM_BP_DIRECT	endonucleolytic cleavage in ITS1 to separate SSU-rRNA from 5.8S rRNA and LSU-rRNA from tricistronic rRNA transcript (SSU-rRNA, 5.8S rRNA, LSU-rRNA)	3	0.0034921	0.9853351
INTERPRO	RNA recognition motif domain	8	0.0066265	0.9463546
GOTERM_BP_DIRECT	positive regulation of G-protein coupled receptor protein signaling pathway	3	0.0079098	0.9999313
INTERPRO	Ubiquitin-associated/translation elongation factor EF1B, N-terminal, eukaryote	4	0.0085902	0.9775403
GOTERM_BP_DIRECT	response to peptide hormone	4	0.0122478	0.9999997
GOTERM_BP_DIRECT	mitochondrial fusion	3	0.0125802	0.9999998
INTERPRO	Fzo/mitofusin HR2 domain	2	0.0186435	0.9997466
INTERPRO	Mitofusin family	2	0.0186435	0.9997466
INTERPRO	Ubiquitin	4	0.0195478	0.9998311
KEGG_PATHWAY	Metabolic pathways	24	0.0200073	0.9894041
GOTERM_BP_DIRECT	cellular response to amino acid stimulus	4	0.0202721	1
GOTERM_BP_DIRECT	regulation of cytoskeleton organization	3	0.0213033	1
GOTERM_BP_DIRECT	protein targeting to mitochondrion	3	0.0299959	1
GOTERM_MF_DIRECT	mRNA binding	7	0.0327507	0.9999946
GOTERM_MF_DIRECT	identical protein binding	25	0.033164	0.9999953

Appendix

Category	Term	Count	PValue	Bonferroni
GOTERM_MF_DIRECT	nucleic acid binding	8	0.0332799	0.9999955
GOTERM_BP_DIRECT	cellular response to mechanical stimulus	4	0.0337972	1
GOTERM_BP_DIRECT	face morphogenesis	3	0.0338038	1
GOTERM_BP_DIRECT	endocytosis	6	0.0349044	1
GOTERM_MF_DIRECT	alpha-1,2-mannosyltransferase activity	2	0.0368116	0.9999988
INTERPRO	Tropomyosin	2	0.0369413	0.9999999
INTERPRO	LUC7-related	2	0.0369413	0.9999999
KEGG_PATHWAY	Oxocarboxylic acid metabolism	3	0.0405607	0.9999101
INTERPRO	Zinc finger, RING/FYVE/PHD-type	10	0.041123	1
UP_KW_BIOLOGICAL_PROCESS	Endocytosis	5	0.0427306	0.9529681
GOTERM_BP_DIRECT	positive regulation of translation	4	0.043174	1
UP_KW_BIOLOGICAL_PROCESS	Nonsense-mediated mRNA decay	3	0.043674	0.9561048
GOTERM_BP_DIRECT	positive regulation of intrinsic apoptotic signaling pathway	3	0.0440832	1
GOTERM_MF_DIRECT	polyubiquitin binding	3	0.0443466	0.9999999
KEGG_PATHWAY	Parkinson disease	7	0.0443736	0.9999633
INTERPRO	Ribonuclease CAF1	2	0.0459626	1
KEGG_PATHWAY	Diabetic cardiomyopathy	6	0.0472548	0.9999814
GOTERM_BP_DIRECT	protein transport	9	0.0492834	1

Table 37: Renal cell carcinoma Caki-1 DAVID gene ontology analysis

Category	Term	Count	PValue	Bonferroni
UP_KW_PTM	Acetylation	210	1.29E-26	3.22E-25
GOTERM_MF_DIRECT	protein binding	428	2.13E-21	1.61E-18
UP_KW_PTM	Phosphoprotein	342	1.78E-17	4.44E-16
GOTERM_MF_DIRECT	RNA binding	82	2.46E-10	1.86E-07
KEGG_PATHWAY	Metabolic pathways	85	1.51E-08	4.56E-06
INTERPRO	Armadillo-type fold	31	2.88E-08	3.06E-05
INTERPRO	Armadillo-like helical	24	2.00E-07	2.13E-04
UP_KW_MOLECULAR_FUNCTION	Transferase	85	8.04E-06	5.70E-04
GOTERM_MF_DIRECT	magnesium ion binding	20	1.61E-05	0.012101
GOTERM_BP_DIRECT	protein folding	17	1.96E-05	0.0465271
KEGG_PATHWAY	Glutathione metabolism	10	4.88E-05	0.0145735
GOTERM_BP_DIRECT	ribosome biogenesis	8	7.85E-05	0.1737251
GOTERM_BP_DIRECT	ribosomal small subunit biogenesis	10	9.96E-05	0.2151631
UP_KW_BIOLOGICAL_PROCESS	Lipid metabolism	41	1.11E-04	0.0125947
UP_KW_BIOLOGICAL_PROCESS	Host-virus interaction	38	1.28E-04	0.014471
UP_KW_MOLECULAR_FUNCTION	Isomerase	14	1.62E-04	0.0114271
KEGG_PATHWAY	Human immunodeficiency virus 1 infection	18	2.45E-04	0.0712389
INTERPRO	Phox homologous domain	8	2.70E-04	0.249701
GOTERM_BP_DIRECT	mRNA processing	17	3.81E-04	0.6037139
UP_KW_BIOLOGICAL_PROCESS	Ribosome biogenesis	11	5.44E-04	0.0601448
INTERPRO	Thioredoxin domain	7	5.67E-04	0.4529428
UP_KW_MOLECULAR_FUNCTION	Oxidoreductase	31	6.09E-04	0.0423321

Appendix

Category	Term	Count	PValue	Bonferroni
KEGG_PATHWAY	Oocyte meiosis	13	6.22E-04	0.1708802
GOTERM_MF_DIRECT	unfolded protein binding	12	7.78E-04	0.4451095
UP_KW_MOLECULAR_FUNCTION	Rotamase	7	7.88E-04	0.054444
INTERPRO	Tetratricopeptide-like helical	16	0.0010941	0.6880101
GOTERM_MF_DIRECT	peptidyl-prolyl cis-trans isomerase activity	7	0.001427	0.6607502
GOTERM_MF_DIRECT	ATP binding	61	0.0015881	0.6997415
GOTERM_MF_DIRECT	identical protein binding	67	0.0017259	0.7295342
INTERPRO	RNA-processing protein, HAT helix	4	0.0018724	0.8638658
INTERPRO	Helicase, C-terminal	10	0.0021443	0.8981172
GOTERM_BP_DIRECT	chromatin remodeling	19	0.0023387	0.9966355
GOTERM_BP_DIRECT	intracellular protein transport	19	0.0024133	0.9971947
GOTERM_MF_DIRECT	phosphatidylinositol binding	10	0.0025933	0.8599368
GOTERM_MF_DIRECT	nucleic acid binding	19	0.0026982	0.8706537
GOTERM_BP_DIRECT	mitochondrial translation	9	0.002964	0.9992676
KEGG_PATHWAY	Estrogen signaling pathway	12	0.0030031	0.5955771
GOTERM_BP_DIRECT	vesicle cytoskeletal trafficking	3	0.0036882	0.9998749
UP_KW_BIOLOGICAL_PROCESS	Endocytosis	11	0.0042614	0.3854341
GOTERM_MF_DIRECT	ubiquitin protein ligase binding	18	0.0045436	0.9681697
GOTERM_BP_DIRECT	proteasome-mediated ubiquitin-dependent protein catabolic process	14	0.0046593	0.9999883
KEGG_PATHWAY	Biosynthesis of nucleotide sugars	6	0.004931	0.7741548
GOTERM_MF_DIRECT	cadherin binding	18	0.0053034	0.9821429
INTERPRO	Armadillo	6	0.0062495	0.998732
KEGG_PATHWAY	Wnt signaling pathway	13	0.0067674	0.8704797
UP_KW_MOLECULAR_FUNCTION	RNA-binding	32	0.0068084	0.3843339
UP_KW_BIOLOGICAL_PROCESS	Protein transport	31	0.0068605	0.5437877
UP_KW_MOLECULAR_FUNCTION	Kinase	32	0.0077222	0.4232819
UP_KW_BIOLOGICAL_PROCESS	Cell cycle	32	0.0079866	0.5991344
GOTERM_BP_DIRECT	rRNA processing	10	0.0080455	1
KEGG_PATHWAY	Carbon metabolism	10	0.0082645	0.9177466
UP_KW_BIOLOGICAL_PROCESS	rRNA processing	9	0.008555	0.6244864
GOTERM_BP_DIRECT	retrograde vesicle-mediated transport, Golgi to ER	6	0.0090799	1
KEGG_PATHWAY	mRNA surveillance pathway	9	0.0092389	0.938813
INTERPRO	Helicase, superfamily 1/2, ATP-binding domain	9	0.0093164	0.9999527
GOTERM_MF_DIRECT	electron carrier activity	7	0.0097977	0.9994206
GOTERM_BP_DIRECT	positive regulation of mitochondrial translation	4	0.0098341	1
UP_KW_BIOLOGICAL_PROCESS	Mitosis	17	0.0100273	0.6830106
UP_KW_BIOLOGICAL_PROCESS	Lipid biosynthesis	12	0.0100449	0.6836514
GOTERM_BP_DIRECT	mRNA polyadenylation	5	0.010212	1
UP_KW_BIOLOGICAL_PROCESS	mRNA processing	21	0.0107843	0.7094809
GOTERM_MF_DIRECT	3'-5'-exoribonuclease activity	5	0.0108052	0.9997319

Appendix

Category	Term	Count	PValue	Bonferroni
GOTERM_BP_DIRECT	positive regulation of protein localization to centrosome	3	0.0122744	1
GOTERM_BP_DIRECT	purine ribonucleoside salvage	3	0.0122744	1
GOTERM_BP_DIRECT	intramembranous ossification	3	0.0122744	1
GOTERM_BP_DIRECT	endocytosis	12	0.0125061	1
INTERPRO	Peptidase C19, ubiquitin-specific peptidase, DUSP domain	3	0.0131956	0.9999993
UP_KW_MOLECULAR_FUNCTION	Allosteric enzyme	6	0.013726	0.6251761
KEGG_PATHWAY	Pentose phosphate pathway	5	0.0138092	0.9847861
UP_KW_MOLECULAR_FUNCTION	Helicase	10	0.0138146	0.6275587
GOTERM_BP_DIRECT	electron transport chain	6	0.0143206	1
GOTERM_BP_DIRECT	response to unfolded protein	6	0.0143206	1
GOTERM_BP_DIRECT	nucleobase-containing compound metabolic process	5	0.015024	1
GOTERM_MF_DIRECT	enzyme binding	19	0.0150501	0.9999897
GOTERM_MF_DIRECT	protein homodimerization activity	31	0.0160054	0.999995
KEGG_PATHWAY	Amino sugar and nucleotide sugar metabolism	6	0.0160721	0.9923801
GOTERM_BP_DIRECT	outer ear morphogenesis	3	0.0160944	1
GOTERM_BP_DIRECT	dendrite morphogenesis	5	0.0164156	1
KEGG_PATHWAY	Relaxin signaling pathway	10	0.016723	0.9937563
KEGG_PATHWAY	Nucleocytoplasmic transport	9	0.0169469	0.9941699
UP_KW_MOLECULAR_FUNCTION	Ribonucleoprotein	16	0.017057	0.7052115
INTERPRO	Glucose/ribitol dehydrogenase	6	0.0177922	1
GOTERM_BP_DIRECT	protein transport	20	0.0183009	1
GOTERM_BP_DIRECT	negative regulation of apoptotic process	23	0.0194365	1
GOTERM_BP_DIRECT	membrane protein ectodomain proteolysis	4	0.01945	1
GOTERM_MF_DIRECT	tau-protein kinase activity	4	0.0195267	0.9999997
GOTERM_BP_DIRECT	Notch receptor processing	3	0.0203504	1
GOTERM_BP_DIRECT	metaphase/anaphase transition of mitotic cell cycle	3	0.0203504	1
KEGG_PATHWAY	Cysteine and methionine metabolism	6	0.0203609	0.9979541
GOTERM_MF_DIRECT	protein serine/threonine kinase activity	19	0.0206536	0.9999999
UP_KW_BIOLOGICAL_PROCESS	Cholesterol biosynthesis	4	0.0213489	0.9145763
UP_KW_MOLECULAR_FUNCTION	Chaperone	13	0.021574	0.7874377
GOTERM_MF_DIRECT	nucleosomal histone binding	3	0.0222496	1
KEGG_PATHWAY	GnRH signaling pathway	8	0.0229192	0.9990687
UP_KW_MOLECULAR_FUNCTION	Ligase	10	0.024471	0.8277925
GOTERM_BP_DIRECT	positive regulation of rRNA processing	3	0.025018	1
GOTERM_BP_DIRECT	endonucleolytic cleavage in ITS1 to separate SSU-rRNA from 5.8S rRNA and LSU-rRNA from tricistronic rRNA transcript (SSU-rRNA, 5.8S rRNA, LSU-rRNA)	3	0.025018	1
GOTERM_BP_DIRECT	glycogen catabolic process	3	0.025018	1

Appendix

Category	Term	Count	PValue	Bonferroni
GOTERM_BP_DIRECT	transcription, DNA-templated	8	0.0255582	1
GOTERM_BP_DIRECT	embryo implantation	5	0.0264436	1
GOTERM_MF_DIRECT	chaperone binding	8	0.0269532	1
UP_KW_BIOLOGICAL_PROCESS	Lipid degradation	8	0.0275481	0.958603
GOTERM_BP_DIRECT	regulation of attachment of spindle microtubules to kinetochore	3	0.0300737	1
UP_KW_MOLECULAR_FUNCTION	Serine/threonine-protein kinase	18	0.0304669	0.8888402
UP_KW_MOLECULAR_FUNCTION	Hydrolase	60	0.0308387	0.8918267
UP_KW_BIOLOGICAL_PROCESS	Cell division	20	0.0309759	0.9723214
KEGG_PATHWAY	Endometrial cancer	6	0.0310324	0.9999243
GOTERM_BP_DIRECT	insulin receptor signaling pathway	6	0.0318147	1
UP_KW_MOLECULAR_FUNCTION	Ribosomal protein	11	0.0318944	0.8998819
INTERPRO	Armadillo repeat-containing domain	3	0.0322482	1
KEGG_PATHWAY	RNA degradation	7	0.0327915	0.9999562
GOTERM_BP_DIRECT	mitochondrial transport	4	0.0328082	1
GOTERM_BP_DIRECT	tRNA modification	4	0.0328082	1
INTERPRO	SANT domain	4	0.0328522	1
INTERPRO	DnaJ domain, conserved site	4	0.0328522	1
GOTERM_BP_DIRECT	protein phosphorylation	19	0.0338035	1
GOTERM_BP_DIRECT	cell division	17	0.0347408	1
GOTERM_MF_DIRECT	beta-catenin binding	7	0.0353015	1
GOTERM_BP_DIRECT	dephosphorylation	6	0.0353278	1
GOTERM_BP_DIRECT	negative regulation of axonogenesis	3	0.0354952	1
GOTERM_BP_DIRECT	nucleotide biosynthetic process	3	0.0354952	1
GOTERM_BP_DIRECT	histone H2A monoubiquitination	3	0.0354952	1
KEGG_PATHWAY	Progesterone-mediated oocyte maturation	8	0.0355963	0.9999817
GOTERM_BP_DIRECT	endosome to lysosome transport	5	0.0370858	1
UP_KW_BIOLOGICAL_PROCESS	Sterol biosynthesis	4	0.0375803	0.9873073
GOTERM_BP_DIRECT	wound healing	7	0.0377827	1
GOTERM_BP_DIRECT	protein targeting to mitochondrion	4	0.039194	1
GOTERM_BP_DIRECT	positive regulation of G1/S transition of mitotic cell cycle	5	0.0394693	1
GOTERM_BP_DIRECT	vesicle-mediated transport	12	0.0399834	1
GOTERM_MF_DIRECT	misfolded protein binding	4	0.0404689	1
GOTERM_BP_DIRECT	neuron projection development	8	0.040754	1
INTERPRO	Serine/threonine-protein kinase, active site	15	0.0407874	1
GOTERM_BP_DIRECT	RNA 3'-end processing	3	0.0412607	1
GOTERM_BP_DIRECT	negative regulation of proteasomal protein catabolic process	3	0.0412607	1
INTERPRO	WD40 repeat, conserved site	9	0.0414034	1
GOTERM_BP_DIRECT	protein autophosphorylation	10	0.0418304	1
GOTERM_BP_DIRECT	cytoskeleton organization	9	0.0418721	1
GOTERM_BP_DIRECT	sphingolipid biosynthetic process	5	0.0419382	1
GOTERM_MF_DIRECT	nucleotide binding	7	0.0420955	1

Category	Term	Count	PValue	Bonferroni
GOTERM_BP_DIRECT	peptidyl-serine phosphorylation	10	0.044312	1
UP_KW_BIOLOGICAL_PROCESS	Stress response	8	0.0443145	0.9942996
KEGG_PATHWAY	Nucleotide metabolism	7	0.0444844	0.9999989
GOTERM_BP_DIRECT	cellular response to reactive oxygen species	5	0.0444925	1
GOTERM_BP_DIRECT	cellular response to glucose stimulus	6	0.0451236	1
UP_KW_BIOLOGICAL_PROCESS	Cholesterol metabolism	6	0.0456406	0.9951341
GOTERM_MF_DIRECT	oxidoreductase activity	12	0.0465681	1
KEGG_PATHWAY	Cushing syndrome	10	0.046808	0.9999995
GOTERM_BP_DIRECT	cell cycle	16	0.0468184	1
INTERPRO	DnaJ domain	5	0.0470563	1
GOTERM_BP_DIRECT	endosomal transport	6	0.0472585	1
GOTERM_BP_DIRECT	response to arsenic-containing substance	3	0.0473496	1
GOTERM_BP_DIRECT	amyloid precursor protein catabolic process	3	0.0473496	1
KEGG_PATHWAY	Lysosome	9	0.0479884	0.9999996
GOTERM_MF_DIRECT	RNA helicase activity	6	0.0485624	1
GOTERM_MF_DIRECT	protein kinase activity	17	0.0489161	1
GOTERM_MF_DIRECT	protein serine/threonine/tyrosine kinase activity	19	0.0494294	1
GOTERM_BP_DIRECT	negative regulation of signaling	2	0.0498448	1
GOTERM_BP_DIRECT	deoxyribose phosphate catabolic process	2	0.0498448	1
GOTERM_BP_DIRECT	cellular response to thyroxine stimulus	2	0.0498448	1
GOTERM_BP_DIRECT	'de novo' cotranslational protein folding	2	0.0498448	1
GOTERM_BP_DIRECT	regulation of anaphase-promoting complex-dependent catabolic process	2	0.0498448	1
GOTERM_BP_DIRECT	retinoid metabolic process	4	0.0498582	1

Table 38: Prostate Carcinoma PC-3 DAVID gene ontology analysis

Category	Term	Count	PValue	Bonferroni
UP_KW_PTM	Acetylation	210	1.29E-26	3.22E-25
GOTERM_MF_DIRECT	protein binding	428	2.13E-21	1.61E-18
UP_KW_PTM	Phosphoprotein	342	1.78E-17	4.44E-16
GOTERM_MF_DIRECT	RNA binding	82	2.46E-10	1.86E-07
KEGG_PATHWAY	Metabolic pathways	85	1.51E-08	4.56E-06
INTERPRO	Armadillo-type fold	31	2.88E-08	3.06E-05
INTERPRO	Armadillo-like helical	24	2.00E-07	2.13E-04
UP_KW_MOLECULAR_FUNCTION	Transferase	85	8.04E-06	5.70E-04
GOTERM_MF_DIRECT	magnesium ion binding	20	1.61E-05	0.012101
GOTERM_BP_DIRECT	protein folding	17	1.96E-05	0.0465271
KEGG_PATHWAY	Glutathione metabolism	10	4.88E-05	0.0145735
GOTERM_BP_DIRECT	ribosome biogenesis	8	7.85E-05	0.1737251
GOTERM_BP_DIRECT	ribosomal small subunit biogenesis	10	9.96E-05	0.2151631
UP_KW_BIOLOGICAL_PROCESS	Lipid metabolism	41	1.11E-04	0.0125947
UP_KW_BIOLOGICAL_PROCESS	Host-virus interaction	38	1.28E-04	0.014471
UP_KW_MOLECULAR_FUNCTION	Isomerase	14	1.62E-04	0.0114271
KEGG_PATHWAY	Human immunodeficiency virus 1 infection	18	2.45E-04	0.0712389
INTERPRO	Phox homologous domain	8	2.70E-04	0.249701

Appendix

Category	Term	Count	PValue	Bonferroni
GOTERM_BP_DIRECT	mRNA processing	17	3.81E-04	0.6037139
UP_KW_BIOLOGICAL_PROCESS	Ribosome biogenesis	11	5.44E-04	0.0601448
INTERPRO	Thioredoxin domain	7	5.67E-04	0.4529428
UP_KW_MOLECULAR_FUNCTION	Oxidoreductase	31	6.09E-04	0.0423321
KEGG_PATHWAY	Oocyte meiosis	13	6.22E-04	0.1708802
GOTERM_MF_DIRECT	unfolded protein binding	12	7.78E-04	0.4451095
UP_KW_MOLECULAR_FUNCTION	Rotamase	7	7.88E-04	0.054444
INTERPRO	Tetratricopeptide-like helical	16	0.0010941	0.6880101
GOTERM_MF_DIRECT	peptidyl-prolyl cis-trans isomerase activity	7	0.001427	0.6607502
GOTERM_MF_DIRECT	ATP binding	61	0.0015881	0.6997415
GOTERM_MF_DIRECT	identical protein binding	67	0.0017259	0.7295342
INTERPRO	RNA-processing protein, HAT helix	4	0.0018724	0.8638658
INTERPRO	Helicase, C-terminal	10	0.0021443	0.8981172
GOTERM_BP_DIRECT	chromatin remodeling	19	0.0023387	0.9966355
GOTERM_BP_DIRECT	intracellular protein transport	19	0.0024133	0.9971947
GOTERM_MF_DIRECT	phosphatidylinositol binding	10	0.0025933	0.8599368
GOTERM_MF_DIRECT	nucleic acid binding	19	0.0026982	0.8706537
GOTERM_BP_DIRECT	mitochondrial translation	9	0.002964	0.9992676
KEGG_PATHWAY	Estrogen signaling pathway	12	0.0030031	0.5955771
GOTERM_BP_DIRECT	vesicle cytoskeletal trafficking	3	0.0036882	0.9998749
UP_KW_BIOLOGICAL_PROCESS	Endocytosis	11	0.0042614	0.3854341
GOTERM_MF_DIRECT	ubiquitin protein ligase binding	18	0.0045436	0.9681697
GOTERM_BP_DIRECT	proteasome-mediated ubiquitin-dependent protein catabolic process	14	0.0046593	0.9999883
KEGG_PATHWAY	Biosynthesis of nucleotide sugars	6	0.004931	0.7741548
GOTERM_MF_DIRECT	cadherin binding	18	0.0053034	0.9821429
INTERPRO	Armadillo	6	0.0062495	0.998732
KEGG_PATHWAY	Wnt signaling pathway	13	0.0067674	0.8704797
UP_KW_MOLECULAR_FUNCTION	RNA-binding	32	0.0068084	0.3843339
UP_KW_BIOLOGICAL_PROCESS	Protein transport	31	0.0068605	0.5437877
UP_KW_MOLECULAR_FUNCTION	Kinase	32	0.0077222	0.4232819
UP_KW_BIOLOGICAL_PROCESS	Cell cycle	32	0.0079866	0.5991344
GOTERM_BP_DIRECT	rRNA processing	10	0.0080455	1
KEGG_PATHWAY	Carbon metabolism	10	0.0082645	0.9177466
UP_KW_BIOLOGICAL_PROCESS	rRNA processing	9	0.008555	0.6244864
GOTERM_BP_DIRECT	retrograde vesicle-mediated transport, Golgi to ER	6	0.0090799	1
KEGG_PATHWAY	mRNA surveillance pathway	9	0.0092389	0.938813
INTERPRO	Helicase, superfamily 1/2, ATP-binding domain	9	0.0093164	0.9999527
GOTERM_MF_DIRECT	electron carrier activity	7	0.0097977	0.9994206
GOTERM_BP_DIRECT	positive regulation of mitochondrial translation	4	0.0098341	1
UP_KW_BIOLOGICAL_PROCESS	Mitosis	17	0.0100273	0.6830106
UP_KW_BIOLOGICAL_PROCESS	Lipid biosynthesis	12	0.0100449	0.6836514

Appendix

Category	Term	Count	PValue	Bonferroni
GOTERM_BP_DIRECT	mRNA polyadenylation	5	0.010212	1
UP_KW_BIOLOGICAL_PROCESS	mRNA processing	21	0.0107843	0.7094809
GOTERM_MF_DIRECT	3'-5'-exoribonuclease activity	5	0.0108052	0.9997319
GOTERM_BP_DIRECT	positive regulation of protein localization to centrosome	3	0.0122744	1
GOTERM_BP_DIRECT	purine ribonucleoside salvage	3	0.0122744	1
GOTERM_BP_DIRECT	intramembranous ossification	3	0.0122744	1
GOTERM_BP_DIRECT	endocytosis	12	0.0125061	1
INTERPRO	Peptidase C19, ubiquitin-specific peptidase, DUSP domain	3	0.0131956	0.9999993
UP_KW_MOLECULAR_FUNCTION	Allosteric enzyme	6	0.013726	0.6251761
KEGG_PATHWAY	Pentose phosphate pathway	5	0.0138092	0.9847861
UP_KW_MOLECULAR_FUNCTION	Helicase	10	0.0138146	0.6275587
GOTERM_BP_DIRECT	electron transport chain	6	0.0143206	1
GOTERM_BP_DIRECT	response to unfolded protein	6	0.0143206	1
GOTERM_BP_DIRECT	nucleobase-containing compound metabolic process	5	0.015024	1
GOTERM_MF_DIRECT	enzyme binding	19	0.0150501	0.9999897
GOTERM_MF_DIRECT	protein homodimerization activity	31	0.0160054	0.999995
KEGG_PATHWAY	Amino sugar and nucleotide sugar metabolism	6	0.0160721	0.9923801
GOTERM_BP_DIRECT	outer ear morphogenesis	3	0.0160944	1
GOTERM_BP_DIRECT	dendrite morphogenesis	5	0.0164156	1
KEGG_PATHWAY	Relaxin signaling pathway	10	0.016723	0.9937563
KEGG_PATHWAY	Nucleocytoplasmic transport	9	0.0169469	0.9941699
UP_KW_MOLECULAR_FUNCTION	Ribonucleoprotein	16	0.017057	0.7052115
INTERPRO	Glucose/ribitol dehydrogenase	6	0.0177922	1
GOTERM_BP_DIRECT	protein transport	20	0.0183009	1
GOTERM_BP_DIRECT	negative regulation of apoptotic process	23	0.0194365	1
GOTERM_BP_DIRECT	membrane protein ectodomain proteolysis	4	0.01945	1
GOTERM_MF_DIRECT	tau-protein kinase activity	4	0.0195267	0.9999997
GOTERM_BP_DIRECT	Notch receptor processing	3	0.0203504	1
GOTERM_BP_DIRECT	metaphase/anaphase transition of mitotic cell cycle	3	0.0203504	1
KEGG_PATHWAY	Cysteine and methionine metabolism	6	0.0203609	0.9979541
GOTERM_MF_DIRECT	protein serine/threonine kinase activity	19	0.0206536	0.9999999
UP_KW_BIOLOGICAL_PROCESS	Cholesterol biosynthesis	4	0.0213489	0.9145763
UP_KW_MOLECULAR_FUNCTION	Chaperone	13	0.021574	0.7874377
GOTERM_MF_DIRECT	nucleosomal histone binding	3	0.0222496	1
KEGG_PATHWAY	GnRH signaling pathway	8	0.0229192	0.9990687
UP_KW_MOLECULAR_FUNCTION	Ligase	10	0.024471	0.8277925
GOTERM_BP_DIRECT	positive regulation of rRNA processing	3	0.025018	1

Appendix

Category	Term	Count	PValue	Bonferroni
GOTERM_BP_DIRECT	endonucleolytic cleavage in ITS1 to separate SSU-rRNA from 5.8S rRNA and LSU-rRNA from tricistronic rRNA transcript (SSU-rRNA, 5.8S rRNA, LSU-rRNA)	3	0.025018	1
GOTERM_BP_DIRECT	glycogen catabolic process	3	0.025018	1
GOTERM_BP_DIRECT	transcription, DNA-templated	8	0.0255582	1
GOTERM_BP_DIRECT	embryo implantation	5	0.0264436	1
GOTERM_MF_DIRECT	chaperone binding	8	0.0269532	1
UP_KW_BIOLOGICAL_PROCESS	Lipid degradation	8	0.0275481	0.958603
GOTERM_BP_DIRECT	regulation of attachment of spindle microtubules to kinetochore	3	0.0300737	1
UP_KW_MOLECULAR_FUNCTION	Serine/threonine-protein kinase	18	0.0304669	0.8888402
UP_KW_MOLECULAR_FUNCTION	Hydrolase	60	0.0308387	0.8918267
UP_KW_BIOLOGICAL_PROCESS	Cell division	20	0.0309759	0.9723214
KEGG_PATHWAY	Endometrial cancer	6	0.0310324	0.9999243
GOTERM_BP_DIRECT	insulin receptor signaling pathway	6	0.0318147	1
UP_KW_MOLECULAR_FUNCTION	Ribosomal protein	11	0.0318944	0.8998819
INTERPRO	Armadillo repeat-containing domain	3	0.0322482	1
KEGG_PATHWAY	RNA degradation	7	0.0327915	0.9999562
GOTERM_BP_DIRECT	mitochondrial transport	4	0.0328082	1
GOTERM_BP_DIRECT	tRNA modification	4	0.0328082	1
INTERPRO	SANT domain	4	0.0328522	1
INTERPRO	DnaJ domain, conserved site	4	0.0328522	1
GOTERM_BP_DIRECT	protein phosphorylation	19	0.0338035	1
GOTERM_BP_DIRECT	cell division	17	0.0347408	1
GOTERM_MF_DIRECT	beta-catenin binding	7	0.0353015	1
GOTERM_BP_DIRECT	dephosphorylation	6	0.0353278	1
GOTERM_BP_DIRECT	negative regulation of axonogenesis	3	0.0354952	1
GOTERM_BP_DIRECT	nucleotide biosynthetic process	3	0.0354952	1
GOTERM_BP_DIRECT	histone H2A monoubiquitination	3	0.0354952	1
KEGG_PATHWAY	Progesterone-mediated oocyte maturation	8	0.0355963	0.9999817
GOTERM_BP_DIRECT	endosome to lysosome transport	5	0.0370858	1
UP_KW_BIOLOGICAL_PROCESS	Sterol biosynthesis	4	0.0375803	0.9873073
GOTERM_BP_DIRECT	wound healing	7	0.0377827	1
GOTERM_BP_DIRECT	protein targeting to mitochondrion	4	0.039194	1
GOTERM_BP_DIRECT	positive regulation of G1/S transition of mitotic cell cycle	5	0.0394693	1
GOTERM_BP_DIRECT	vesicle-mediated transport	12	0.0399834	1
GOTERM_MF_DIRECT	misfolded protein binding	4	0.0404689	1
GOTERM_BP_DIRECT	neuron projection development	8	0.040754	1
INTERPRO	Serine/threonine-protein kinase, active site	15	0.0407874	1
GOTERM_BP_DIRECT	RNA 3'-end processing	3	0.0412607	1
GOTERM_BP_DIRECT	negative regulation of proteasomal protein catabolic process	3	0.0412607	1

Appendix

Category	Term	Count	PValue	Bonferroni
INTERPRO	WD40 repeat, conserved site	9	0.0414034	1
GOTERM_BP_DIRECT	protein autophosphorylation	10	0.0418304	1
GOTERM_BP_DIRECT	cytoskeleton organization	9	0.0418721	1
GOTERM_BP_DIRECT	sphingolipid biosynthetic process	5	0.0419382	1
GOTERM_MF_DIRECT	nucleotide binding	7	0.0420955	1
GOTERM_BP_DIRECT	peptidyl-serine phosphorylation	10	0.044312	1
UP_KW_BIOLOGICAL_PROCESS	Stress response	8	0.0443145	0.9942996
KEGG_PATHWAY	Nucleotide metabolism	7	0.0444844	0.9999989
GOTERM_BP_DIRECT	cellular response to reactive oxygen species	5	0.0444925	1
GOTERM_BP_DIRECT	cellular response to glucose stimulus	6	0.0451236	1
UP_KW_BIOLOGICAL_PROCESS	Cholesterol metabolism	6	0.0456406	0.9951341
GOTERM_MF_DIRECT	oxidoreductase activity	12	0.0465681	1
KEGG_PATHWAY	Cushing syndrome	10	0.046808	0.9999995
GOTERM_BP_DIRECT	cell cycle	16	0.0468184	1
INTERPRO	DnaJ domain	5	0.0470563	1
GOTERM_BP_DIRECT	endosomal transport	6	0.0472585	1
GOTERM_BP_DIRECT	response to arsenic-containing substance	3	0.0473496	1
GOTERM_BP_DIRECT	amyloid precursor protein catabolic process	3	0.0473496	1
KEGG_PATHWAY	Lysosome	9	0.0479884	0.9999996
GOTERM_MF_DIRECT	RNA helicase activity	6	0.0485624	1
GOTERM_MF_DIRECT	protein kinase activity	17	0.0489161	1
GOTERM_MF_DIRECT	protein serine/threonine/tyrosine kinase activity	19	0.0494294	1
GOTERM_BP_DIRECT	negative regulation of signaling	2	0.0498448	1
GOTERM_BP_DIRECT	deoxyribose phosphate catabolic process	2	0.0498448	1
GOTERM_BP_DIRECT	cellular response to thyroxine stimulus	2	0.0498448	1
GOTERM_BP_DIRECT	'de novo' cotranslational protein folding	2	0.0498448	1
GOTERM_BP_DIRECT	regulation of anaphase-promoting complex-dependent catabolic process	2	0.0498448	1
GOTERM_BP_DIRECT	retinoid metabolic process	4	0.0498582	1

Danksagung

Ich möchte diese Gelegenheit nutzten, um allen Personen zu danke, welche mich beim Erstellen dieser Doktorarbeit maßgeblich unterstützt haben.

Mein ganz besonderer Dank gilt meinem Doktorvater Prof. Dr. Daniel Nettersheim. Ich möchte mich bei Ihm für das sehr spannende Projekt, seine umfangreiche und engagierte Betreuung, sowie der wissenschaftlichen Anleitung und dem facettenreichen Austausch in seiner Arbeitsgruppe herzlichst bedanken. Du hast mich und alle anderen Mitglieder der Arbeitsgruppe immer wieder dazu gebracht das Beste aus uns hervorzubringen, gute Ergebnisse zu liefern und diese auch zu präsentieren.

Des Weiteren möchte ich meiner Betreuerin Dr. Margaretha Skowron für die ebenfalls sehr engagierte Unterstützung im Labor bedanken, aber auch für die Beratung beim Schreiben dieser Arbeit, zu jeder Zeit und von jedem Ort.

Außerdem möchte ich auch allen weiteren Teammitgliedern der Arbeitsgruppe, für die stets sehr harmonische und produktive Arbeitsatmosphäre danken. Ihr habt mir beigebracht, wie man richtig forscht und vor allem, dass es auch neben der einen oder anderen Frustration sehr viel Spaß machen kann. Auch abseits der Forschung habe ich mich bei euch extrem gut aufgehoben gefühlt und ich vermisse die Kaffee und Mittagspausen immer noch. Es war für mich eine sehr schöne Zeit, in der ich viele Erfahrungen sammeln konnte. Ich war gerne bei euch und habe mich nicht nur fachlich, sondern auch persönlich weiterentwickeln können.

Schlussendlich gilt mein besonderer Dank noch meiner Familie und meiner Partnerin Jana Herbst, welche mich während des gesamten Prozesses des Forschens und Schreibens mit vollem Einsatz unterstützt haben.

Vielen Dank für alles!